Isolation and identification of the toxic compounds of *Tapura fischeri* Engl.

Marelie Taljaard

26178746

Submitted in partial fulfilment of the requirements for the degree

MSc (Medicinal Plant Science)

Department of Plant Science

Faculty of Natural and Agricultural Sciences

University of Pretoria

Supervisor: Prof. J.J.M. Meyer

November 2014

UNIVERSITEIT VAN PRETORIA
UNIVERSITY OF PRETORIA
YUNIBESITHI YA PRETORIA

DECLARATION OF ORIGINALITY
UNIVERSITY OF PRETORIA

Full names of student: **Marelie Taljaard**

Student number: **26178746**

Topic of work: **Isolation and identification of the toxic compounds of *Tapura fischeri* Engl.**

Declaration

1. I understand what plagiarism is and am aware of the University's policy in this regard.

2. I declare that this **dissertation** (eg essay, report, project, assignment, dissertation, thesis, etc) is my own original work. Where other people's work has been used (either from a printed source, Internet or any other source), this has been properly acknowledged and referenced in accordance with departmental requirements.

3. I have not used work previously produced by another student or any other person to hand in as my own.

4. I have not allowed, and will not allow, anyone to copy my work with the intention of passing it off as his or her own work.

SIGNATURE

.....

Abstract

Tapura fischeri is a member of the family Dichapetalaceae and the only other member of this family naturally occurring in South Africa is *Dichapetalum cymosum.* Poisoning by *D. cymosum* results in the deaths of many domestic livestock each year due to the presence of fluoroacetate. The aim of the study was to determine if monofluoroacetate or another fluorinated compound is present in *T. fischeri,* and the possible role endophytes might play in the production of these compounds. Through NMR and GCMS studies it was established that trifluoroacetate is present in *T. fischeri*. Bacterial endophytes were isolated from plant material and shown to produce a fluorinated compound other than mono and tri-fluoroacetate. Since trifluoroacetic acid is extremely volatile, and evaporate from the plant extract over time, column chromatography, together with NMR was employed to isolate and identify other compounds responsible for antibacterial activity against the bacterium *Enterococcus faecalis* previously observed on TLC plates. Two compounds were isolated, and identified with NMR as a fatty acid and a fatty acid attached to glycerol. The names of the compounds could not be established with GCMS due to insufficient derivatization of the compounds. The antibacterial activity of the compounds were also analyzed using 96 well microtitre plates in liquid media, where it was determined that the compounds do not have antibacterial activity against *E. faecalis*. This indicated that previous results on TLC plates were false positives due to the hydrophobic nature of the fatty acid compounds. Transmission electron microscopy was done on leaf material to determine the presence of bacterial endophytes in the intracellular spaces of plant material, but none was detected. These results suggest a possitive correlation between the plant, its endophytes and the production of the fluorinated compound.

Keywords: *Tapura fischeri,* mono-fluoroacetate, trifluoroacetate, endophytes, NMR, GCMS

Acknowledgements

Prof J.J.M. Meyer – Thanks for being a great supervisor, and always providing support and encouragement.

Dr. F.P. Senejoux – I appreciate all the help with the compound isolation and NMR analysis. I have learned a lot about solvent polarities, and how to isolate compounds.

Dr. A.A. Yusuf – Thank you for not only running my samples on the GCMS, but also providing a learning opportunity. I appreciate your patience and the time you provided to help me understand the principles and out come of the results

Dr. H.M Heyman – You have been the rock, I could rely on always. You explained when I did not understand difficult concepts, and encouraged when I was disheartened.

Mr. C.F. van der Merwe – I appreciate the help you provided with the microscopy work, you made black and white images look exciting, and opened a door to a world few people get to see.

Mr. C. van der Westhuizen – Thanks for allowing us to run our samples on the 400 MHz NMR at the CSIR.

InPheno, Basil Switzerland – Thanks for testing our samples against HIV, the effort is appreciated.

Without the help of the above-mentioned people, the study would not have been completed. They were there to give guidance when needed, and support during rough times.

Table of Contents

List of Figures

List of Tables

List of abbreviations

BCl_3-methanol: Boron trichloride methanol

BSA: Brine shrimp assay

BSTFA: N,O,-Bis(trimethylsilyl)trifluoroacetamide

BuOH: Butanol

$CDCl_3$: Deutorated chloroform

CFU: Colony forming units

CVC: Citrus variegated chlorosis

D_2O: Deuterium oxide

DCM: Dichloromethane

dH_2O: Distilled water

DMSO: Dimethyl sulfoxide

EC_{50}: Concentration at which a drug is 50% effective for a targeted response.

EtOAc: Ethyl acetate

FA: Fatty acid

FAG: Fatty acid glycerol

FAMEs: Fatty acid methyl esters

FDA: 5-fluoro-5-deoxyfluoroadenosine

FID: Film ionization detector

GC: Gas chromatography

GCMS: Gas chromatography mass spectrometry

H_2SO_4: Sulphuric acid

Hex: Hexane

HFC's: Hydrofluorocarbons

HOAc: Acetic acid

HOFC's: Hydrochlorofluorocarbons

HS: Head space

HSV: Herpes simplex virus

INT: 2-(4-iodophenyl)-3-(4-nitrophenyl)-5-phenyltetrazolium chloride

KZN: KwaZulu-Natal

LBG: Lowveld botanical garden

LD_{50}: Lethal dose at which 50% of test subjects are killed

m/z: Mass to charge ratio

MeOH: Methanol

MFA: Monofluoroacetate

MIC: Minimum inhibitory concentration

MTFA: Methyl ester of trifluoro-acetic acid

NAD^+: Nicotinamide adenine dinucleotide

NMR: Nuclear magnetic resonance

OP: Onderstepoort

SAM: S-adenosyl methionine

SFM: Soy flower medium

SIM EI$^+$: Selected ion monitoring for positive electron ionization

TEM: Transmission electron microscopy

TFA: Trifluoro-acetic acid

TLC: Thin layer chromatography

TMSH: Trimethylsulfonium

UV: Ultra violet

Chapter 1:

Literature review

1.1 Background of *Tapura fischeri*

Tapura fischeri Engl. is a member of the family Dichapetalaceae (Figure 1.1 A). It is commonly known as the leaf-berry tree, and occurs mostly in the forest margins of coastal forest in the Zululand-Maputuland region of KwaZulu-Natal (KZN) (Pooley, 1993). *T. fischeri* was collected for the first time in 1895 in Tanzania, it was later found to extend south into South-Africa, along the coastal forest of Zululand (Palmer, 1972). It is known to occur in forests around Lake Sibayi in KZN (Palmer, 1972). Figure 1.1 B shows the distribution map for *T. fischeri* in Africa.

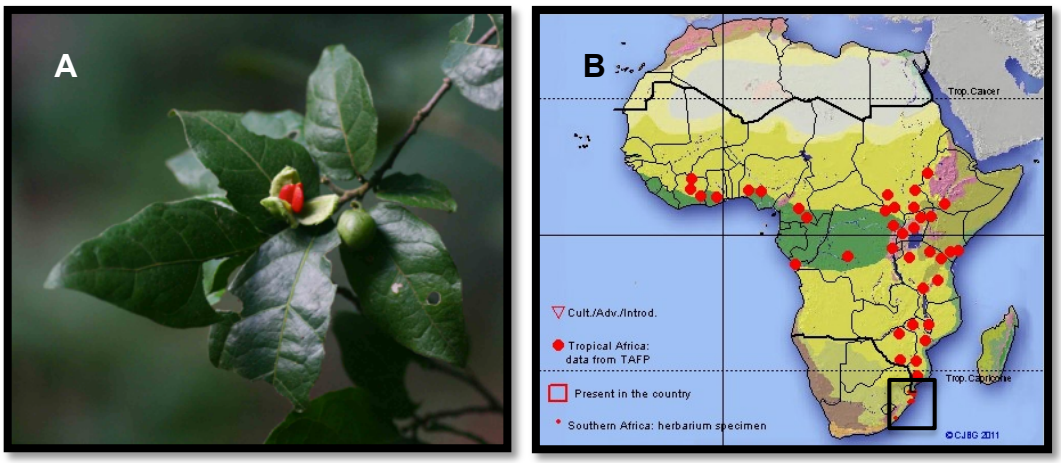

Figure 1.1: (A) The plant *T. fischeri.* (B) Distribution map of *T. fischeri* in Africa. The black box shows the distribution in South-Africa and the northern parts of KZN (African Plant Database, 2012).

T. fischeri is a small tree, mostly between 4 and 6 m in height (Coates Palgrave, 2002), however some have been recorded to reach up to 21 m (Palmer, 1972). The flowers are white and very small (2-3 mm in diameter), with a sweet scent. They are born in clusters on a stalk, which is fused to the petiole (Coates Palgrave, 2002). They can be seen from October to December (Boon, 2010). The fruit is fleshy, very small (±4 mm in diameter), occur at the base of the leaf blade and is present from January to April (Boon, 2010).

Eighty-six *Dichapetalum* species have been described in Africa, of which twenty-six are found in east and southern Africa. The only other member of this family found in South-Africa is *Dichapetalum cymosum* (Hook.) Engl. (poison-leaf). This plant is known to contain the poison fluoroacetate and is responsible for many deaths of domestic livestock each year. Unlike some of the other species in this family, *D. cymosum* dies off during winter, limiting livestock poisonings to the growing season (spring and summer). *T. fischeri* has apparently also been demonstrated to contain fluoroacetate (this was established through personal communication with P.P. Minnaar of the Veterinary Faculty at Onderstepoort in 1995) (Kellerman *et al*., 2005). This has however not been published.

The toxicity of the *Tapura* genus is well known, with the leaves and seeds of many species being used as poisons against rats and mice (Cornejo & Janovec, 2010). The toxicity of *Tapura amazonica* Poepp., a species known from the Amazon has been tested for its toxicity using the brine shrimp assay (BSA). BSA is used to determine the toxicity of compounds, since it correlates well with the oral lethal dose (LD_{50}) in mice (Quignard *et al*., 2004). From the plants tested, the roots of *T. amazonica* was the most active with a LD_{50} of 1.2 µg/ml. These results can be linked to the toxicity in vertebrates and perhaps even in humans (Quignard *et al*., 2004). In another study the toxicity of Amazonian plants were tested against the larvae *Aedes aegypti*. Once again the root extracts of *T. amazonica* showed the best results, with 100% mortality (Pohlit *et al*., 2004).

1.2 Fluorine in nature

Of all the halogens fluorine is the most abundant in the earth's crust. It is the 13th most abundant element although most of it is in an insoluble form and therefore biologically unavailable. Even though only a small percentage is biologically available, many marine and terrestrial organisms still contain a relatively large amount of inorganic fluorine. Some

terrestrial plants can concentrate inorganic fluorine from a low percentage in the soil, e.g. the genus *Camelia* (which includes the tea plant) can contain 70-80 µg/g of dry weight. Fluorine that is organically bound is however very rare in nature and has been identified in only a small number of tropical and subtropical plants and in only two actinomycetes (Harper & O'Hagan, 1994).

The unique chemical attributes of fluorine is the reason why only a small percentage can be used biologically, as compared to other halogens. For this reason it is referred to as a superhalogen. Some of these attributes include the small radius of fluorine, which is even smaller than hydrogen. It is also the most electronegative of all the elements, meaning that it forms the strongest single bond with carbon. The toxicity of fluorine results from its electronegativity. During enzyme-substrate binding the presence of fluorine can change the acidity of neighboring functional groups, which affects the affinity of the enzyme for the substrate (Harper & O'Hagan, 1994)

1.2.1 Organic fluorine compounds

So far only 13 organic fluorine compounds have been found in nature, eight of these are fluorinated homologous of long chain fatty acids. Therefore only six discrete natural fluorinated compounds are natural products (Figure 1.2). The first fluorinated compound to be isolated was fluoroacetate in 1943 from the southern African plant *Dichapetalum cymosum* (O'Hagan & Harper, 1999). The most recent compound isolated was 4-fluorothreonine from the bacterium *Streptomyces cattleya* in 1986 (O'Hagan & Harper, 1999). Other fluorinated compounds include fluoroacetone, fluorocitrate and nucleocidin (Harper & O'Hagan, 1994).

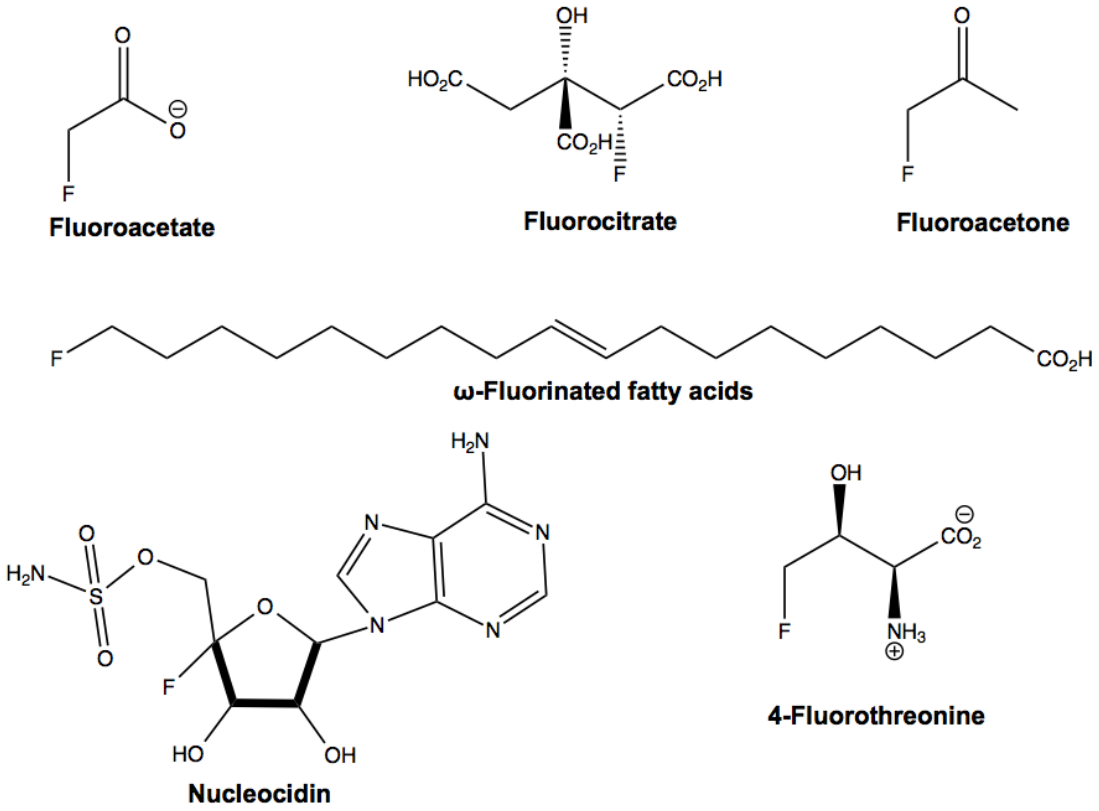

Figure 1.2: Structures of the six discrete natural fluorinated compounds in nature (Compiled from O'Hagan & Harper, 1999).

The most abundant naturally occurring organic fluoride compound is fluoroacetate. It is found in many plants at low concentrations, in some plants such as *D. cymosum* it can accumulate in high concentrations. Due to fluoroacetate the plant is extremely toxic, and causes large numbers of cattle losses in South-Africa each year. The leaves can accumulate up to 2.5mg/g dry weight during early spring. Other members of *Dichapetalum* (*D. braunii, D. toxicarium, D. heudelotti* and *D. stuhllmannii*) as well as certain Australian plants (*Acacia georginae*, as well as various species of the family Legumonisae, belonging mainly to two genera, namely: *Gastrolobium*, and *Oxylobium*) also contain fluoroacetate (Harper & O'Hagan, 1994; O'Hagan & Harper, 1999).

A salt derived from fluoroacetate known as sodium monofluoroacetate (1080) has been developed as a pest control. 1080 has been shown to be toxilogically and chemically identical to fluoroacetate. It has been used to kill rodents in the United States of America (USA) and possums in New Zealand. In the USA its use has been restricted for protection of cattle and sheep against coyotes. Fluoroacetate is converted into fluorocitrate in the body of animals where it inhibits energy production in the Krebs cycle. This results in citrate accumulation in the blood, and eventual death (Eason, 2002).

It has been demonstrated that the bacterium *S. cattleya* produce both 4-fluorothreonine and fluoroacetate in the presence of inorganic fluoride (Figure 1.2). During studies on these compounds a striking similarity has been discovered between the labeling pattern of C-1 and C-2 of fluoroacetate and the C-3 and C-4 of fluorothreonine. This indicates a common origin for both compounds and a single enzyme. The most likely prescursor for both compounds was fluoroacetylaldehyde (Harper & O'Hagan, 1994; O'Hagan & Harper, 1999; Murphy *et al*., 2003).

The initial step in the formation of fluorinated compounds have been studied in the bacterium *S. cattleya*. It was determined that a fluorinase enzyme converts a fluoride ion and S-adenosylmethionine (SAM) into 5-fluoro-5-deoxyfluoroadenosine (5-FDA) (Figure 1.3). 5-FDA in turn is converted into the precursor fluoroacetaldehyde, which in turn is converted into fluoroacetate or 4-fluorothreonine (O'Hagan *et al*., 2002).

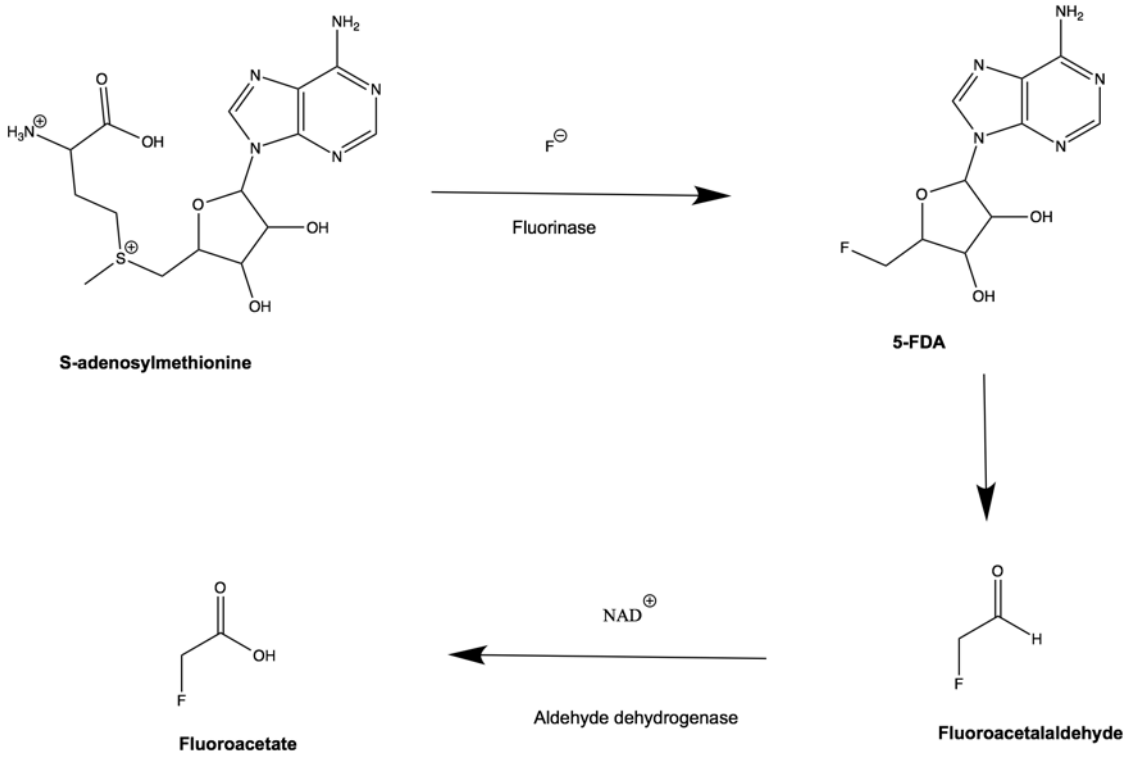

Figure 1.3: Biosynthesis of fluoroacetate from SAM, yieldind 5-FDA and fluoroacetaldehyde as intermediatery molecules (O'Hagan *et al*., 2002)

In later studies it was found that there are in fact two enzymes in *S. cattleya* responsible for forming fluoroacetate and 4-fluorothreonine from fluoroacetaldehyde. The first enzyme form fluoroacetate from fluoroacetaldehyde and NAD^+, indicating that this enzyme is an aldehyde dehydrogenase (Figure 1.3). Through substrate specificity studies it has been determined that the enzyme has a much higher affinity for fluoroacetaldehyde than for any other aldehyde. A second enzyme is responsible for the formation of 4-fluorothreonine. It was previously reported that 4-fluorothreonine is formed from fluoroacetaldehyde and glycine. However through labeling studies it has been determined that glycine do not play a role in the synthesis of 4-fluorothreonine. The molecule is formed from fluoroacetaldehyde and L-threonine by a threonine transaldolase (Murphy *et al*., 2003).

1.3 Other compounds isolated from Dichapetalaceae

Many members of the Dichapetalaceae family have been reported to be highly toxic, specifically due the presence of fluorinated compounds, of which the most common toxic compounds being fluoro-carboxylic acids (Addae-Mensah *et al*., 1996).

Except for the fluorine toxicity not much else is known about this plant family. In previous studies N-methylserine and N-methylalanine have been isolated form *Dichapetalum cymosum*. N-methylserine has never before been isolated from plants, it was further determined that similarly to fluoroacetate the concentration of N-methylserine is much lower in older leaves than it is in younger leaves. The Australian plant *Acacia georginae* also known to contain fluoroacetate did not contain N-methylserine, thereby ruling out the possibility that the metabolism of the two compounds are linked (Eloff, 1969).

In an attempt to gain further knowledge in the non-fluorinated compounds of *Dichapetalum* spp., Achenbach *et al*. (1995), isolated a new compound, belonging to the triterpenoid group, known as dichapetalin A (Figure 1.4), from *Dichapetalum madagascariensis*. This species is one of the lesser toxic members of the plant family, and is known to be traditionally used in folk medicine for the treatment of jaundice, sores and urethritis (Osei-Safo *et al*., 2012). Since then dichapelins A-H and M have been discovered in *D. madagascariensis* (Addae-Mensah *et al*., 1996; Osei-Safo *et al*., 2008). Four dichapetalins have been discovered in *D. gelonioides*, namely I, J, K and L (Fang *et al*., 2006). Six more dichapetalins namely dichapetalins N-S have been isolated from *D. mombuttense, D. zenkeri* and *D. leucosia*. Five dichapetalin-derived triterpenoids, known as the acutissimatriterpenes have been isolated form a non-Dichapapetalaceae member, *Phyllanthus acutissima* (Long *et al*., 2013).

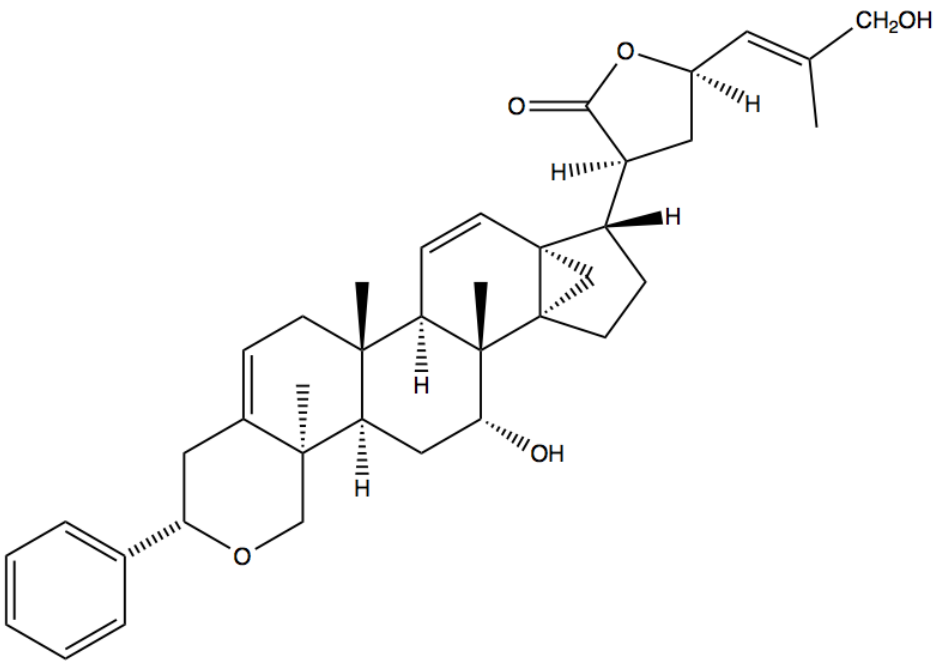

Figure 1.4: Structure of dichapetalin A (Long *et al*., 2013)

The basic structure of dichapetalins consist of two main parts, namely the dammarane-triterpene skeleton and a C6-C2 unit. The C6-C2 unit attaches to ring A of the dammarane skeleton to form a phenylpyrano moiety (Figure 1.5) (Osei-Safo *et al*., 2012)

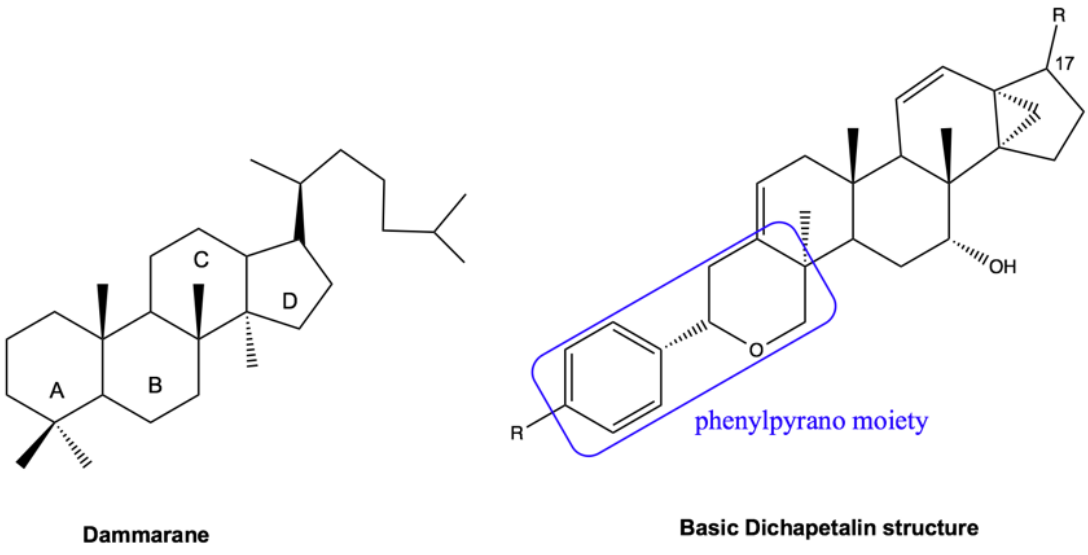

Figure 1.5: Basic dichapetalin structure, consisting of a C6-C2 unit attached to a dammarane (Osei-Safo *et al*., 2012)

The dichapetalins thus far discovered contains either a lactone group or a methyl ester attached to C-17 (Figure 1.6). Thus far biological activity have only been observed in dichapetalins comprising a lactone side chain. Dichapetalins containing the lactone side chain are dichapetalins A, B, I, J, K, L, M, N and P (Osei-Safo *et al*., 2012; Long *et al*., 2013).

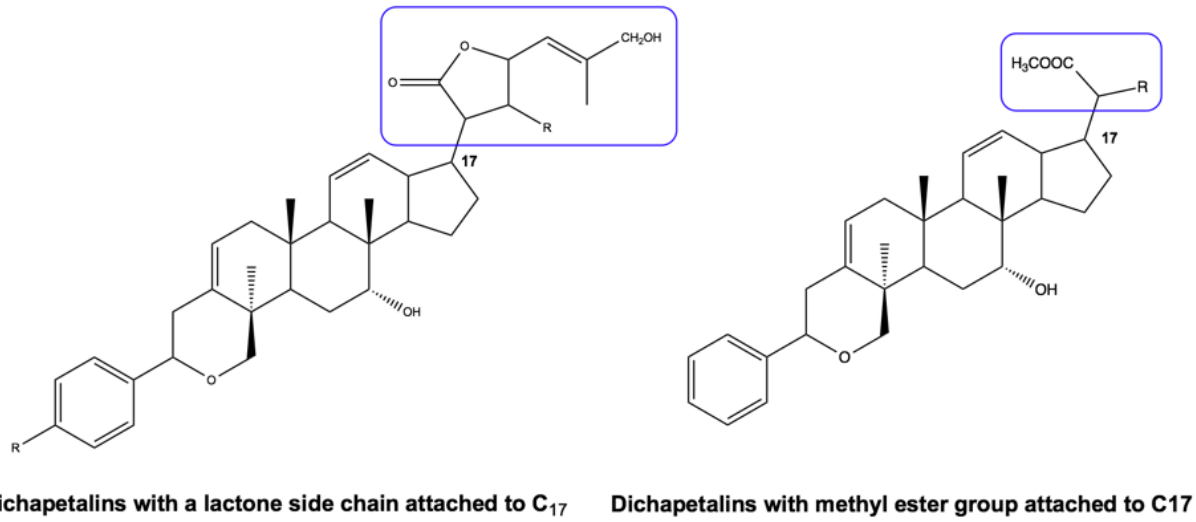

Dichapetalins with a lactone side chain attached to C_{17} **Dichapetalins with methyl ester group attached to C17**

Figure 1.6: The two different dichapetalin structures, giving rise to either toxic or non toxic dichapetalins. (Osei-Safo *et al*., 2012).

Toxicity studies thus far have been conducted against brine shrimp larvae and various cancer cell lines. Dichapetalin A showed a n LC_{50} of 0.31 µg/ml, while dichapetalin M was 28 times more active with an LC_{50} of 0.011 µg/ml. (Addae-Mensah *et al*., 1996; Osei-Safo *et al*., 2008).

Dichapetalin A activity against various cancer cell lines varied greatly, L1210 Murine leukemia cells were highly sensitive with an EC_{90} of less than 0.0001 µg/ml. Human KB carcinoma and Murine bone marrow cells only showed an effect when concentrations four orders of magnitude higher were tested (Addae-Mensah *et al*., 1996). Fang *et al*. (2006) tested dichapetalins A, I, J, K an L against various cancer cell lines, dichapetalins A, I and J

showed significant activity against the SW626 human ovarian cencer cell line, with IC_{50} values between 0.2 and 0.5 µg/ml. *In vivo* studies of dichapetalin A against LNCaP (human-dependant prostate), SW 626 (ovarian adenocarcinoma), MCF-7 (breast adenocarcinoma) and Lu1 (Lung) cell lines showed no significant growth inhibition. The loss of activity of dichapetalin A *in vivo* might be a result of enzymatic activity, in which case the lactone ring might be hydrolyzed to form an open carboxylic acid chain (Osei-Safo *et al*., 2012).

Long *et al*. (2013) tested dichapelin A against 16 cancer cell lines (Table 1.1). Human colorectal carcinoma (HCT116) was the most sensitive with an EC_{50} of 2.5 x 10^{-7} M, while the human melanoma (WM266-4) cell line showed the most resistance with an EC_{50} of 1.7 x 10^{-5} M. These cell lines were then used to test for cytotoxicity of dichapetalins B, C, I, L, M, O, P, Q, R and S. All dichapetalins tested showed activity against HCT116. Dichapetalin M was the most active with an EC_{50} of 9.9 x 10^{-9} M against HCT116 and EC_{50} = 7.8 x 10^{-8}M for MW 266-4 (Table 1.2).

Table 1.1: Dichapetalin A tested for cytotoxicity against 16 cancer cell lines (Long *et al.*, 2013)

Cell Line	**Tumor Types**	**Dichapetalin A EC_{50} (M)**
HCT-116	Human colorectal carcinoma	2.5 x 10^{-7}
NAMALWA	Human Burkitt's lymphoma	3.0 x 10^{-7}
SKOV-3	Human ovarian adenocarcinoma	8.6 x 10^{-7}
HOP-62	Human lung cancer	9.1 x 10^{-7}
A549	Human lung adenocarcinoma	1.2 x 10^{-6}
NCI-H460	Human prostrate carcinoma	1.4 x 10^{-6}
T47D	Human breast ductal carcinoma	2.3 x 10^{-6}
BxPC3	Human pancreatic adenocarcinoma	3.0 x 10^{-6}
KM-12	Human colon carcinoma	8.7 x 10^{-6}

OvcAR	Human ovarian adenocarcinoma	1.0×10^{-5}
HL-60	Human acute promyelocytic leukemia	1.1×10^{-5}
Colo-205	Human colorectal adenocarcinoma	1.2×10^{-5}
TK10	Human renal adenocarcinoma	1.2×10^{-5}
MDAMB231	Human breast adenocarcinoma	1.3×10^{-5}
DUI 145	Human prostrate carcinoma	1.3×10^{-5}
WM 266-4	Human melanoma	1.7×10^{-5}

Table 1.2: Cytotoxic activities of Dichapetalins agains the HCT 116 and MW 266-4 cancer cell lines (Long *et al*., 2012)

Dichapetalin derivatives	HCT-116 EC_{50} (M)	WM 266-4 EC_{50} (M)
A	2.5×10^{-7}	1.7×10^{-5}
B	8.1×10^{-8}	3.4×10^{-7}
C	5.0×10^{-7}	2.5×10^{-6}
I	2.8×10^{-7}	1.0×10^{-5}
L	6.8×10^{-7}	3.1×10^{-6}
M	9.9×10^{-9}	7.8×10^{-8}
N	9.2×10^{-8}	1.5×10^{-6}
O	8.9×10^{-7}	8.4×10^{-6}
P	5.8×10^{-8}	2.3×10^{-7}
Q	2.5×10^{-6}	2.7×10^{-5}
R	4.2×10^{-6}	3.1×10^{-5}
S	4.5×10^{-7}	1.3×10^{-6}

Dichapetalins B and P also exhibited good cytotoxic results against these cell lines. Dichapetalin M (Figure 1.7) has some modifications which up until the discovery of dichapetalin P has not been observed in other dichapetalins, these include an oxygenation

of C6 of the basic skeleton as well as a spiroketal moiety and an acetoxy group on C25 of the lactone side chain (Osei-Safo *et al*., 2008). The nature of the side chains of dichapetalin B and M, suggests a possible conversion of dichapetalin B to dichapetalin M (Osei-Safo *et al*., 2012). The structure of dichapetalin P closely resembles that of dichapetalin M, it also contains the spiroketal moiety and the C25 acetoxy goup but lacks an oxygen on C6 of the basic skeleton (Long *et al*., 2013). It is speculated that the spiroketal bicyclic side chain of dichapetalin M and P might result in a higher stability of the lactone ring, suggesting positive cytotoxic results against cancer cell lines *in vivo* (Osei-Safo *et al*., 2012).

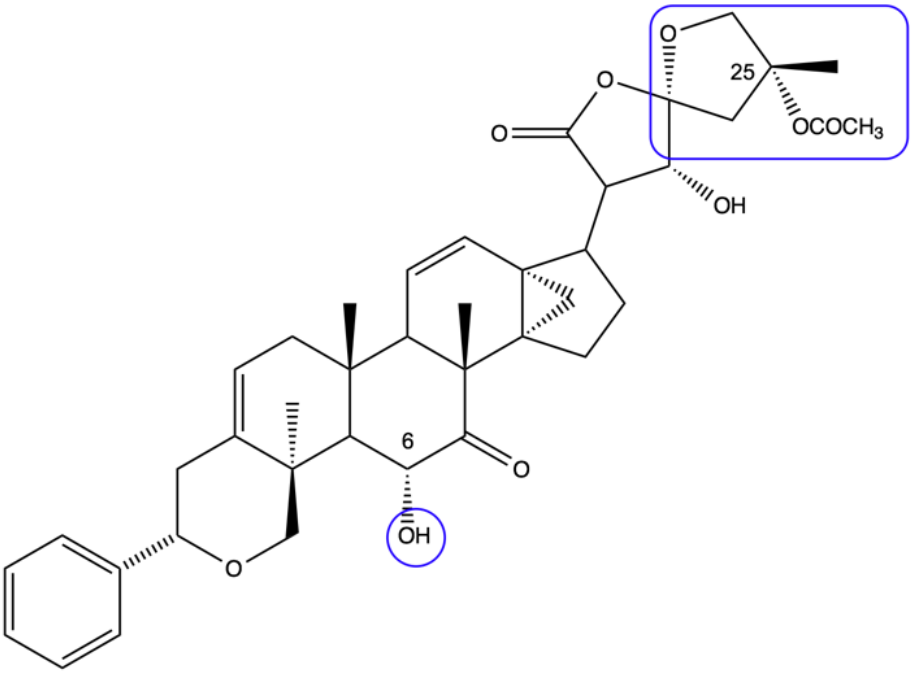

Figure 1.7: Chemical structure of dichapetalin M (Osei-Safo *et al*., 2012)

Most research done regarding the Dichapetalaceae family have been done on *Dichapetalum*. Thus far no extensive research have been done regarding the *Tapura* genus. Schwikkard *et al*. (1998), isolated compounds from *Tapura fischeri* in an attempt to possibly isolate dichapetalins form this genus. No dichapetalins were isolated, however four novel pheophytins were isolated (Figure 1.8). These are 17^3-ethoxyphaeophorbide a, phaeophytin

a-13^2-carboxylic acid, 17^3-ethoxy-phaephorbide a-13^2-carboxylic acid and 17^3-ethoxyphaeophytin b. They also isolated their known compound phaeophytin a (Schwikkard *et al*., 1998).

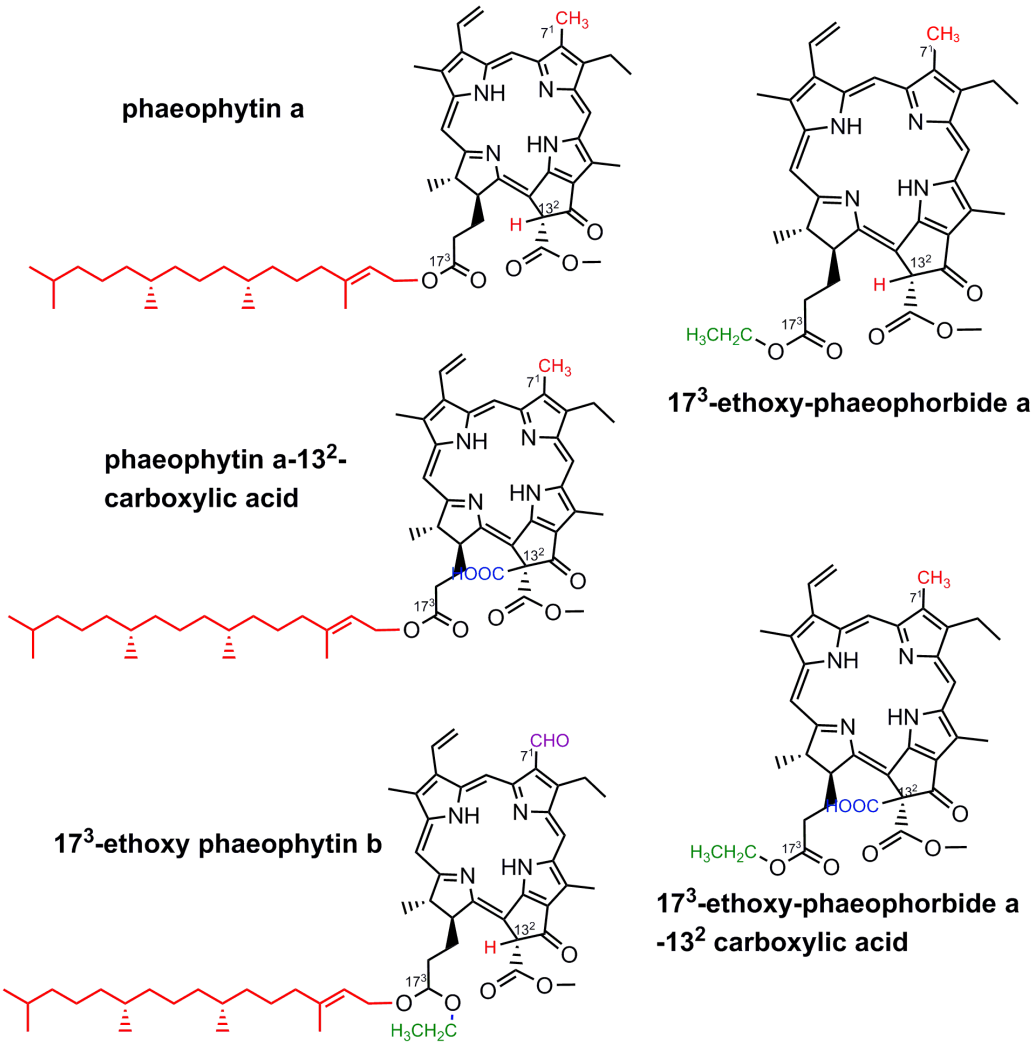

Figure 1.8: Phaeophytin a as well as four novel phaeophytins isolated from *T. fischeri* (Adapted from Souza Chaves *et al*., 2013).

1.4 Endophytes and plants

Endophytes are organisms which live in the intercellular space (apoplast) or within cells (symplast) of the host organism (Gliménez *et al*., 2007). They have been isolated from all plant organs including the seeds (Figure 1.9) (Ryan *et al*., 2008). They can be fungal or bacterial organisms which cause no apparent damage to the host (Gliménez *et al*., 2007). Endophytes can be classified into facultative and obligate endophytes. Obligate endophytes are completely dependent on the host for growth and survival, while facultative endophytes can exist outside of the host for a certain stage of their lifecycle (Hardoim *et al*., 2008)

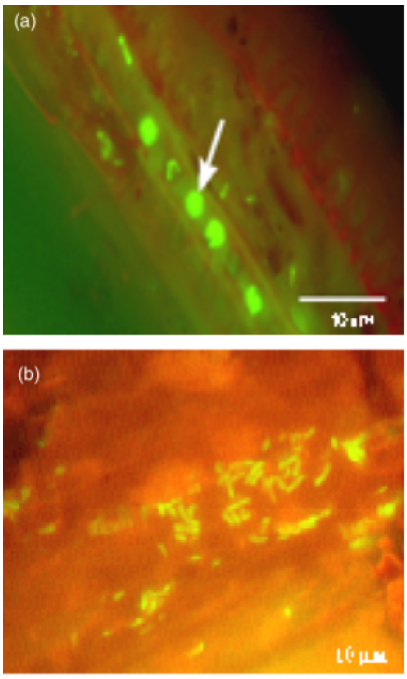

Figure 1.9: The endophyte *Pseudomonas putida* in different regions of the plant. A) *P. putida* in the xylem tracheid pits of the poplar trees. B) *P. putida* within the root cortex of the pea plant (Ryan *et al*., 2008).

Endophytic bacteria have been isolated from both monocots and dicots, both woody tree species (oak and pear) and herbaceous species (maize). Different endophytes can result in different advantages for the plant (Ryan *et al*., 2008).

Some endophytes can act as biocontrol agents by controlling plant pathogens, insects or nematodes. It has been shown that some bacterial endophytes prevent disease development by producing novel compounds and antifungal metabolites. This characteristic of certain endophytes creates the opportunity for many novel medicinal compounds to be discovered. Some soil bacteria of the genera *Burkholderia* and *Bacillus* also include endophytic members. These genera are known for the wide range of secondary compounds that they produce, which include antibiotics, anticancer drugs and antifungal agents (Ryan *et al*., 2008).

In other instances endophytes can increase seedling emergence, promote plant establishment under adverse conditions or increase plant growth (Ryan *et al*., 2008). It is extremely difficult to culture certain plant species in the absence of bacteria, indicating a role for endophytes in plant growth. For some plants the presence of endophytes is essential for their growth and establishment in a specific environment (Hardoim *et al*., 2008).

Plants with endophytes normally have an advantage over those plants without endophytes, while endophytes profit from the plant due to the enhanced availability of nutrients. The plant-endophyte relationship is therefore generally a mutualistic symbiotic relationship. However some endophytic fungi can cause harm to the host during stressful conditions. This scenario refers to an antagonistic relationship between the fungus and the host (Gliménez *et al*., 2007). In an extreme view plant pathogens can also be classified as endophytes, since they can occur in some instances in the avirulent form in plants (Hardoim *et al*., 2008).

1.5 Aim & Objectives

The main aim of the study was to identify the toxic compounds present in *T. fischeri* and to establish their toxicity towards bacteria and HIV.

The objectives of the study were as follows:

- Identify the fluorinated compound in *T. fischeri*.
- Establish the relationship between the compound and endophytes capable of producing fluorinated compounds.
- Determine the toxicity of *T. fischeri* towards micro-organisms through bacterial assays.
- Isolate other compounds responsible for the toxicity of the plant.
- Establish the similarity between plants growing in different regions, with special focus on the fluorinated compounds.

1.5.1 Hypothesis

Fluorinated compounds are also present in *Tapura fischeri*, a characteristic of many Dichapetalaceae members.

1.6 References

Achenbach, H., Asunka, S.A., Waibel, R., Addae-Mensah, I., Oppong, I.V., 1995. Dichapetalin A, A Novel Plant Constituent from *Dichapetalum madagascariense* with Potential Antineoplastic Activity. Natural Products Letters 7(2), 93-100

Addae-Mensah, I., Waibel, R., Asunka, S.A., Oppong, I.V., Achenbach, H., 1996. The Dichapetalins – A new class of triterpenoids. Phytochemistry 43(3), 649-656

African Plants Database., 2012 *Tapura fischeri* Engl. Conservatoire et Jardin botaniques & South African National Biodiversity Institute. [Online available: http://www.ville-ge.ch/musinfo/bd/cjb/africa/details.php?langue=an&id=13406] [Last accessed: 25/03/14]

Boon, R., 2010. Pooley's Trees of Eastern South Africa. Flora and Fauna Publications Trust, Durban.

Coates Palgrave, K., 2002. Trees of Southern Africa. Struik Publishers, Cape Town.

Cornejo, F., Janovec, J., 2010. Seeds of Amazonia Plants. Princeton University Press, New Jersey.

Eason, C., 2002. Sodium monofluoroacetate (1080) risk assessment and risk communication. Toxicology 181-182, 523-530.

Eloff, J.N., Grobbelaar, N., 1969. Isolation and Characterization of N-methyl- L-serine from *Dichapetalum cymosum*. Phytochemistry 8, 201-204

Fang, L., Ito, A., Chai, H.B., Mi, Q., Jones, W.P., Madulid, D.R., Oliveros, M.B., Gao, Q., Orjala, J., Farnsworth, N.R., Soejarto, D.D., Cordell, G.A., Swanson, S.M., Pezzuto, J.M., Kinghorn, A.D., 2006. Cytotoxic Constituents from the Stem Bark

of *Dichapetalum gelonioides* Collected in the Phillippines. Journal of Natural Products 69, 332-337

Gliménez, C., Cabrera, R., Reina, M., González-Coloma, A., 2007. Fungal Endophytes and their role in Plant Production. Current Organic Chemistry 11, 707-720.

Hardoim, P.R., van Overbeek, L.S., van Elsas, J.D., 2008. Properties of bacterial endophytes and their proposed role in plant growth. Trends in Microbiology 16, 463-471.

Harper, D.B., O'Hagan, D., 1994. The Fluorinated Natural products. Natural Products Report 11, 123-133.

Kellerman, T.S., Coetzer, J.A.W., Naude, T.W., Botha. C.J., 2005. Plant Poisonings and mycotoxicoses of Livestock in Southern Africa. Oxford University Press Southern Africa, Cape Town.

Long, C., Aussagues, Y., Molinier, N., Marcourt, L., Vendier, L., Samson, A., Poughon, V., Chalo Mutiso, P.B., Ausseil F., Sautel, F., Arimondo, P.B., Massiot, G., 2013. Dichapetalins from *Dichapetalum* species and their cytotoxic properties. Phytochemistry 94, 184-191.

Murphy, C.D., Schaffrath, C., O'Hagan, D., 2003. Fluorinated natural products: the biosynthesis of fluoroacetate and 4-fluorothreonine in *Streptomyces cattleya*. Chemosphere 52, 455-461.

O'Hagan, D., Harper, D.B., 1999. Fluorine containing natural products. Journal of Fluorine Chemistry 100, 127-133.

O'Hagan, D., Schaffrath, C., Cobb, S.L., Hamilton, J.T.G., Murphy, C.D., 2002. Biosynthesis of an organofluorine molecule. Nature 416, 279.

Osei-Safo, D., Chama, M.A., Addae-Mensah, I., Waibel, R., Asomaning, W.A., Oppong, I.V., 2008. Dichapetalin M from *Dichapetalum madagascariensis*. Phytochemistry Letters 1, 147-150.

Osei-Safo, D., Chama, M.A., Addae-Mensah, I., Waibel, R., 2012. The Dichapetalins - Unique Cytotoxic Constituents of the Dichapetalaceae, Phytochemicals as Nutraceuticals - Global Approaches to Their Role in Nutrition and Health, Dr Venketeshwer Rao (Ed.), ISBN: 978-953-51-0203-8, InTech, [Online available: http://cdn.intechopen.com/pdfs-wm/32905.pdf] [Last accessed: 27/06/14]

Palmer, E.,Pitman, N., 1972. Trees of Southern Africa: covering all known indigenous species in the Republic of South Africa, South-West Africa, Botswana, Lesotho & Swaziland. A.A. Balkema, Cape Town.

Pohlit, A., Quignard, E., Nunomura, S., Tadei, W., Hidalgo, A., Pinto, A., dos Santos, E., de Morais, S., Saraiva, R., Ming, L., Alecrim, A., Ferraz, A., Pedroso, A., Diniz, E., Finney, E., Gomes, E., Dias, H., de Souza, K., de Oliveira, L., Don, L., Queiroz, M., Henrique, M., dos Santos, M., Lacerda Junior, O., Pinto, P., Silva, S., Graca, Y., 2004. Screening of plants found in the State of Amazonas, Brazil for larvicidal activity against *Aedes aegypti* larvae. Acta Amazonica 34, 97-105.

Pooley, E., 1993. The complete field guide to trees of Natal, Zululand and Transkei. Flora Publications Trust, Durban.

Quignard, E.L.J., Nunomura, S.M., Pohlit, A.M., Alecrim, A.M., Pinto, A.C.D.S., Portela, C.N., De Oliveira, L.C.P., Don, L.D.C., Rocha E Silva, L.F., Henrique, M.C., Dos

Santos, M., Pinto, P.D.S., Silva, S.G., 2004. Median lethal concentrations of amazonian plant extracts in the brine shrimp assay. Pharmaceutical Biology 42, 253-257.

Ryan, R.P., Germaine, K., Franks, A., Ryan, D.J., Dowling, D.N., 2008. Bacterial endophytes: recent developments and applications. FEMS Microbiology Letters 278, 1-9.

Schwikkerd, S.L., Mulholland, D.A., Hutchings, A., 1998. Phaeophytins from *Tapura fischeri*. Phytochemistry 49(8), 2391-2394

Souza Chaves, O., Gomex, R.A., De Andrade Tomaz, A.C., Fernandez, M.G., Des Graças Mendes Jr, L., De Fatima Agra, M., Braga, V.A., De Souza, M.D.F.V., 2013. Secondary metabolites from *Sida rhombifolia L*. (Malvaceae) and the vasorelaxant activity of cryptolepinone. Molecules 18(3), 2769-2777

Chapter 2:

Fluorinated compounds of *Tapura fischeri*

2.1 Introduction

T. fischeri is a member of the family Dichapetalaceae, the same family to which *Dichapetalum cymosum* belongs. The toxic compound present in *D. cymosum* is the fluorinated compound known as mono-fluoroacetate (MFA). Only a single reference to the presence of fluoroacetate in *T. fischeri* has been reported thus far (personnel communication) (Kellerman *et al*., 2005).

Originally detection of fluorine compounds was done using gas chromatography (GC), however in 1972 it was suggested that ^{19}F NMR (nuclear magnetic resonance) could also be used. Although it is not as sensitive as GC, it is easier to use in practice, and it can be used to detect fluorinated compounds other than fluoroacetate (Baron *et al*., 1986). Fluorine contains only a single naturally occurring isotope, with a spin quantum number of one half (I = ½), the same as hydrogen. The fluorine coupling constants and chemical shifts are also at least an order of magnitude larger that the corresponding proton analogues. These characteristics of fluorine are what make ^{19}F NMR so effective (Harper & O'Hagan, 1994).

In this part of the study, it was determined whether the fluorinated compound; mono-fluoroacetate is present in *T. fischeri*, or a different fluorinated compound. This was done using ^{19}F NMR. If monofluoroacetate is present in the extract a peak at about -216 ppm will be expected (Baron *et al*., 1986). Gas chromotography will be used together with ^{19}F NMR to identify the compound if the fluorinated compound is not monofluoroacetate.

2.2 Methodology

2.2.1 Plant extraction and NMR

Plant material was collected at two sites, from the Onderstepoort (OP) campus of the University of Pretoria as well as the Lowveld Botanical Garden (LBG) in Mbombela (Nelspruit). At OP only leaf material were collected, while both leaves and stems were collected form the LBG. In previous toxicity studies on *T. amazonica*, the highest toxicity was obtained with methanol extractions (Pohlit *et al*., 2004; Quignard *et al*., 2004), for this reason methanol was used as extraction solvent. The plant material (3.0 g of each plant) was extracted with 100 % methanol using a Buchi Speedextractor E-916. The extraction was done at a temperature of 50 °C and a pressure of 100 kPa, the extract was then dried using a rotavapor to form an extract with a viscous like consistency. The OP and LBG plant material were extracted separately, to determine whether the fluorinated compound is present in plants from both regions.

Leave material was collected a second time from OP and first extracted with 100 % methanol, followed by 100 % distilled water, monofluoroacetate (MFA) can be effectively extracted from plant material using water (Vickery *et al*., 1972). For this reason the plant material was also extracted with water, to ensure the extraction of MFA if the compound is present in *T. fischeri*. The extraction was once again done at a temperature of 50 °C and a pressure of 100 kPa, using the Buchi Speedextractor E-916. The extracted material was again dried with a rotavapor. The methanol and water extracts were dried separately.

The extracts were prepared for ^{19}F NMR using D_2O (deuterium oxide) as solvent. The extracted material was allowed to dissolve in 1ml of D_2O. The NMR was set up for fluorine

NMR. The extracts were scanned 16 000 times to determine the presence of mono-fluoroacetate or another fluorinated compound.

After it was determined that a fluorinated compound are present in both plant extracts, plant samples were prepared for gas chromatography mass spectrometry (GCMS).

2.2.2. Gas chromatography mass spectrometry

Fresh leaf material was again collected from OP and the LBG. Plant material was extracted with 100 % methanol using a Buchi Speed extractor E-916, as described previously. Each extraction tube (40 ml) contained between 2.93 g and 3.01 g fresh leaf material. The extracted samples were then dried individually and treated as separate samples.

Trifluoroacetate (TFA) standards and samples were derivatized to the methyl ester, forming methyl ester trifluoroacetate (MTFA) prior to analysis on the GCMS. Trifluoracetic acid standards were prepared in various concentrations to obtain the mass spectra, and produce a quantification curve. Six standards (0.25 mg/ml, 0.5 mg/ml, 0.75 mg/ml, 1 mg/ml, 1.5 mg/ml and 2.0 mg/ml) were used to produce a quantification curve. The standards were derivatized by dissolving the TFA in water to obtain the desired concentration, 500 µl of each concentration were then transferred to head space GC (HS) vials, this was followed by the addition of 200 µl methanol (MeOH) and 200 µl concentrated sulphuric acid (H_2SO_4). The samples were placed in an 80 °C water bath for one hour, and allowed to cool down before GCMS analysis (Adapted from Bayer *et al*., 2002).

Samples from both OP and LBG were prepared by dissolving 31.0 mg and 29.1 mg of extract respectively in 2.0 ml MeOH, of which 500 µl was placed in a HS vial, this was followed by the addition of 500 µl concentrated H_2SO_4. For each location two HS vial

samples were prepared. The vials were sealed, and placed in the 80 °C water bath for an hour.

Standards and samples were analyzed using a Shimadzu QP2010 Ultra GCMS, fitted with an Agilent HP PLOT/Q column (30 m x 0.320 mm diameter; film thickness of 20.0 µm). The oven temperature program started at 100 °C, increased by a heating rate of 15 °C/min to 220 °C where it was held for two minutes. The injector temperature was set at 250 °C, and the column pressure at 100 kPa. Helium was used as the carrier gas with a flow rate of 3.59 ml/min. 1 µl of sample was injected and ran with split injection with a split ratio of 7:1. The mass spectrum was operated on the SIM EI^+ mode, with both the ion source and interface temperatures set at 250 °C (Adapted from Bayer *et al.,* 2002). The ions monitored were *m/z* 59, 69, 99 as these are the most prominent ions in the MTFA mass spectrum (Zehavi & Seiber, 1996).

2.3 Results and discussion

2.3.1 NMR spectroscopy of plant extracts

The NMR results (Figure 2.1) showed fluorine peaks at -76 ppm for both collection sites. These results showed no signs of monofluoroacetate (MFA) being present in the plant, since a MFA peak would have been expected at -216 ppm (Baron *et al*., 1986).

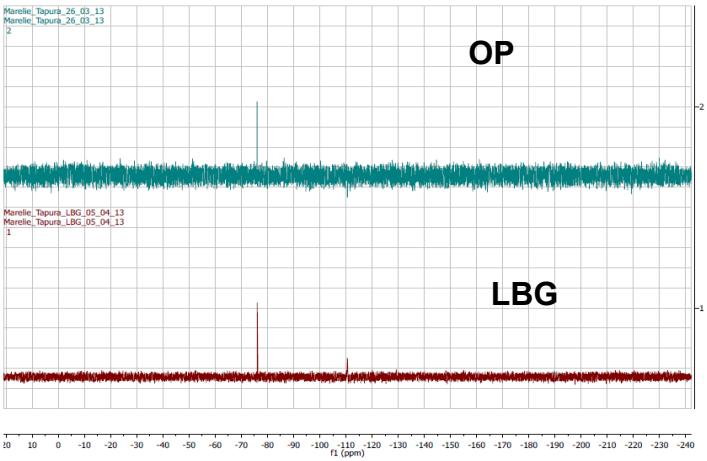

Figure 2.1: 19F NMR peak at -76 ppm, obtained from *T. fischeri* extracts, from both the OP as well as the LBG collection sites.

The second extraction was done with young leaves, and a serial extraction of 100 % methanol and 100 % water was done, using the same leaves. This was done to ensure that all of the fluorinated compounds are extracted. Although methanol effectively extracted the fluorinated compound, it was unsure whether MFA, if present in the plant, can be effectively extracted with methanol, since it is known to be very soluble in water (Vickery *et al.*, 1972).

From Figure 2.2 it is clear that only the methanol extract (green) contain a fluorinated compound, with the single peak again at -76 ppm. The water extract (red) seems to show a peak at -110 ppm, this however is an artifact present in most NMR scans, a small peak at the same place can be seen in the methanol extract as well as in the two scans shown in Figure 2.1, and therefore do not indicate the presence of a fluorinated compound. At the -216 ppm region, no triplet is observed, which would be the expected result if MTFA were present in the extract.

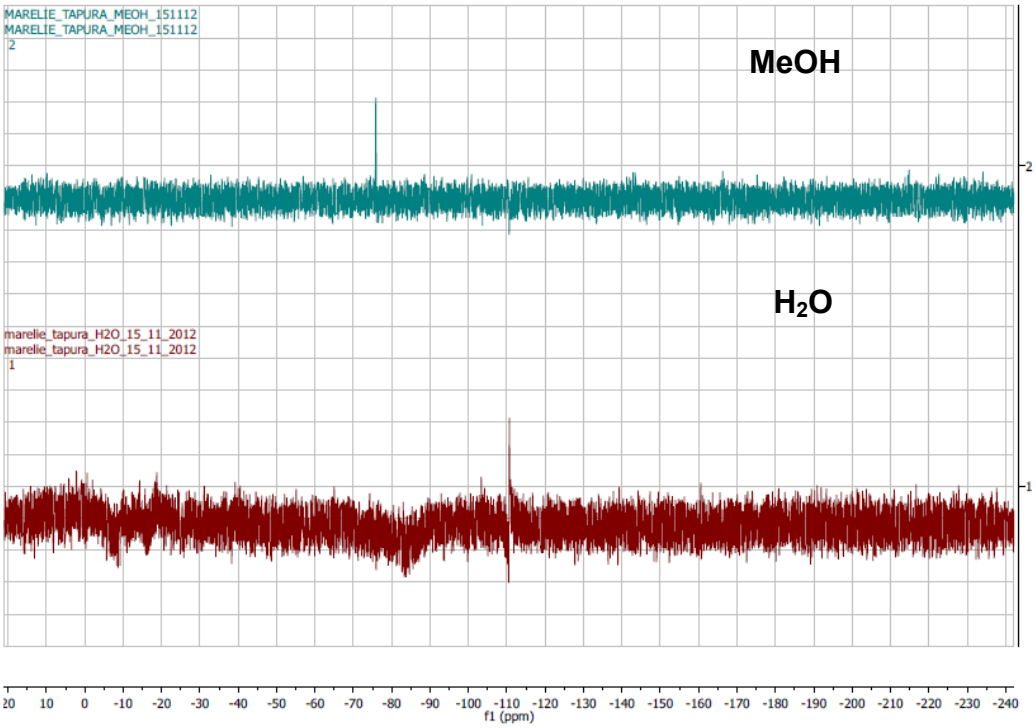

Figure 2.2: Methanol and water extracts of *T. fischeri* leaves indicating the presence of the fluorinated compound at -76 ppm only in the methanol extract. The peak seen in the water extract at -110 ppm is a general artifact present in most fluorine scans.

Only a single fluorinated compound is therefore present in *T. fischeri*, with no fluoroacetate being extracted in either methanol or water. The compound present in *T. fischeri* might be trifluorinated, due to the occurrence of the single peak with a chemical shift of -75.87 ppm, which corresponds to the trifluorinated compounds in Figure 2.3 (CF_3-C forming peaks -50 to -90 ppm). Figure 2.3 shows the chemical shifts of fluorinated compounds, from the figure it can be seen that al trifluorinated compounds (CF_3-C, CF_3-vinylic and CF_3-aryl) have chemical shifts close to -75 ppm. Trifluoroacetate with a chemical shift of -76.55 ppm also suggests the presence of a trifluorinated compound in *T. fischeri* (Dolbier Jr, 2009).

Both CF_2=C and Vinylic-F (Figure 2.3) also form peaks in the region of -75 ppm. This suggests that the fluorine containing compound in *T. fischeri* could also be a di-fluorinated

compound double bonded to carbon, or a mono-fluorine bound to a vinylic group (Dolbier Jr, 2009).

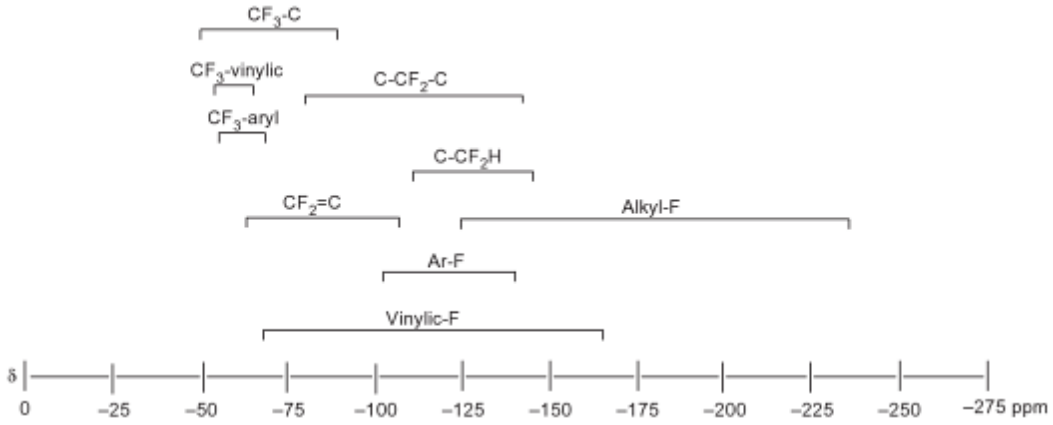

Figure 2.3: An overview of fluorine chemical shifts, relative to $CFCl_3$ with a chemical shift of 0 ppm (Dolbier Jr, 2009).

Focus were then placed on isolating the unidentified fluorinated compound, however it was observed that the fluorinated compound seemed to disappear after about a month of storage. Since no fluorinated peaks are observed after such time, it was established that the fluorinated compound are not broken down, but are volatile. Since trifluoroacetate (TFA) also form a peak at -76 ppm (Dolbier Jr, 2009) and volatile, it was hypothesized that the unknown compound in *T. fischeri* might be TFA.

^{19}F NMR of *T. fischeri* and TFA, both show a single peak both at -76 ppm, (Figure 2.4). Since the peaks are so similar and the concentration of TFA in *T. fischeri* relatively low, it is difficult to accurately determine whether the compound in *T. fischeri* is TFA for certain, and was therefore confirmed using GCMS.

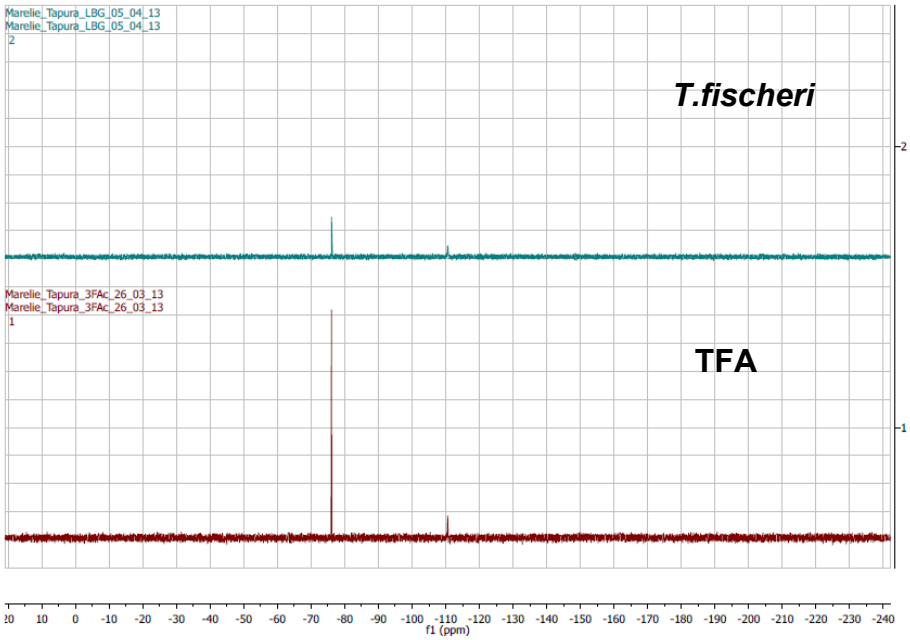

Figure 2.4: ^{19}F NMR indicating a single peak at -76 ppm for both the fluorinated compound in *T. fischeri* as well as TFA.

2.3.2 Gas chromatography mass spectrometry

The retention time for MTFA standards was determined to be 4.6 minutes, as is shown in Figure 2.5.

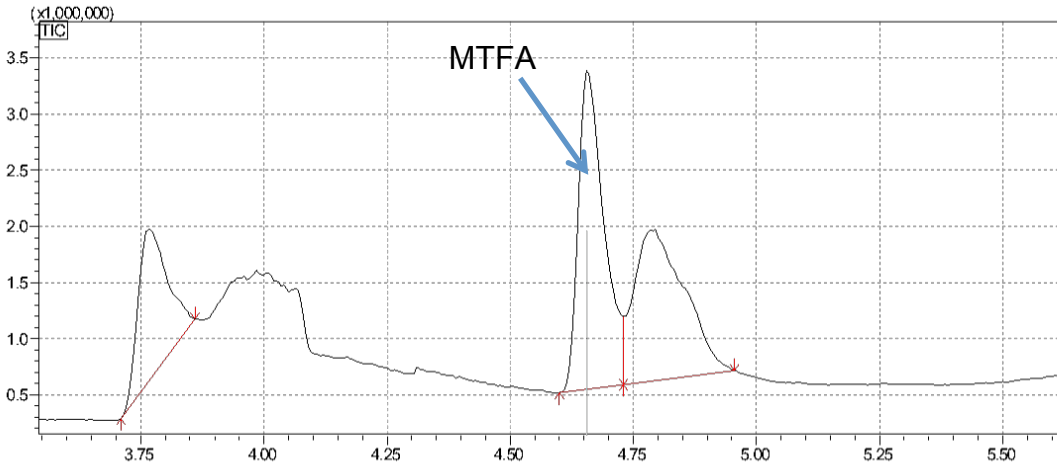

Figure 2.5: MTFA formed during the derivatization of the TFA standards eluted after 4.6 minutes.

The mass spectrum breakdown pattern of MTFA can be seen in Figure 2.6, with *m/z* 59, 69 and 99 being the most abundant ions.

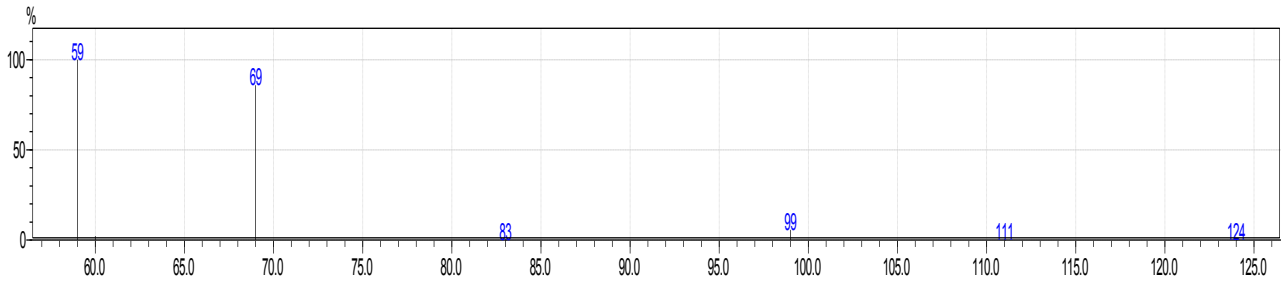

Figure 2.6: Mass spectrum of MTFA derivatized from the standards.

The molecular mass of MTFA is 128 Da, and the fractionation to the three most prominent ions (*m/z* 59, 69 and 99) can be seen in Figure 2.7. The CF_3 group is removed to form the *m/z* 59 ion ($COOCH_3$). The other two ions form by a different fractionation pattern where a H-atom is first lost to form *m/z* 127. In order to form *m/z* 99, 28 units need to be lost from *m/z* 127, for this to occur an O-atom (16 Da) bound to C-atom (12 Da) need to be removed. This is achieved by the removal of the carbonyl carbon (C=0), through the migration of CF_3 from this carbon to the ether oxygen forming CF_3OCH_2. The loss of OCH_2, result in the formation of the *m/z* 69 ion (CF_3) (Sekigutchi *et al.,* 1998). It should be considered that the formation of *m/z* 69 might also derive from the removal of the *m/z* 59 ($COOCH_3$) ion.

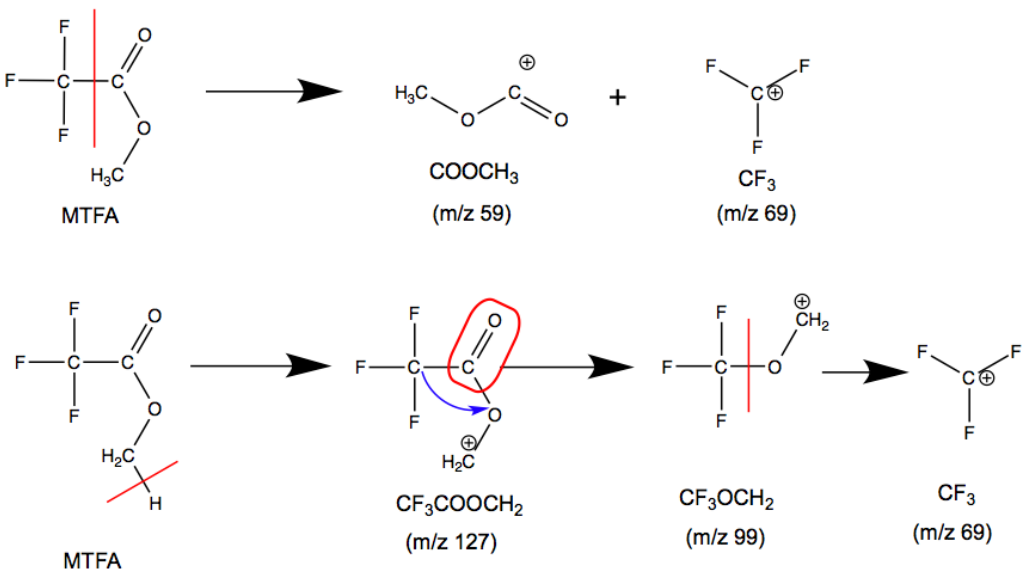

Figure 2.7: Fractionation pattern of MTFA to form the most abundant ions (Adapted from Sekigutchi *et al.,* 1998).

The standards were plotted onto a graph by using the concentrations for the x-axis and the area under the curve for the y-axis. The 2 mg/ml concentration formed an outlier and was removed, in order to form a better quantification curve. The best-fit line (R^2-value of 0.99454) was drawn through the concentrations plotted to form the quantification curve (Figure 2.8).

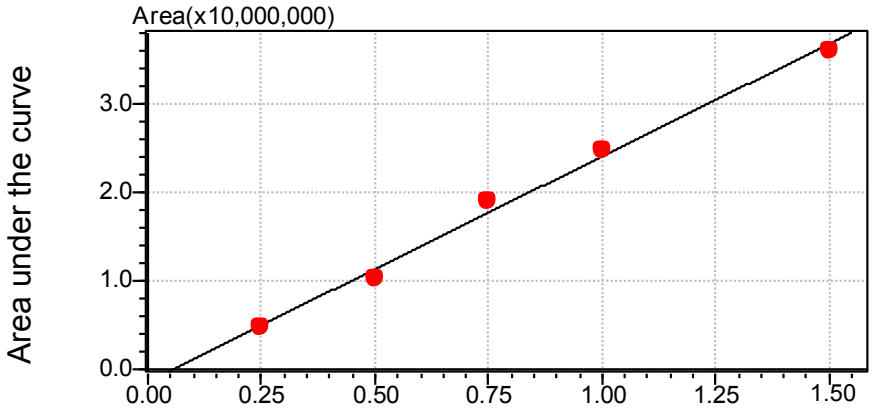

Figure 2.8: Quantification curve of methyl trifluoroacetate using standard concentrations.

The quantification curve was incorporated into the SIM EI^+ GCMS method, in order to automatically quantify MTFA, if present in a sample.

The sample was again run in SIM EI^+ mode for *m/z* 59, 69 ND 99 ions, and showed an MTFA peak at 4.6 minutes (Figure 2.9). The MTFA concentration for OP (average of the two sample replicates) was quantified to be 0.029035 mg/ml (29.035 µg/ml) in an extract concentration of 7.75 mg/ml, and for LBG the MTFA concentration (average of two replicates) was 0.028975 mg/ml (28.975 µg/ml) in an extract concentration of 7.325 mg/ml. The fresh weight of the OP sample was 2.93 g and yielded 186.45 mg of dried plant extract, while the fresh weight for the LBG sample was 3.01 g and yielded only 116.9 mg of dried plant extract. The amount of MTFA in the two plant extracts was calculated as follows:

$$\left(\frac{total\ mass\ dried\ plant\ extract}{mass\ extract\ used\ for\ derivatization} \times mass\ of\ MTFA\ quantified\right) \div fresh\ weight\ plant\ material$$

$$= MTFA\ /\ gram fresh\ plant\ material$$

For the OP sample:

$$\therefore \left(\frac{186.45\ mg}{7.75\ mg} \times 29.035\ \mu g\right) \div 2.93\ g = 238.40\ \mu g/g$$

The amount of TFA per gram fresh leaf material is therefore 238.40 µg/g. This indicates that MTFA constitute 0.02384 %, of leaf material in the OP plant; a remarkably high number.

For the LBG sample:

$$\therefore \left(\frac{116.9\ mg}{7.325\ mg} \times 28.975\ \mu g\right) \div 3.01\ g = 153.63\ \mu g/g$$

For the LBG sample the amount of TFA is therefore 153.63 µg/g fresh leaf material. Although the percentage is still high (0.01536%), is significant lower than that of the OP sample.

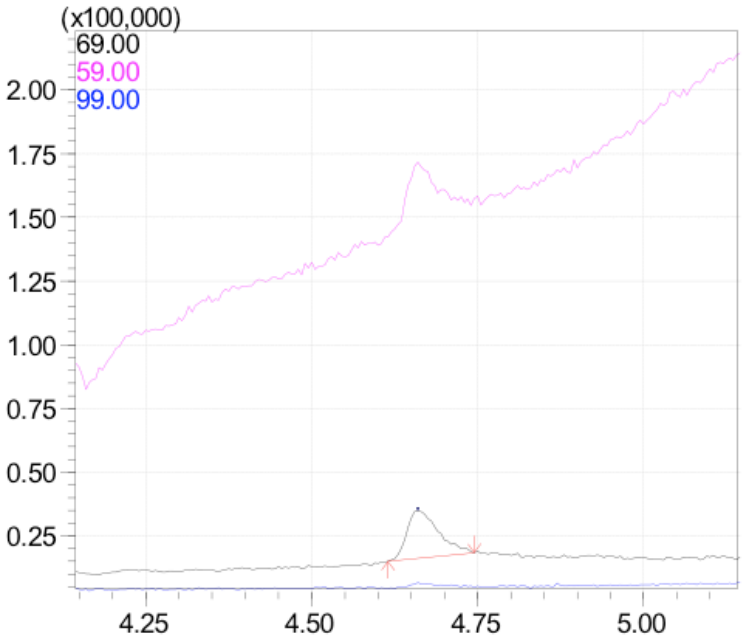

Figure 2.9: *T. fischeri* Onderstepoort sample showing the MTFA peak at 4.6 minutes.

Trifluoroacetate (TFA) occurs mostly in nature as a pollutant, known to form as by-product in the troposphere from refrigerants such as hydrofluorocarbons (HFC's) and hydrochlorofluorocarbons (HCFC's) (Cahill *et al.,* 1999). Due to the high water solubility of TFA it return to earth in rainwater, and become highly cumulative in water bodies (Cahill *et al.,* 1999; Smit *et al.,* 2009). Similar to monofluoroacetate it is extremely stable due to its inability to be oxidized and dehalegenized. It is further reported to be of environmental concern due to its toxicity to plants in particular. Although certain algae such as *Raphidocelis subcapitata* are affected by concentrations of 360 µg/L, most plant species tested thus far were only affected by concentrations of mg/L. (Cahill, *et al.,* 1999).

Although TFA are highly accumulative in plants, no reports could be obtained of such high concentrations as reported in this study being observed in plants. Most studies were done to observe the effect TFA might have on plants, and test subjects were exposed to higher levels of TFA that are currently observed in nature. In a study conducted by Smit *et al.*

(2009), *Phaseolus vulgaris* and *Zea mays* plants were exposed to concentrations of NaTFA ranging from 0.625 to 160 mg/L for 14 days. Clear reductions in the size of both species were seen with increased concentrations of TFA. The TFA levels the plants were exposed to are much higher than current hydrospheric TFA levels, which are at 41 µg/L (Smit *et al.,* 2009).

In another study by Likens *et al*. (1997), they measured the amount of TFA accumulation in plants. They found the highest concentration accumulated in a tree occurring in a wetland known as *Acer pensylvanicum.* The tree received an additional 500 mg/m^2 TFA at its base. The TFA concentration in this plant was measured to be 79.80 ± 15.8 µg/g leaf material.

Cahill *et al.* (2001) measured the amount of TFA of a vernal pool system in the California wetlands. They measured the TFA levels of three plant species in and around the pool system. *Avena sativa* (wild oats) were collected outside the pools in order to determine background levels of TFA. *Downingia insignis* (calicolflowers) was collected from intermediate depths and *Eryngium vaseyi* (cayoti-thistles) were collected from the deepest parts. As was expected the plants collected from the deepest parts has the highest TFA concentrations (279 ng/g dry weight) due to these plants being exposed to larger TFA concentrations.

From the above experiments previously reported in literature, it is clear that no plants exposed to natural environmental levels or even spiked levels of TFA, have accumulated TFA in amounts as high as reported in this study (238.40 µg/g fresh weight OP leaf material and 153.63 µg/g fresh weight LBG leaf material). It therefore seems unlikely that the amounts of TFA observed in *T. fischeri* are only due to pollutant TFA accumulation. Considering also that other Dichapetalaceae members such as *D. cymosum* are known to contain fluorinated compounds, specifically monofluoroacetate (O'Hagan & Harper, 1999),

and other *Tapura* spp. such as *T. amazonica* are known to be toxic (Pohlit *et al.,* 2004), it is very likely that TFA are produced in *T. fischeri* as a natural toxic compound, possibly serving a similar defensive role as in *D. cymosum*.

2.4 Conclusion

T. fischeri contains a fluorinated compound other that fluoroacetate, which is known to be the toxic compound in the South African related species *D. cymosum*. It was confirmed to be a trifluorinated compound, based on the similarity of the chemical shift (-75.87 ppm) to that of CF3-C (-50 to -90 ppm) and trifluoroacetate (-76.55 ppm), as well as with GCMS analysis.

The identity of the compound was confirmed with GCMS, and showed a 97 % similarity to trifluoroacetate. The quantity of TFA in the OP tree was calculated to be 238.40 µg/g and for the sample from LBG to be 153.63 µg/g. Since TFA is a well-known pollutant, it is possible that the TFA might have accumulated in the plants through the uptake of TFA from soil water. The concentrations reported in this study are however much higher than previously reported in studies where elevated levels of TFA have been added to plant test subjects. The fact that these high levels were found in plants from Pretoria and Mbombela (Nelspruit), about 300 km apart, also indicates that pollution is an unlikely cause for this compound in *T. fischeri.* It is therefore highly unlikely that these high concentrations of TFA are purely from pollution, but that the plant possibly produces TFA as a defense mechanism.

2.5 References

Baron, M.L., Bothroyd, C.M., Rogers, G.I., Staffa, A., Rae, I.D., 1986. Detection and measurements of fluoroacetate in plant extracts by ^{19}F NMR. Phytochemistry 26, 2293-2295.

Bayer, T., Amberg, A., Bertermann. R., Rusch, G.M., Anders, M.W., Dekant, W., 2002. Biotransformation of 1,1,1,3,3-pentafluoropropane (HFC-245fa). Chemical Resonance Toxicology 15, 723-733.

Cahill, T.M., Benesch, J.A., Gustin, M.S., Zimmerman, E.J., Seiber, J.N., 1999. Simplified method for trace analysis of trifluoroacetic acid in plant, soil and water samples using head space gas chromatography. Analytical Chemistry 71, 4465-4471.

Cahill, T.M., Thomas, C.M., Schwarzbach, S.E., Seiber, J.N., 2001. Accumulation of trifluoroacetate in Seasonal wetlands in California. Environmental Science and Technology 35, 820-825.

Dolbier, W.R., 2009. Guide to fluorine NMR for organic chemists. John Wiley & Sons, New Jersey.

Harper, D.B., O'Hagan, D., 1994. The Fluorinated Natural products. Natural Products Report 11, 123-133.

Kellerman, T.S., Coetzer, J.A.W., Naude, T.W., Botha. C.J., 2005. Plant Poisonings and mycotoxicoses of Livestock in Southern Africa. Oxford University Press Southern Africa, Cape Town.

Likens, G.E., Tartowski, S.L., Berger, T.W., Richey, D.G., Driscoll, C.T., Franks, H.G., Klein, A., 1997. Transport and fate of trifluoroacetate in upland forest and wetland ecosystems. The National Academy of Sciences of the USA 94, 4499-4503.

O'Hagan, D., Harper, D.B., 1999. Fluorine containing natural products. Journal of Fluorine Chemistry 100, 127-133.

Pohlit, A., Quignard, E., Nunomura, S., Tadei, W., Hidalgo, A., Pinto, A., dos Santos, E., de Morais, S., Saraiva, R., Ming, L., Alecrim, A., Ferraz, A., Pedroso, A., Diniz, E., Finney, E., Gomes, E., Dias, H., de Souza, K., de Oliveira, L., Don, L., Queiroz, M., Henrique, M., dos Santos, M., Lacerda Junior, O., Pinto, P., Silva, S., Graca, Y., 2004. Screening of plants found in the State of Amazonas, Brazil for larvicidal activity against *Aedes aegypti* larvae. Acta Amazonica 34, 97-105.

Quignard, E.L.J., Nunomura, S.M., Pohlit, A.M., Alecrim, A.M., Pinto, A.C.D.S., Portela, C.N., De Oliveira, L.C.P., Don, L.D.C., Rocha E Silva, L.F., Henrique, M.C., Dos Santos, M., Pinto, P.D.S., Silva, S.G., 2004. Median lethal concentrations of amazonian plant extracts in the brine shrimp assay. Pharmaceutical Biology 42, 253-257.

Sekigutchi, O., Tajima, S., Koitabashi, R., Tajima, S., 1998. Decomposition of metastable methyl trifluoroacetate and ethyl trifluoroacetate upon electric impact. International Journal of mass spectrometry 177, 23-30.

Smit., M.F., van Heerden, P.D.R., Pienaar, J.J., Weissflog, L., Strasser, R.J., Krüger, G.H.J., 2009. Effect of trifluoroacetate, a persistent degradation product of fluorinated hydrocarbons, on *Phaseolus vulgaris* and *Zea mays*. Plant Physiology and Biochemistry 47, 623-643.

Vickery, B., Vickery, M.L., Ashu, J.T., 1972. Analysis of plants for fluoroacetic acids. Phytochemistry 12, 145-147.

Zehavi, D., Seiber, J.N., 1996. An analytical method for trifluoroacetic acid in water and air samples using head space gas chromatographic determination of the methyl ester. Analytical chemistry 68, 3450-3459.

Chapter 3:

Isolation of antibacterial compounds from *Tapura fischeri*

3.1 Introduction

As was mentioned previously, many species of the *Tapura* genus is known to be toxic, as well as a number of the *Dichapetalum* species (Cornejo & Janovec, 2010). No literature could be obtained to establish the toxicity of *T. fischeri*, although the presence of the fluorinated compound and literature published for other members of the Dichapetalaceae family suggest that it might indeed be toxic (Harper & O'Hagan, 1994).

During the onset of the project the aim was to isolate the fluorinated compound, however as observed earlier, it was discovered that the fluorinated compound in *T. fischeri*, is highly volatile due to the disappearance of the compound upon storage of the extract. The extract from which the fluorinated compound was lost however still showed antibacterial activity against the bacterium *Enterococcus faecalis* as will be shown in section 3.3.1. The aim for this part of the study was therefore focused on the isolation of the compounds showing antibacterial activity on TLC plates.

3.2 Methodology

3.2.1 Antibacterial activity using thin layer chromatography (TLC)

Antibacterial activity was initially determined using thin layer chromatography (TLC). The extract was spotted on TLC plates in varying concentrations, and developed with different solvent systems, to obtain good separation of the compounds. For each solvent system two plates were developed, the one was sprayed with vanillin, while the second were sprayed with the Gram-positive bacterium, *Enterococcus faecalis*, to determine the toxicity of the plant. *E. faecalis* was cultured in a nutrient broth medium for 24 hours prior to spraying of the plates. The bacteria were spun down using the centrifuge setting on the genevac EZ-2 plus. The old media was removed, new broth was added to the bacteria and the cells were

re-suspended in the new media. The plates sprayed with *E. faecalis* were left to develop for 24 hours at a temperature of 36°C, in an incubation chamber. After 24 hours the plates were sprayed with 0.4 mg/ml INT (2-(4-iodophenyl)-3-(4-nitrophenyl)-5-phenyltetrazolium chloride) solution and allowed to develop. A purple/pink reaction indicates bacterial growth, while white spots indicate bacterial inhibition.

3.2.2 Liquid liquid partitioning

The following protocol served as the basis for the isolation of the compounds responsible for showing antibacterial activity. About 450 g of plant material was collected form the Lowveld botanical gardens, and comprised of both leaf and stem material (200 g stems, 250 g leaves). The plant material was freeze-dried using a Virtis freeze-dryer. After drying the weight of the plant material were 64.14 g and 70.20 g for the leaf and stem material respectively. Only 46.5 g leaf material and 68.5 g stems were used for extraction purposes. The leaves yielded 3.66 g extract while only 0.53 g of extract were obtained from the stems. Comparison of the extracts on TLC showed no significant differences, and the extracts were therefore combined for further analysis.

The extract was partitioned into different polar fractions through liquid-liquid partitioning. The extract was dissolved in distilled water, hexane was added and the extract was then partioned between the upper non-polar hexane phase and the lower polar water phase. Upon removal of the hexane phase, ethyl acetate was added to the water phase and partitioning done a second time to yield a phase with intermediate polarity. The three phases were dried and yielded 4.36 g, 0.48 g and 2.25 g for the hexane, ethyl acetate and water fractions respectively. 20 mg of each extract were dissolved in 500 µl of its corresponding solvent. The fractions were spotted on TLC plates and dissolved in three different mobile phase systems with increasing polarity: 1.) 80 % hexane (hex): 20 % ethyl

acetate (EtOAc), 2.) 95 % dicloromethane (DCM): 5 % methanol (MeOH) and 3.) 40 % buthanol (BuOH): 10 % acetic acid (HOAc): 50 % distilled water (dH_2O). Two plates were prepared for each mobile solvent system, the one set of plates were sprayed with vanillin while the other were sprayed with the Gram positive bacterium, *E. faecalis* as described in section 3.2.1.

3.2.3 Isolation of antibacterial compounds using column chromatography

3.2.3.1 Silica column 1

The hexane and ethyl acetate fractions were combined, and 4.40 g of extract used for isolation purposes. Isolation was done, using a silica column 30 cm high and 4 cm in diameter. The extract was mixed with 8 g silica in DCM and allowed to dry overnight before it was added to the column, this allowed the extracted material to bind to the silica, which can then be added tot the column in the form of a powder. The compounds were separated using two solvent systems with increasing polarity. The first solvent system was a mixture of hexane and ethyl acetate, starting with 5 % EtOAc in 95 % Hex. The polarity was then increased to 7.5 %, 10 %, 20 % and 25 % EtOAc in Hex. After 25 % EtOAc in Hex the solvent system was changed to DCM and MeOH, starting with 1 % MeOH in DCM. The polarity was then increased to 3 %, 5 %, 7.5 %, 15 % and 25 % MeOH in DCM until all fractions were collected.

The fractions were spotted onto TLC plates during the separation process and developed using various solvent systems with increasing polarity. Similar fractions were then combined resulting in 32 different fractions. The remaining fractions were spotted onto TLC plates to determine which fractions contain the antibacterial compounds. Three different solvent systems were used depending on the mobile phase used to isolate the specific fractions. Again two plates were spotted for each solvent system. Fractions 1-12 were separated on

TLC using 80 % Hex: 20 % EtOAc mobile phase, while fractions 12 – 18 were developed in 95 % DCM: 5 % MeOH, and fractions 18-32 in 90 % DCM: 10 % MeOH. The plates were again sprayed with *E. faecalis* to determine which fractions contained antibacterial activity as described in section 3.2.1

3.2.3.2 Sephadex columns 1 and 2

Fractions 14 and 15 were combined and separated a second time into more fractions using a Sephadex column (268 mg). The compounds were separated with a 50 % DCM: 50 % MeOH mobile phase. Fractions was spotted onto TLC plates and developed in a 95 % DCM: 5 % MeOH mobile phase.

Similar fractions were again combined, and fraction 2 of the first Sephadex column was further separated on a second Sephadex column. The mobile phase used was 25 % DCM: 75 % MeOH. Similar fractions were again combined, resulting in eight different fractions obtained from the two Sephadex columns. The fractions were spotted onto TLC plates and developed in a 95 % DCM: 5 % MeOH mobile phase. One plate was sprayed with *E. faecalis* for antibacterial activity testing as described in section 3.2.1.

3.2.3.3 Silica column 2

The fraction showing antibacterial activity was separated further using a second silica column, 10 cm high and a 1 cm diameter. The extract was dissolved in DCM, and the first mobile phase 1 % MeOH in DCM. The polarity was increased to 2 %, 3 % and 6 % MeOH in DCM. Similar fractions were combined, and 10 fractions were obtained. The pure compounds were further analyzed with NMR and GCMS.

3.2.4 Nuclear Magnetic Resonance

Pure compounds obtained from the column where analyzed with ^{1}H and ^{13}C NMR on a 200 MHz NMR apparatus. All pure compounds were analyzed even if they did not show antibacterial activity on TLC.

Compounds with antibacterial activity were initially analyzed with the 200 MHz NMR for ^{1}H and ^{13}C NMR data, but were then analyzed on a 400 MHz NMR. The 400 MHz ^{1}H and ^{13}C NMR spectra were obtained with the help of Mr. Chris van der Westhuizen at the CSIR.

All compounds were dissolved in $CDCl_3$ (deutorated chloroform) for NMR analysis.

3.2.5 Gas chromatography of antibacterial compounds

It was necessary to derivatise the compounds to their methyl ester forms to increase their volatility. 10 µl of the derivitisation agent BSTFA (N,O-Bis(trimethylsilyl)trifluoroacetamide) was added to 10 µl of each sample. This was allowed to stand for 24 hours in 4 °C fridge.

The fatty acid methyl esters (FAME's) were analyzed on an Agilent 6890 N GC system, equipped with an HP1-MS column and an FID (flame ionization detector). 1 µl was injected, and the samples ran on a splitless mode, with the injection temperature set at 250 °C. Helium was used as the carrier gas with a flow rate of 1 ml/min. The oven temperature started at 50 °C, where it was held for 2 minutes, it was then increased by 10 °C/min up to 170 °C, held for 3 min, increased by 12 °C/min up to 230 °C and held for 8 minutes. The total run time was 30 minutes.

Due to no FAME's being detected the column was changed to a fatty acid specific column, namely, HP innowax column, using the same Agilent 6890N GC system and FID detector. The injection temperate was held at 250 °C, with 1 µl being injected in the splitless mode.

Helium was still used as carrier gas at a flow rate of 1ml/min. The oven temperature program was changed to start at 60 °C and hold for 3 minutes, where after it was increased by 10 °C/min up to 240 °C and hold for 29 minutes. The total run time was 50 minutes.

After no FAME's were detected the derivatization method was changed. 2 ml of the derivatization agent, BCl_3-methanol was added to the 1 mg of each sample and heated for 10 minutes at 60 °C. The reaction vessel was cooled down before 1 ml water and 1 ml hexane was added. The reaction vessel was shaken in order to move the methyl esters into the non-polar solvent. After the layers have formed, the upper organic layer was removed and placed in a clean vial. The organic layer was dried by the addition of anhydrous sodium sulphate (Na_2SO_4), to the vial, and shaking it (Sigma Aldrich, 2014). The samples were analyzed using the method set up for the HP innowax column.

A third derivatization technique was used after no FAME's were detected. 500 µg of sample was dissolved in 500 µl of methyl-tert-butyl eter. 100 µl was pipetted into an HS vial, 50 µl of the derivatization agent TMSH (trimethylsulfonium) was added, and the sample was left to stand for 30 minutes at room temperature prior to GC analysis (Gomez-Brandon *et al.*, 2008). The FAME's were once again analyzed using the method set up for the HP innowax column.

3.2.6 Microtitre antibacterial activity testing

The compounds that showed antibacterial activity on TLC were screened again in liquid media to rule out any false positive fatty acid results obtainable with TLC. The test was conducted in a 96 well microtitre plate, using nutrient broth as liquid media. The same bacterium *Enterococcus faecalis* was used. Two antibiotics, Ciproflaxin and Tetracyclin were used as the positive controls, these were chosen as they are common antibiotics with activity against a wide range of aerobic and anaerobic Gram positive and negative

organisms (Pinheiro *et al*., 2004). Other controls included a solvent control, media control and bacterial control.

Due to low quantities for the active compounds the experiment was first conducted with the controls only, to ensure the accuracy of the results. Ciproflaxin and Tetracyclin were tested at concentrations of 2 µg/ml and 50 µg/ml respectively. The compounds were dissolved in DCM, for this reason DCM was used for the solvent control and tested from 10 %. A bacterial control in which only the bacteria is added to the media, as well as a media control, was included.

The experiment was repeated with the active compounds. Only tetracyclin was used for the positive control, and again was tested at a concentration of 50 µg/ml. The pure compounds were tested at a concentration of 200 µg/ml, and were dissolved in DCM, while the plant extract was tested at 1000 µg/ml and dissolved in DMSO. For this reason solvent controls for both DCM and DMSO were included, bacteria and media controls were also included.

The bacteria were grown in nutrient broth overnight, and diluted to a 0.5 McFarland [1.5 x 10^8 CFU (colony forming units)/ml] standard using a spectrophotometer (reading between 0.1 and 0.13 A). The bacterial solution was then further diluted 300 times to a final inoculum concentration of 5 x 10^5 CFU/ml (Sahm *et al*., 1991)

3.3 Results and Discussion

3.3.1 Antibacterial activity using TLC

The plant extract was separated on TLC (thin layer chromatography) plates, and sprayed with the bacterium *Enterococcus faecalis* and then with INT solution, to visualize bacterial growth on the plates.

The original mobile phase used for the TLC's were 100 % methanol, however the separation obtained were weak, with an accumulation of the compounds at the top of the plate. The same extract was spotted onto the TLC plate using different volumes (varying amounts of drops on a single spot). The volumes applied increases from left to right, starting from 2 spots to 10, each spot increasing with 2. The plate from Figure 3.1 shows bacterial inhibition even at the lowest concentration (2 spots). The compound or group of compounds responsible for the inhibition is uncertain, due to the weak separation.

Figure 3.1: Bacterial inhibition (white spots) of *E. faecalis* by *T. fischeri* extract. The extract concentration increases from left to right. Inhibition is seen even at the lowest concentration. Mobile phase: 100 % MeOH.

In order to try and improve the separation between the compounds, various concentrations of MeOH to DCM were used. The best separation was obtained with 90 % DCM: 10 %

MeOH, resulting in a better spread of compounds on the TLC plate (Figure 3.2 A). A protocol to separate polar compounds containing fluoroacetate was described by Vickery *et al*. (1972), in which they used a ratio of (95:3:1:1) ethanol (EtOH): ammonium solution (NH4OH): pyridine (pyr): water (H_2O). The protocol was modified for this scenario to 96:3:1 EtOH: pyr : NH_4OH (Figure 3.2 B). Separation of the compounds was also improved from the 100 % MeOH, using this mobile phase.

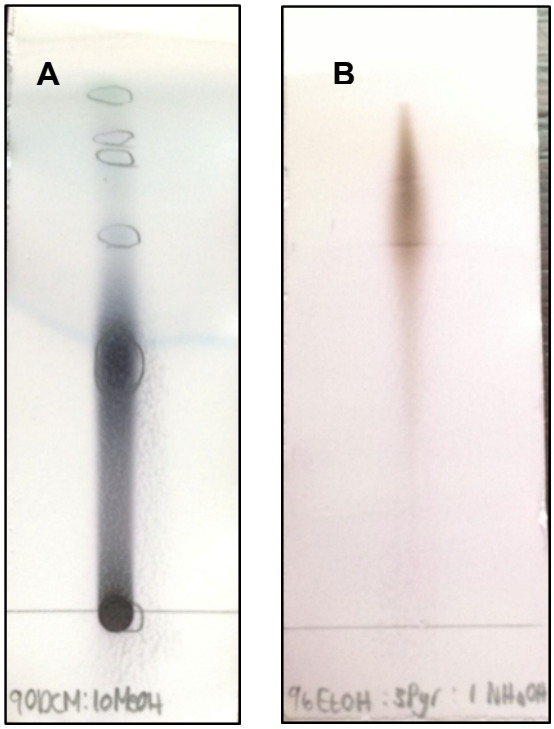

Figure 3.2: Seperation of the plant extract using two new mobile phases. (A) Mobile phase: 90:10 DCM: MeOH. (B) Mobile phase 96:3:1 EtOH: Pyr: NH_4OH.

From Figure 3.3 it seems that the compound in the middle of the plate is the toxic compound, since this is the only spot showing bacterial inhibition while the active compound in Figure 3.4 is more towards the top and seems to fall between the two compounds, with the upper and lower portion of the smear not exhibiting bacterial inhibition.

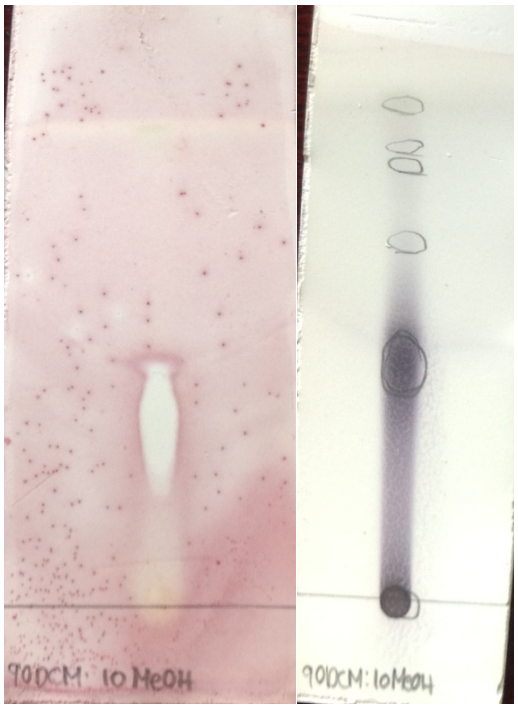

Figure 3.3: *E. faecalis* inhibition, observed by the compounds present in the middle of the plate. The mobile phase was 90:10 DCM: MeOH.

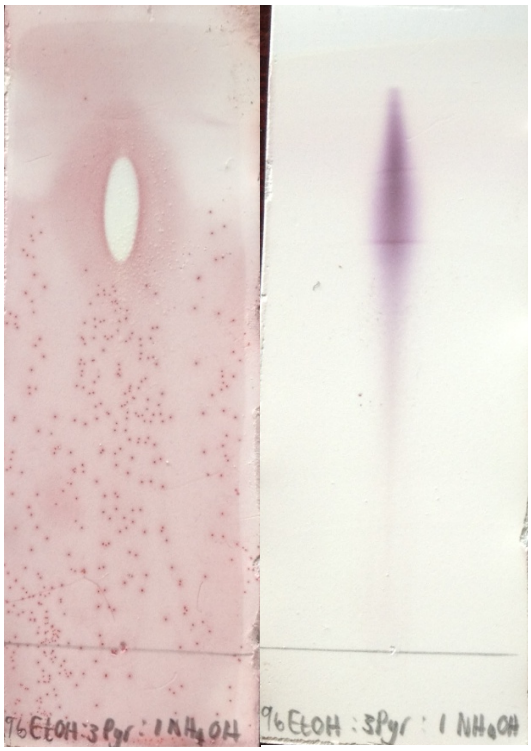

Figure 3.4: *E. faecalis* inhibition observed in the middle of the smear. The mobile phase was 96:3:1 EtOH: Pyr: NH_4OH.

3.3.2 Liquid-liquid partitioning

As described in the material and methods section, plant material were collected and dried on a freeze drier. Comparison of the leaf and stem extracts on TLC showed no significant differences, and the extracts were therefore combined for further analysis.

Liquid–liquid partitioning of the extract was done with three different solvents, hexane, ethyl acetate and water. The various fractions yielded 4.36 g, 0.48 g and 2.25 g for the hexane, ethyl acetate and water fractions respectively. The extracts were spotted onto TLC and developed in three different solvent systems, after which the plates were sprayed with *E. faecalis*. Figure 3.5 indicate that both the hexane and ethyl acetate fractions contain compounds responsible for the antibacterial activity observed on TLC. Due to the similarity of the profiles of these two fractions, they were combined and used for isolation of the antibacterial compounds through column chromatography.

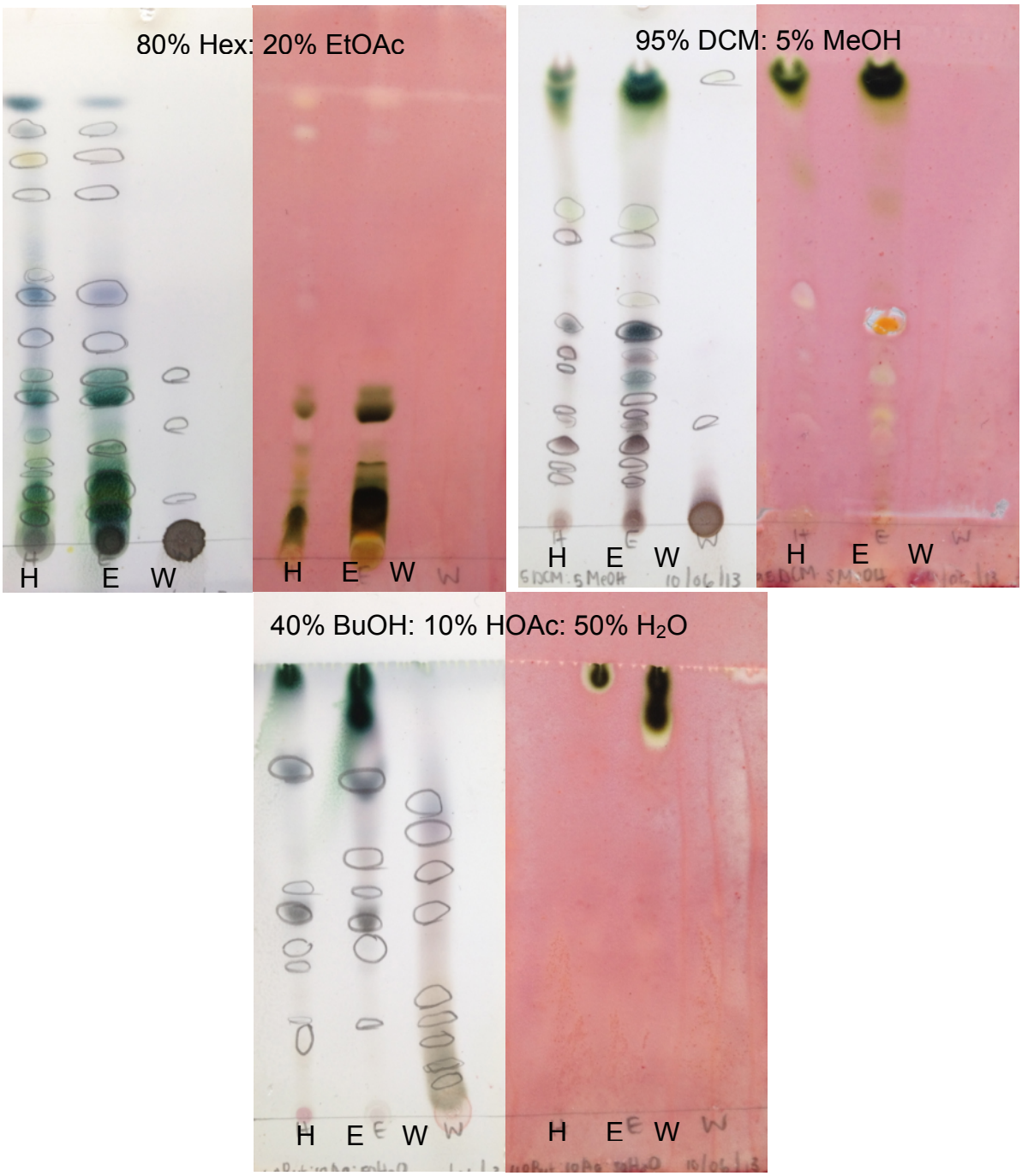

Figure 3.5: Antibacterial results of the three fractions, hexane, ethyl acetate and water, developed in three different solvent systems. White plates were treated with vanillin, while pink plates were sprayed with *E. faecalis*. White spots indicate antibacterial activity.

3.3.3. Isolation of antibacterial compounds through column chromatography

In total four columns were done in order to isolate two compounds responsible for the antibacterial activity seen on TLC. Column 1 (Figure 3.6) made use of a silica gel, which yielded 108 fractions, these were combined based on similarity to yield 32 fractions (Figure 3.6).

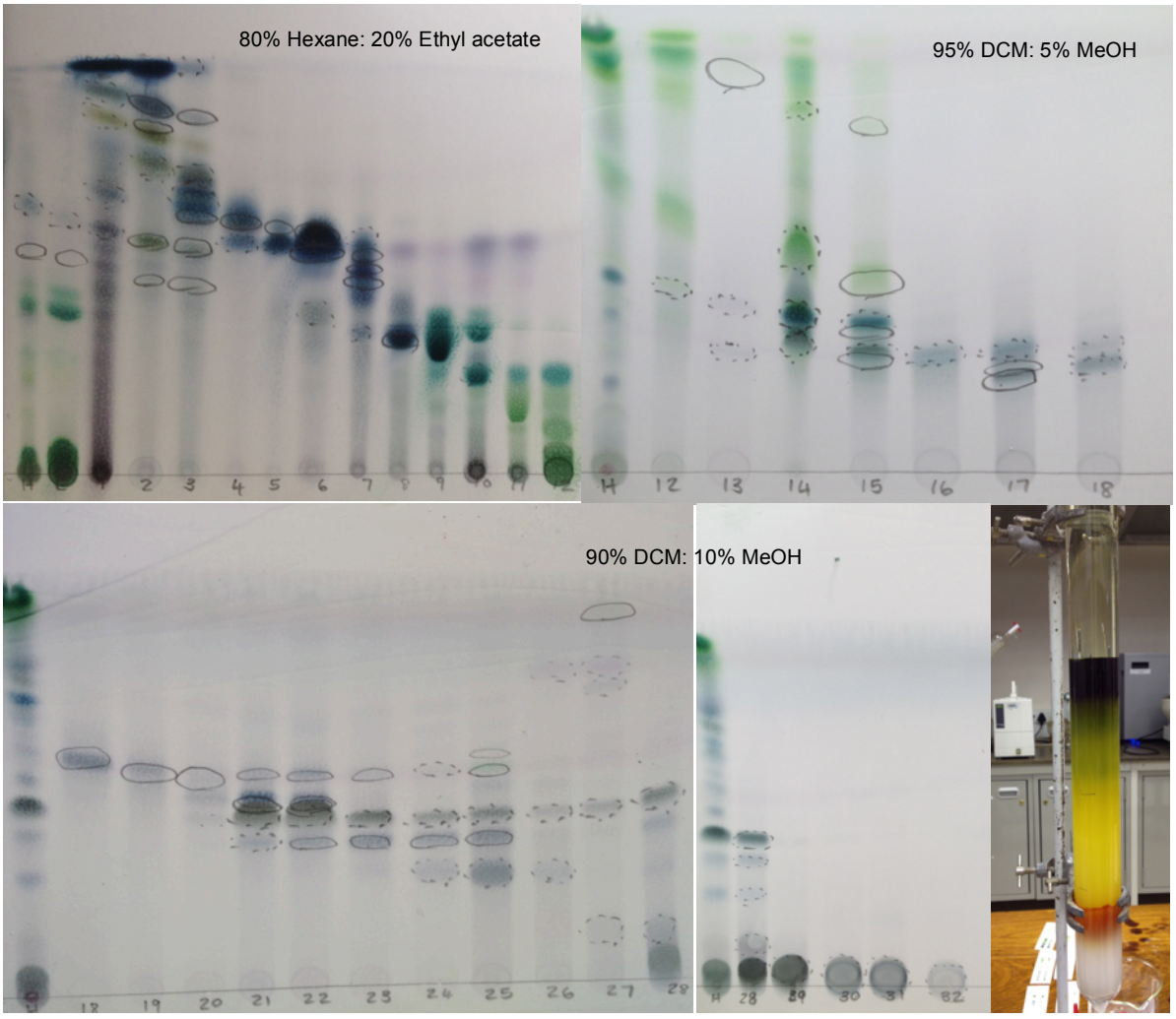

Figure 3.6: Isolation of compounds from *Tapura fischeri* using a silicia column for separation.

The plates were then sprayed with *Enterococcus faecalis* to determine which fractions are responsible for the white antibacterial spots seen on previous TLC plates. Antibacterial

activity was observed for the first 7 fractions (Figure 3.7). Due to the low polarity of these fractions, it was concluded that these fractions contain mostly hydrophobic carbon chains such as fatty acids, and therefore of little interest as antibacterial compounds. Fractions 14 and 15 (Figure 3.7) also showed antibacterial activity. The two fractions were combined and separated on a second column.

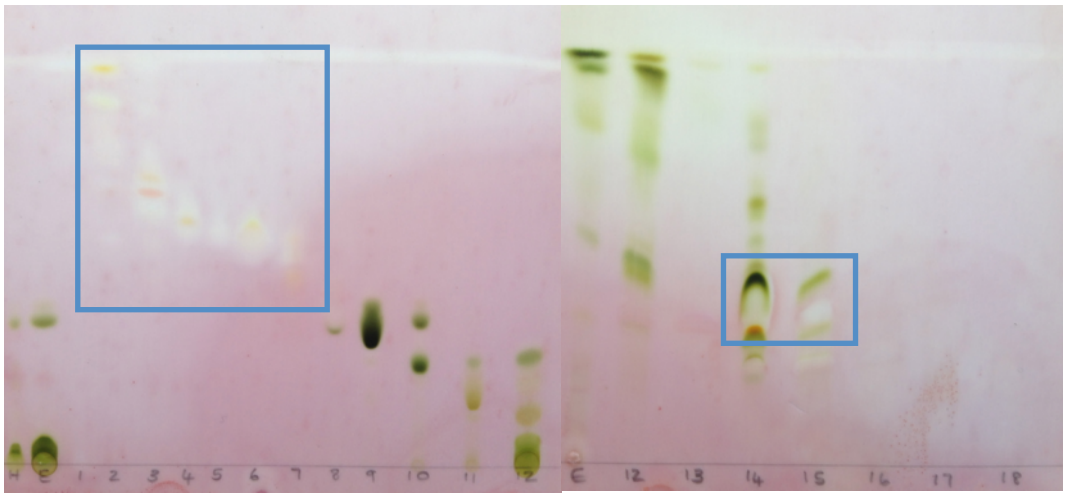

Figure 3.7: Isolated fractions with antibacterial activity, as indicated by the white spots. Blue rectangles indicate regions with antibacterial activity. Fractions 1-7 and 14-15 contained compounds with antibacterial activity.

The first Sephadex column done with fractions 14 and 15, yielded 4 fractions after combining the original fractions. Due to weak separation of the second fraction of this column, a second Sephadex column was done for fraction 2. The antibacterial results of these fractions are shown in Figure 3.8. From the figure it can be seen that fraction 4 of the first Sephadex column, named C1F4 on the TLC plate are responsible for the antibacterial activity and consist of two main compounds (plate 1 Figure 3.8). This fraction was used for a second silica column, in order to separate the two main compounds from each other.

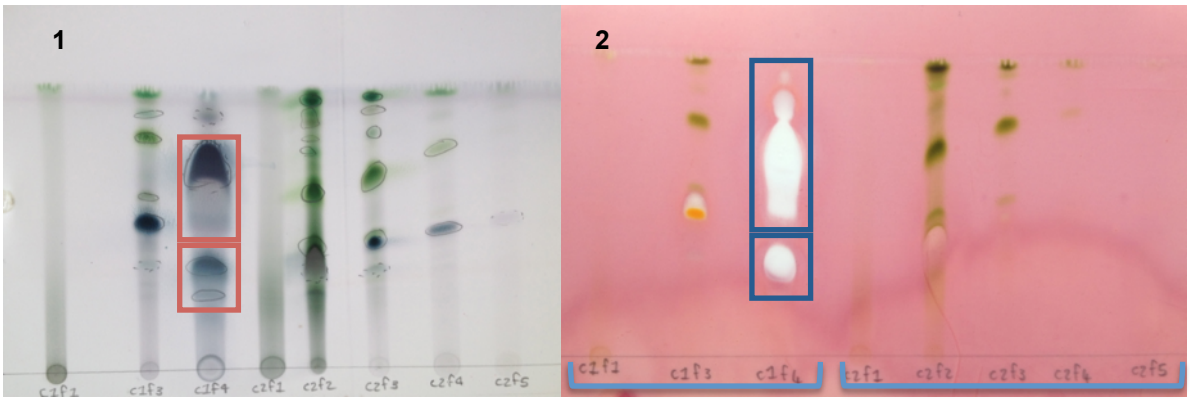

Column 1 Column 2

Figure 3.8: TLC's of the two Sephadex columns used to separate antibacterial compounds. Antibacterial activity observed in the fourth compound of the first Sephadex column.

The fraction C1F4 was used to conduct a second silica column (column 4). Seperation of the compounds was difficult due to the colourless nature of most of the compounds; they further also did not absorb UV light. The fractions from column 4 were spotted onto TLC and could only be visualized after the plates were treated with vanillin. Figure 3.9 indicates all the fractions collected. The combined fractions indicated by the black numbers in Figure 9 were never spotted onto a single TLC or sprayed with the bacteria, since it was previously determined (Figure 3.8) that all the compounds from fraction C1F4 are antibacterial.

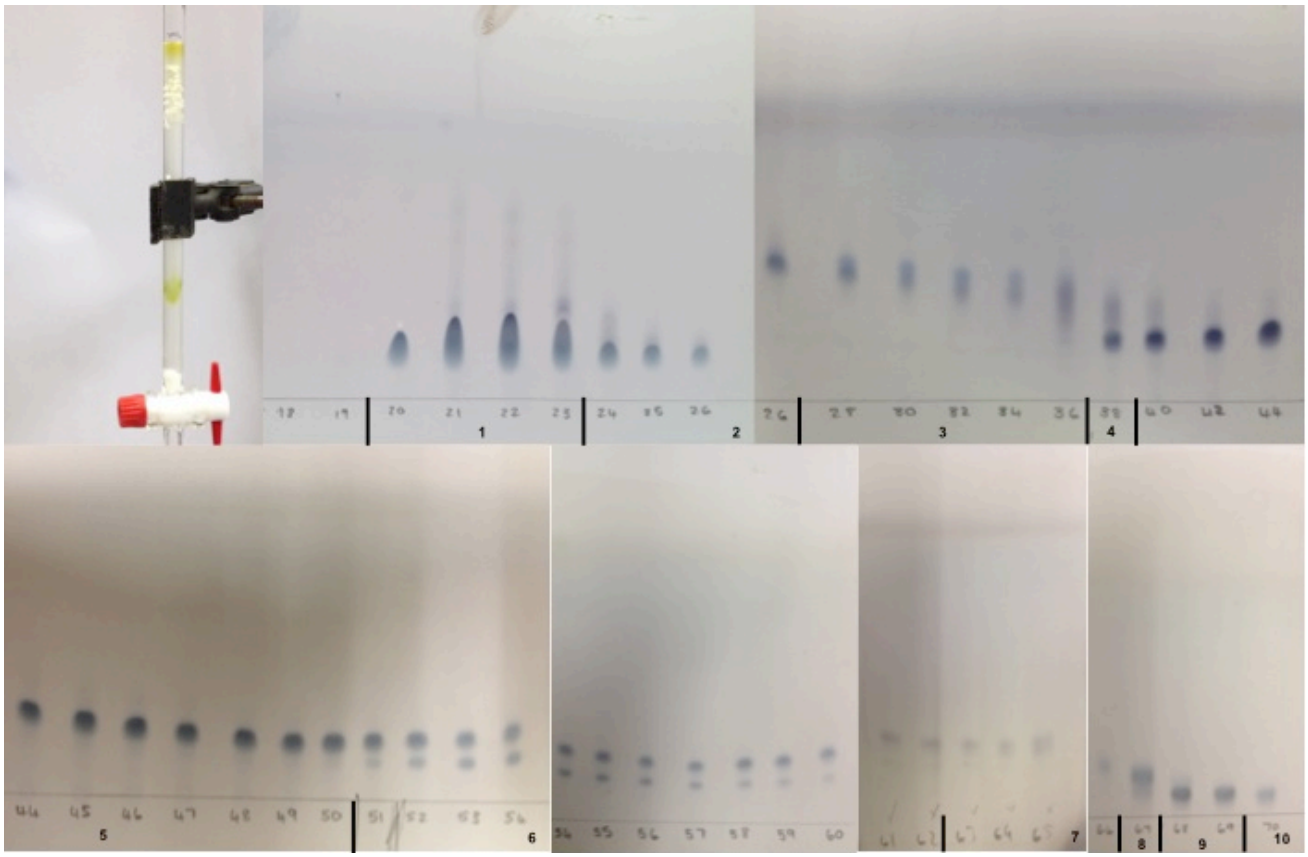

Figure 3.9: Fractions collected from column 4 (Silica column 2), and combined into 10 fractions.

Fraction 1 from Figure 3.9 are believed to be the large upper antibacterial compound observed in Figure 3.8, due to the shape of the compound on TLC. Fractions 3 and 4 appear to have traces of both compounds, while fraction 5 are believed to be the lower antibacterial compound as can be seen in Figure 3.8. The remaining fractions appear to contain at least two compounds. Fractions 1 and 5 were also the two fractions with the highest masses, 10.3 mg and 3.5 mg respectively, and were used for analysis on NMR.

3.3.4 Nuclear magnetic resonance of isolated compounds

3.3.4.1 Pheophytin a

As was mentioned in the methodology all relatively pure fractions of the first silica column was analyzed with a 200 MHz NMR Varian spectrometer. This was done mainly in an attempt to determine whether dichapetalins might be present in *T. fischeri*.

Similar to Schwikkard *et al*. (1998), no dichepetalins were isolated, however pheophytin a, was isolated. The fraction in which pheophytin a, was obtained was fraction 9. The ^{1}H NMR data of fraction 9 (Figure 3.11) fits well with the ^{1}H NMR results of pheophytin a published by Schwikkard *et al*. (1998) (Table 3.1). Due to lower resonance of the 200 MHz spectrometer compared to the 300 MHz Gemini spectrometer used in the literature, as well as the impurities still present in the sample it was difficult to clearly match the ^{13}C data to that of published results.

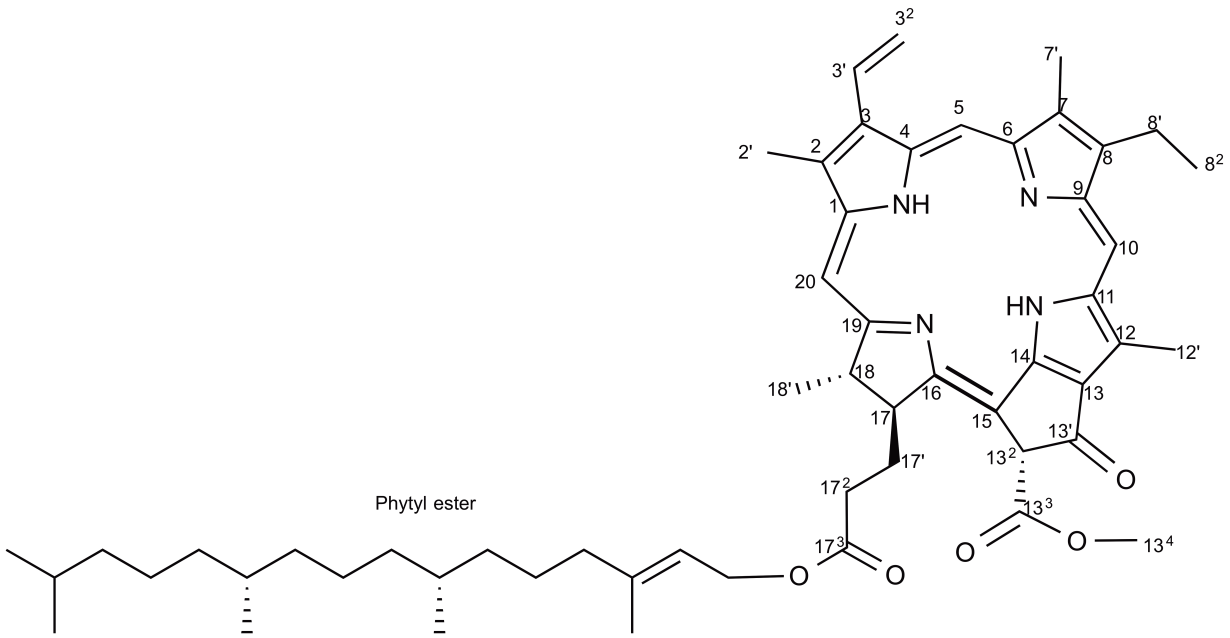

Figure 3.10: Chemical structure of pheophytin a (Adapted from Souza Chaves *et al.* 2013)

Table 3.1 Proton NMR data as compared with published data from Schwikkard *et al.* (1998) for pheophytin a.

^{1}H NMR				
Proton	Current results		Schwikkard *et al.* (1998)	
	Peak type	Signal (ppm)	Peak type	Signal (ppm)
Me	S	0.77	S	0.76
Me	S	0.79	S	0.79
Me	S	0.81	S	0.8
Me	S	0.83	D	0.85
Me	S	0.86	D	0.85
H-8[2]	T	1.69	T	1.68
H-18'	D	1.81	D	1.8
H-7'	S	3.22	S	3.21
H-2'	S	3.40	S	3.39
H-8'	S	3.66	Q	3.66
H-12'	S	3.69	S	3.68
H-13[4]	D	3.89	S	3.88
H-17	M	4.21	M	4.2
H-17[4]	-	-	DD	4.35
H-18	M	4.46	M	4.45
H-17[5]	T	5.1	T	5.1
H-3[2] (Z)	DD	6.18	DD	6.17
H-13[2]	S	6.27	S	6.26
H-32 (E)	DD	6.29	DD	6.28
H-3'	DD	7.99	DD	7.98
H-20	S	8.56	S	8.55
H-5	S	9.37	S	9.36
H-10	S	9.51	S	9.5

As can be seen from Table 3.1 proton NMR data fits well with the results published by Schwikkard *et al*. (1998). There are a few differences in the type of peak observed however the chemical shifts for all proton signals differ by no more than 0.1 for all peaks. The differences in the peak types are possibly due to the lower resonance of the 200 MHz spectrometer. This is possibly the reason why the proton H-8' are seen as a singlet instead

of a quartet as in published results. The two-methyl groups described as doublets in the literature are seen as two singlets at different positions, it is however possible that again it is not seen as doublets due to the lower resonance of the spectrometer, and that both occur at 0.86 ppm, resulting the peak at 0.83 being an impurity. Proton H-13^4 is however observed as a doublet instead of a singlet, which might be due to an underlying impurity splitting the singlet in two. The absence of H-17^4 is unexplainable; it is possible that the size of the peak in relation to the others might be relatively small and therefore not clearly seen on the lower resonance spectrometer.

In a previous study by Sakdarat *et al*. (2009) they isolated two closely related analogs of pheophytin a, namely 13^2-hydroxy-(13^2-S)-pheophytin a, and 13^2-hydroxy-(13^2-R)-pheophytin a from *Clinacanthus nutans*, a plant known to have antiviral activity against the herpes simplex virus. These compounds were tested against HSV, both compounds showed 100 % inhibition against HSV-1F, at specifically the pre-viral infection stage, with an IC_{50} for both compounds of 3.11 nM. Due to close relationship of HSV and HIV co-infection, and literature indicating that HSV infected individuals being at greater risk for HIV infection (Tan *et al*., 2009 and Freedman & Mindel, 2004), it was decided to test the activity of pheophytin a against the HIV virus. Tests were conducted at InPheno in Basil, Switzerland as described by Heyman (2014). Activity was tested for varying concentrations up to 200 µg/ml, but no activity was observed.

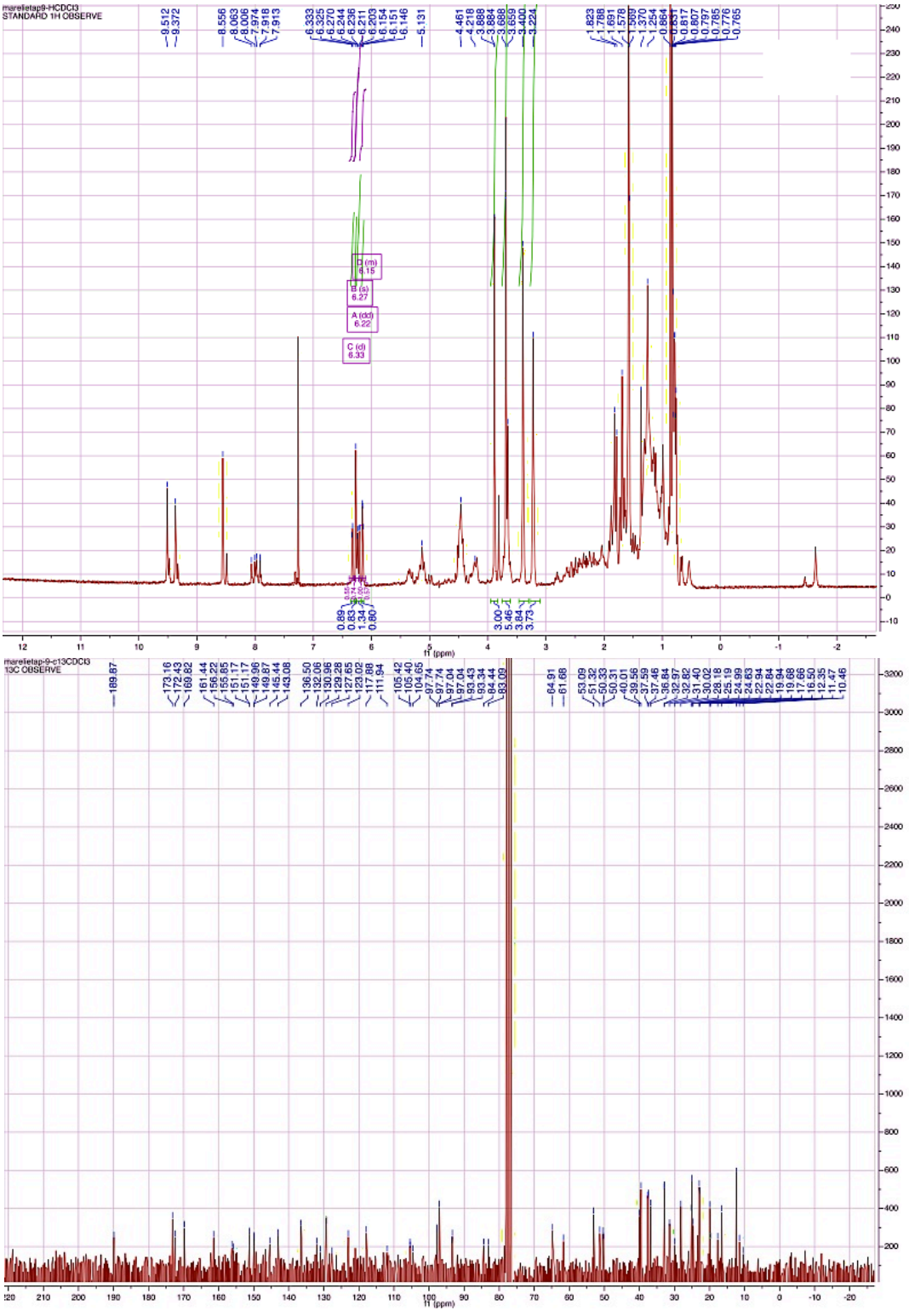

Figure 3.11: ^{1}H and ^{13}C NMR spectra of fraction 9 – Pheophytin a.

3.3.4.2 Antibacterial compounds

Initial ^{1}H and ^{13}C NMR results from the 200 MHz spectrometer were too weak to make clear identifications as to the type of compounds responsible for the antibacterial results. For this reason the samples were analysed at the CSIR in Pretoria on the 400 Mhz spectrometer. When compared with literature both the ^{1}H and ^{13}C data fits well with that of fatty acid compounds. Table 3.2 shows the comparison of the current data with literature.

The first antibacterial compound C4F1 showed NMR results consistent with a long chain saturated fatty acid. It is however not possible to accurately determine the length of the carbon chain due to the central part of the carbon tail, shown as $(CH_2)_x$ in Figure 3.12 A, forming a single large peak at 1.23 ppm as indicated in Table 3.2 and Figure 3.13.

The second antibacterial compound C4F5 is consistent with a glycerol molecule with a long chain saturated fatty acid attached to the first carbon of the glycerol, known as a mono-acyl glycerol. The length of the fatty acid chain couldn't be determined for the same reason as mentioned in the above paragraph. NMR data is indicated in Table 3.2 and Figure 3.14

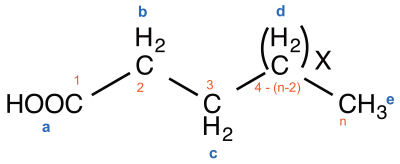

A: Saturated Fatty acid

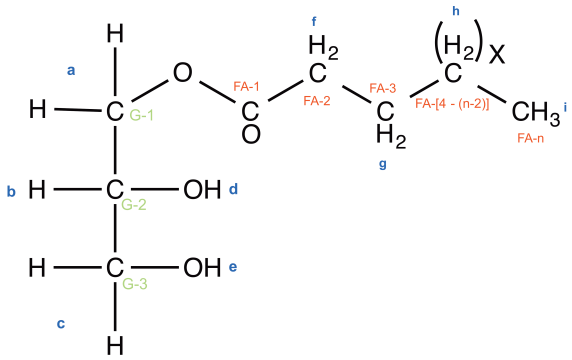

B: Glycerol with saturated fatty acid attached at position 1

Figure 3.12: Structures of the isolated antibacterial compounds, A: long chain fatty acid, B: glycerol with attached fatty acid.

Table 3.2: ^{1}H and ^{13}C NMR data for the antibacterial compounds, compared to literature

Antibacterial compound 1: Long chain saturated fatty acid									
^{1}H NMR					^{13}C NMR				
Proton	Current results		Knothe (2006)		Carbon	Current results		Gunstone (2007)	
	Peak type	Signal (ppm)	Peak type	Signal (ppm)		Peak type	Signal (ppm)	Peak type	Signal (ppm)
a	s	9.74	s	10.5	1	s	179.57	s	180.6
b	t	2.31	t	2.35	2	s	34.18	s	34.2
c	m	1.60	m	1.65	3	s	24.93	s	24.8
d	s	1.23	s	1.3-1.4	n	s	14.3	s	14.1
e	t	0.85	t	0.88	n-1	s	22.89	s	22.8
					n-2	s	32.13	s	32.1
					4 - (n-3)	m	29.29 - 29.9	m	29.3 - 29.8

Table 3.2 Continued

Antibacterial compound 2: Glycerol with a saturated fatty acid attached to carbon 1									
^{1}H NMR					^{13}C NMR				
Proton	Current results		Knothe (2014)		Carbon	Current results		Gunstone (1991) & Bus *et al.* (1976)	
	Peak type	Signal (ppm)	Peak type	Signal (ppm)		Peak type	Signal (ppm)	Peak type	Signal (ppm)
a	2 x dd	4.13 & 4.19	2 x dd	4.18 & 4.25	G-1	s	63.62	s	63.34
b	2 x m	3.68 & 3.58	2 x m	3.64 & 3.73	G-2	s	70.51	s	70.26
c	m	3.92	m	3.97	G-3	s	65.45	s	65.11
d	Signals of d & e overlap triplet of f	3.2	Signals of d & e overlap triplet of f	2.40	FA-2	s	34.40	s	34.07
e					FA-3	s	24.81	s	24.91
f					FA-n	s	14.3	s	14.11
g	m	1.61	m	1.65	FA-(n-1)	s	22.91	s	22.73
h	s	1.24	s	1.3-1.4	FA-(n-2)	s	32.14	s	31.98
i	t	0.86	t	0.88	FA-[4-(n-3)]	s	29.36 - 29.91	s	29.3-29.8

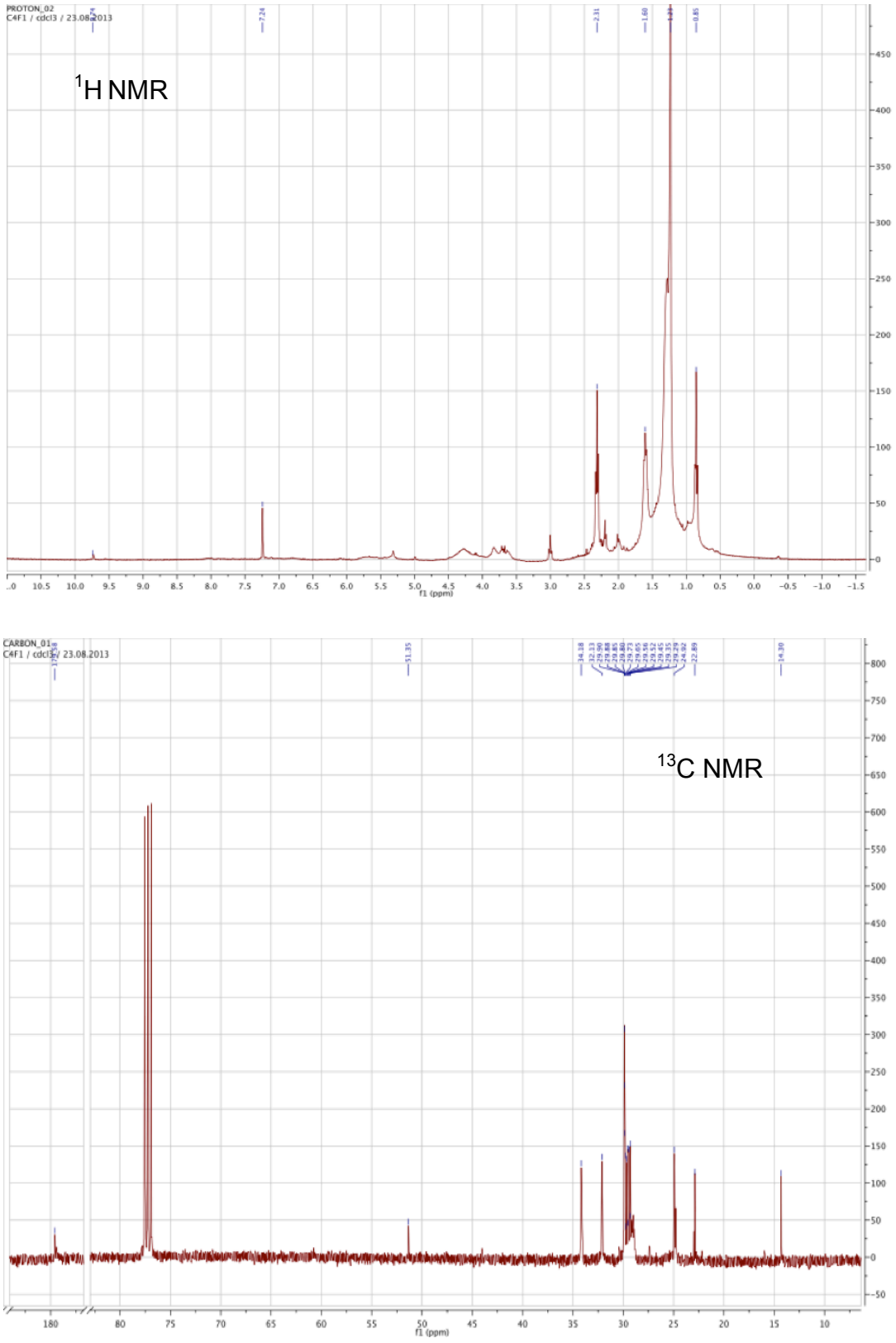

Figure 3.13: ^{1}H and ^{13}C NMR data for antibacterial compound 1: Saturated fatty acid

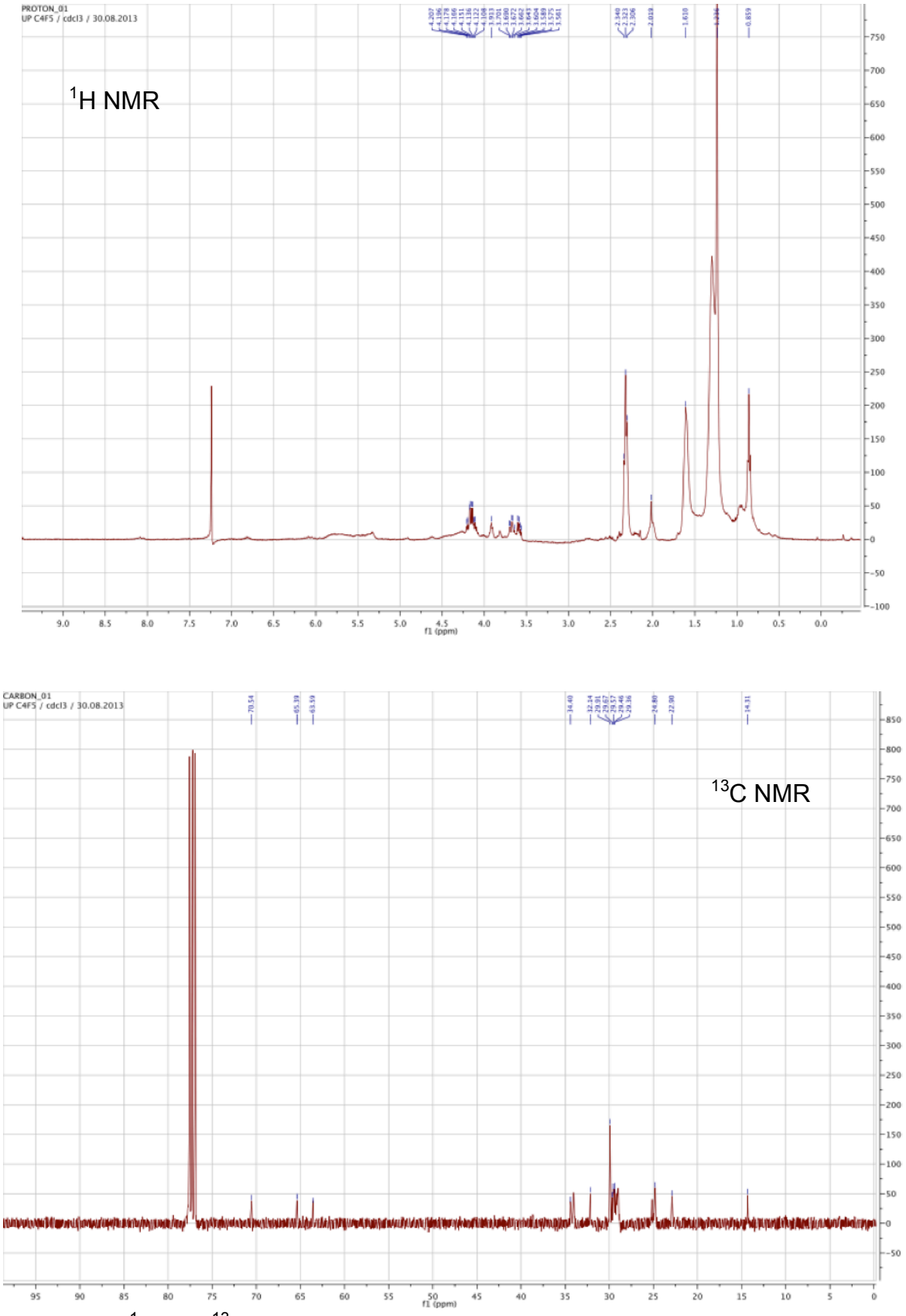

Figure 3.14: ^{1}H and ^{13}C NMR data for antibacterial compound 2: Glycerol with saturated fatty acid attached to position 1.

Since the antibacterial compounds are fatty acids and therefore hydrophobic molecules the possibility exist that the antibacterial results obtained with the TLC plates might be false positives. Since it was not possible to determine the length of the fatty acid structures, the molecular mass can be determined with the use of GCMS, which might help with the determination of the length of the carbon chain.

3.3.5 Gas chromatography

Three different derivatisation methods were used, however none were successful in derivatising the fatty acids to their methyl ester forms (FAMEs). The first method used DCM to dissolve the fatty acids, and results initially were promising when DCM without derivatisation was used as the control. However in order to confirm the results the DCM was also derivitised similarly to the fatty acids. From Figure 3.15 it can be seen that the fatty acid profiles look the same as the derivitised DCM. The small peaks seen in the derivatised FA (fatty acid) and FAG (fatty acid with glycerol), is also present in the derivatised DCM however they are smaller, and therefore difficult to clearly observe.

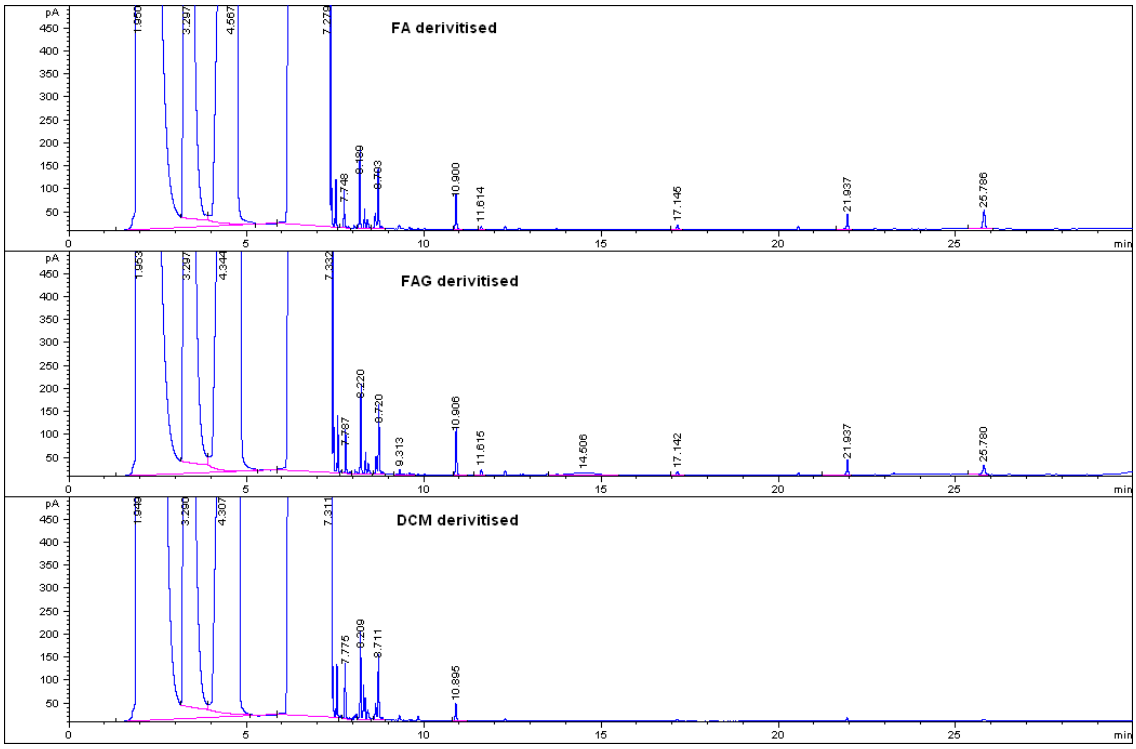

Figure 3.15: FA and FAG dissolved in DCM, derivatised to their FAMEs using BSTFA and analyzed with an HP1-MS column during GC.

The column was changed to a fatty acid specific column, and again analyzed, still no difference could be seen between the derivatised DCM and the fatty acids (Figure 3.16). It can be seen from the figure that the underivatised DCM show no GC peaks, and that derivatisation are responsible for the change in the DCM profile.

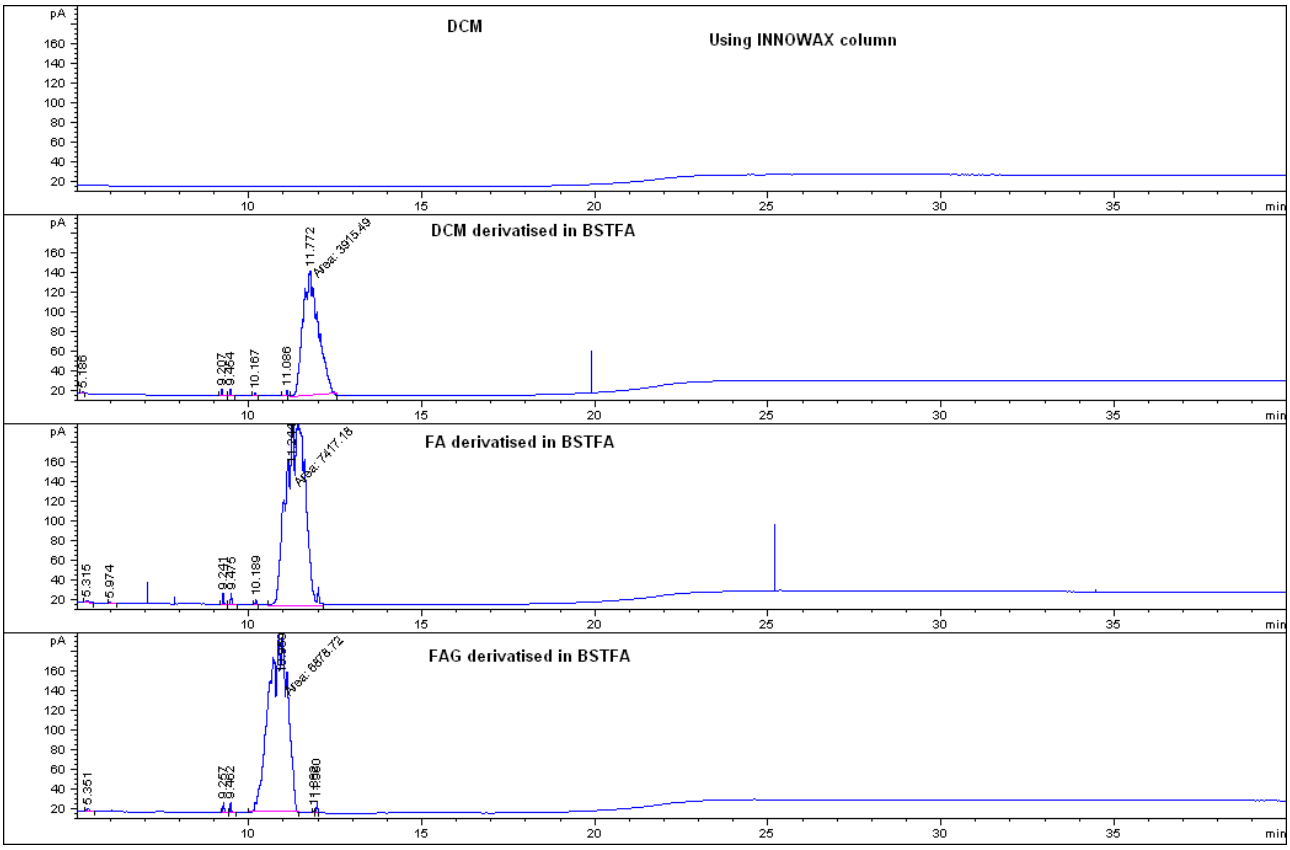

Figure 3.16: FA and FAG dissolved in DCM, derivatised to their FAMEs using BSTFA and analyzed with an innowax column during GC.

The fatty acids were then dissolved in hexane instead of DCM, in an attempt to improve the solubility of the fatty acids before derivatisation. However again no additional peaks were observed in the FA and FAG, showing the same pattern observed in the derivatised hexane (Figure 3.17).

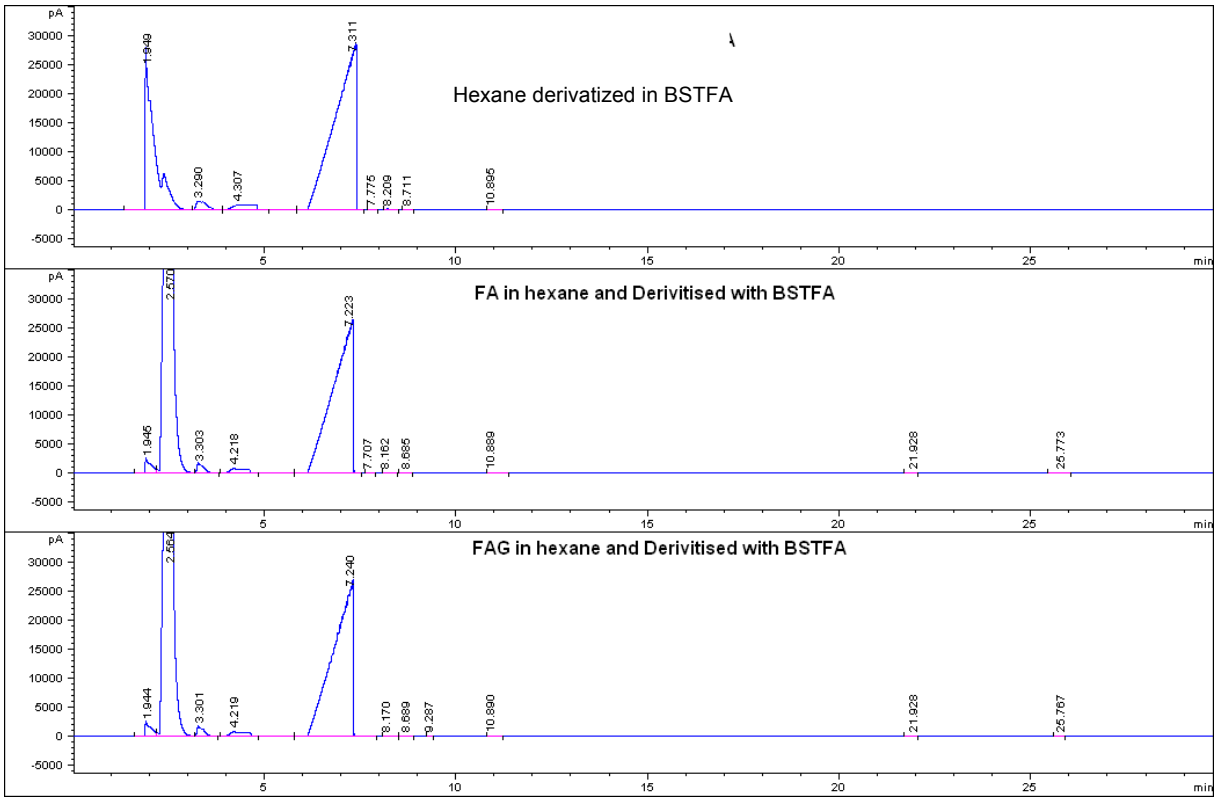

Figure 3.17: FA and FAG dissolved in hexane, derivatised to their FAMEs using BSTFA and analyzed with an innowax column during GC.

A second derivatisation method, making use of BCl_3-metahol was used with the innowax column. As shown in Figure 3.18 the derivation of the fatty acids to their methyl esters was again unsuccessful.

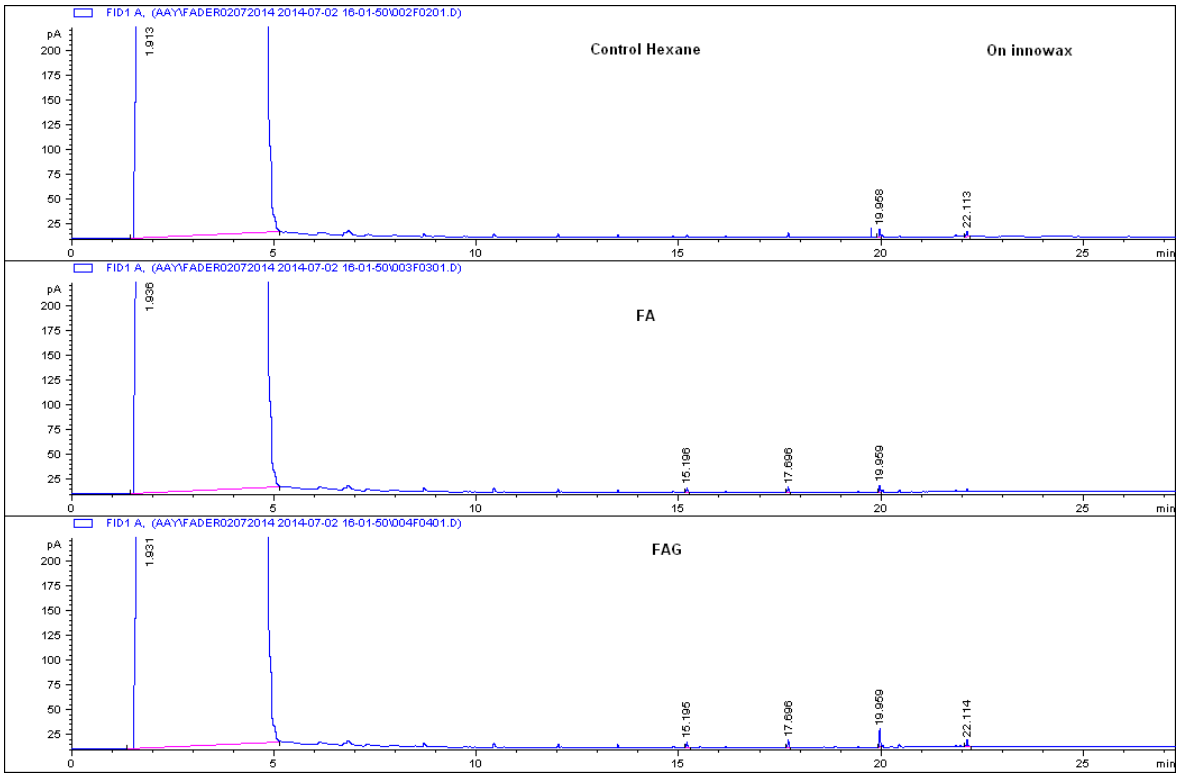

Figure 3.18: FA and FAG dissolved in hexane, derivatised to their FAMEs using BCl_3-methanol and analyzed with an innowax column during GC.

A last derivatisation was used, TMSH as derivatisation agent, and methyl-tert-butyl-eter (MTBE) as solvent to dissolve the fatty acids prior to derivatisation. No FAMEs was detected on the GC and the profiles of FA and FAG was again similar to the derivatisation of the dissolving chemical MTBE (Figure 3.19).

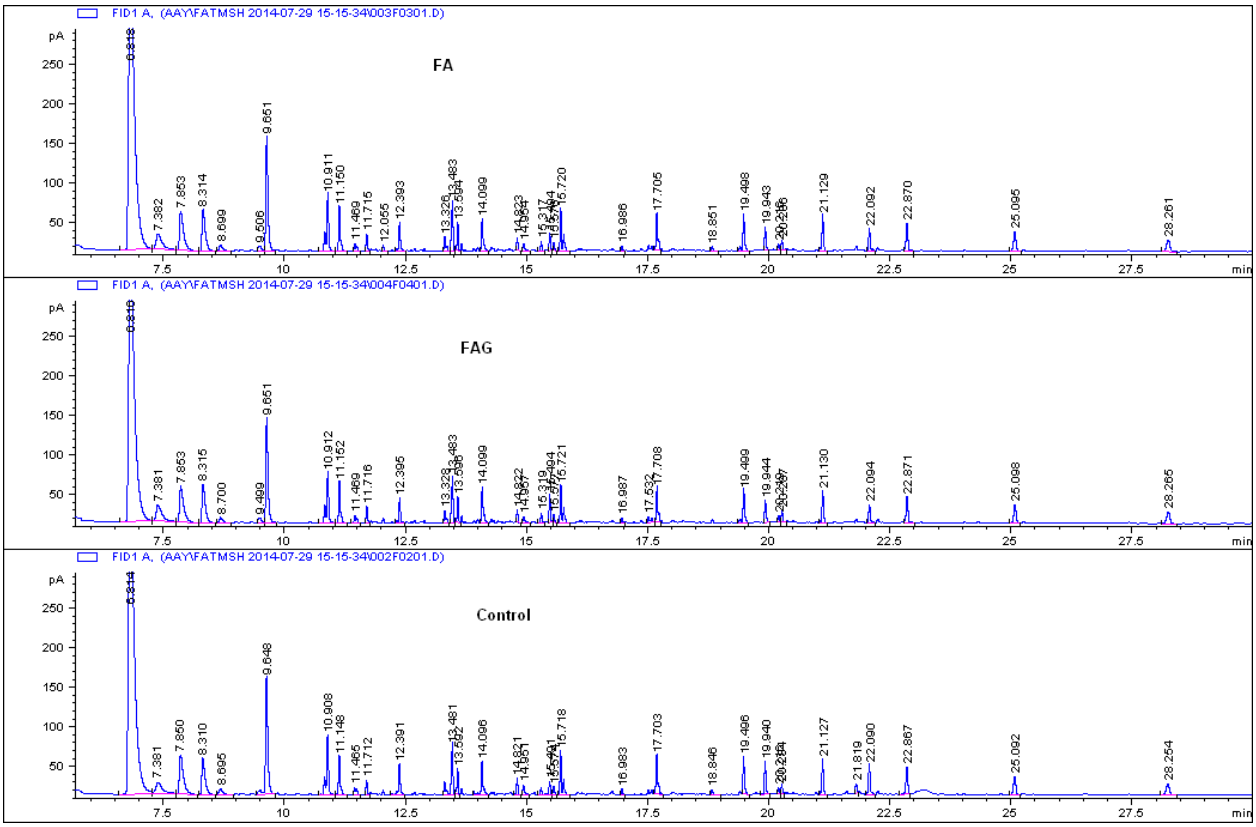

Figure 3.19: FA and FAG dissolved in MTBE, derivatised to their FAMEs using TMSHI and analyzed with an innowax column during GC

Since the results are speculated to be false positive antibacterial results, it was decided not to continue with the GC work on the fatty acids.

3.3.6 Microtitre antibacterial assay

Since it was established that the two antibacterial compounds are in fact fatty acids, the possibility that the antibacterial results might be false positives had to be considered. During antibacterial assays on TLC the bacteria in a water based nutrient broth are sprayed onto the plate. Since the compounds are fatty acids and therefor mainly hydrophobic, meaning water is repelled by the compounds (Campbell *et al.,* 2008), the possibility exist that the bacteria don't grow on the areas where the fatty acids are present. The reaction media (INT) also are water based, resulting in a second possibility where the bacteria might actually be

growing on these spots, but the compound repel the reaction media, thereby preventing the INT to react with the living bacteria on these spots to cause the pink colouring.

For this reason it was decided to redo the antibacterial assay on a 96 well microtitre plate. This allows the reaction to take place in liquid media, and the fatty acid cannot simply repel the bacteria from growing. Due to the low quantities on the antibacterial fatty acid compounds the controls was used as a trial run to ensure the conditions are optimum for the experiment (Figure 3.20).

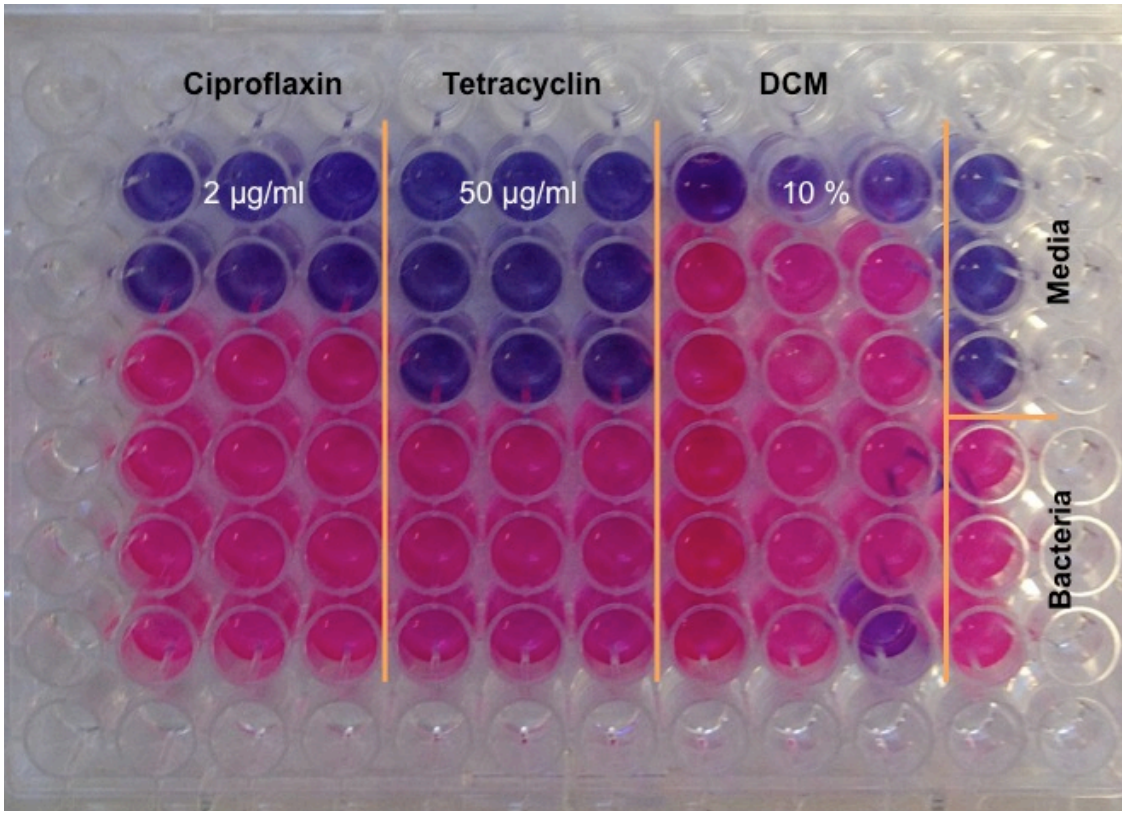

Figure 3.20: 96 well microtitre plate preliminary control results.

Blue wells are indicative of no bacterial growth, while pink wells indicate living cells. The two positive controls ciproflaxin and tetracyclin both showed good bacterial inhibition. Each control was done in 3 replicates. The concentration as indicated on Figure 3.20, is the concentration of the highest concentration in the first row of wells. After which the

concentration was serially diluted downwards, meaning that the following wells have half the concentration of compound than the previous wells. Ciproflaxin are more active than tetracyclin with an MIC of 0.5 µg/ml (indicated by the first 3 pink wells), while tetracyclin have an MIC of 6.25 µg/ml. The solvent control shows bacterial inhibition when 10 % DCM is present in the wells, but from 5 % downward it is save to use as dissolving solvent. The media control shows no bacterial growth indicating that the bacteria seen actively growing can only be from the *E. faecalis* added to the other wells. Lastly the bacterial control shows living cells, indicating the bacteria added to the wells are alive and actively growing.

The antibacterial compounds were then tested as well as the plant extract. The pure compounds were tested from a concentration of 100 µg/ml, while the extract was tested from a 1000 µg/ml. The results are shown in Figure 3. 21

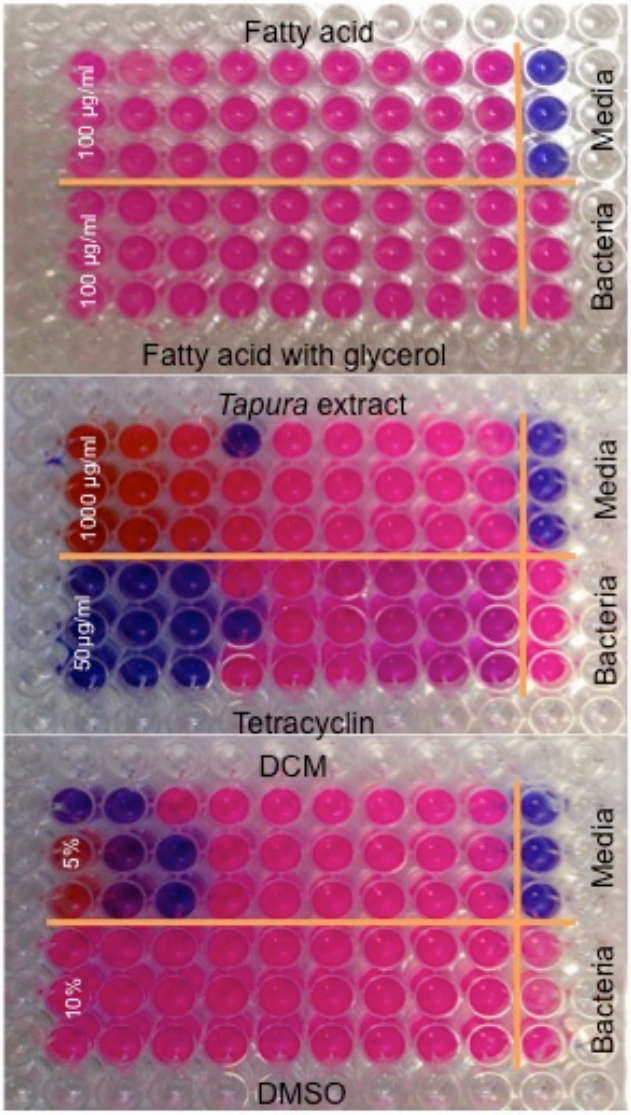

Figure 3.21: Antibacterial results of the two fatty acids tested from 100 µg/ml as well as the plant extract tested at 1000 µg/ml.

Figure 3.21 indicates that neither of the two fatty acid compounds showed any antibacterial activity at 100 µg/ml and lower concentrations. The test was done horizontally testing at eight instead of only six concentrations, as was previously the case as shown in Figure 3.20. The plant extract also showed no antibacterial activity, not even at the highest concentration of 1000 µg/ml. The orange colour observed at the 1000 µg/ml, 500 µg/ml and 250 µg/ml concentrations are due to the green colour of the extract being present before bacterial growth are observed. Only tetracycline was included as the positive control and

again showed an MIC of 6.25 µg/ml. The two out of place blue wells observed at the 125 µg/ml concentration of the *Tapura* extract as well as the middle well from the 6.25 µg/ml concentration of tetracycline, is irregular and its possible that no bacteria was added to these wells.

Two solvent controls were included; since the pure compounds were dissolved in DCM while the extract was dissolved in DMSO. The DMSO showed no bacterial inhibition. The DCM results show antibacterial activity at 2.5 %, as well as two of the wells at 1.25 %. It's possible that bacteria were not added to these wells seeing as previous results showed no bacterial inhibition from 5 %, as well as two wells at 5 % also showed no bacterial inhibition. These unwanted results can be ignored, seeing as the highest DCM concentration in the fatty acid test wells are 2 %, and no bacterial inhibition has occurred. None of the media wells showed any bacterial growth while all of the bacteria controls showed growth, leaving the only possibility for the wells with unexpected antibacterial activity being that bacteria were not added to those wells.

The experiment was repeated starting the antibacterial compounds at a concentration of 200 µg/ml. These results are shown in Figure 3.22.

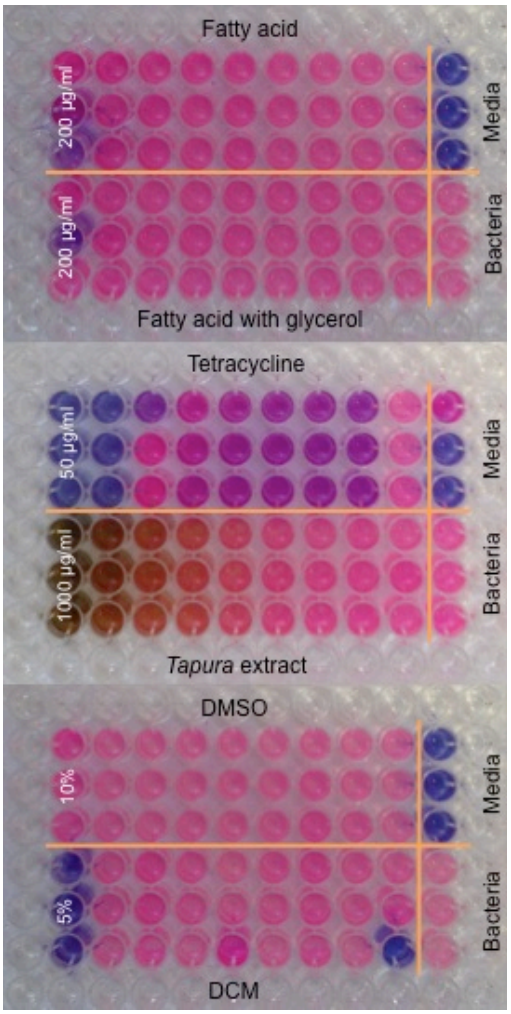

Figure 3.22: Antibacterial results of the two fatty acid compounds tested at 200 µg/ml and the *Tapura* extract tested at 1000 µg/ml

Again no bacterial activity was observed for either of the two fatty acid compounds (Figure 3.22). One well of each of the two compounds has a purple colour, suggesting possible antibacterial activity. Since all the tests were done in triplicate and the other wells were pink in colour, the antibacterial activity are ruled out. The DCM control showed antibacterial activity at the 5 % DCM concentration, although the concentration of DCM in the test compounds are only 2 %, it is possible that a higher concentration were added to the purple wells, seeing as DCM is not very soluble in water (O'Neill, 2006), and might not have mixed well with the water based broth it was diluted with prior to it being added to the wells.

No activity was observed once again for the *Tapura* extract while the tetracycline control only showed an MIC at 12.5 µg/ml. From these results we can finally conclude that neither of the two isolated compounds or the *Tapura* extract have antibacterial properties against the Gram positive bacterium *E. faecalis*, and that the results obtained on the TLC plates were in fact false positive results, stemming from the hydrophobic properties of fatty acids.

3.4 Conclusion

Bioassays can be used as the bases for isolation of the specific compounds responsible for the observed activity, but care must be taken to avoid false positive results. The aim for this part of the work was to isolate compounds responsible for antibacterial activity, as tested against the bacterium *Enterococcus faecalis*. Activity was tested for on TLC plates in which a liquid media containing the bacteria was sprayed onto the developed TLC plates, and after 24 hours sprayed with a reactant, namely INT. Two active compounds were isolated and identified as a long chain saturated fatty acid (compound 1), and a glycerol molecule with a long chain saturated fatty acid attached at position 1 (compound 2), using NMR. This indicated possible false positive results since fatty acids are known to be hydrophobic molecules, repelling water. The antibacterial activity was tested for again in liquid form using 96 well microtitre plates. From these results it was concluded that the compounds were in fact not antibacterial.

A third compound was isolated, known as pheophytin a. This compound has been isolated previously in various plant species, and has been tested before against the HS (herpes simplex) virus, where it showed good antiviral properties. Due to the similarity of HSV and the HIV virus, the compound was tested for anti-HIV activity, but none was detected.

3.5 References

Bus, J., Sies, I., Lie Ken Jie, M.S.F., 1976. ^{13}C-NMR of methyl, methylene, and carbonyl carbon atoms of methyl alkenoates and alkynoates. Chemistry & Physics of Lipids, 17, 501-518

Campbell, N.A., Reece, J.B., Urry, L.A., Cain, M.L., Minorsky, P.V., Wasserman, S.A., Jackson, R.B., 2008. Biology. 8th Ed. Pearson Benjamin Cummings. San Francisco.

Souza Chaves, O., Gomex, R.A., De Andrade Tomaz, A.C., Fernandez, M.G., Des Graças Mendes Jr, L., De Fatima Agra, M., Braga, V.A., De Souza, M.D.F.V., 2013. Secondary metabolites from *Sida rhombifolia* L. (Malvaceae) and the vasorelaxant activity of cryptolepinone. Molecules 18(3), 2769-2777

Cornejo, F., Janovec, J., 2010. Seeds of Amazonian Plants. Princeton University Press, New Jersey.

Freedman, E., Mindel, A., 2004. Epidimiology of herpes and HIV co-infection. Journal of HIV therapy 9(1), 4-8.

Gómez-Brandón, M., Lores, M., Domínguez, J., 2008. Comparison of extraction and dervatization methods for fatty acid analysis in solid environmental matrixes. Analytical Bioanalytical Chemistry 392, 505-514.

Gunstone, F.D., 1991. ^{13}C-NMR studies of mono-, di- and triacylglycerols leading to qualitative and semiquantitative information about mixtures of these glycerol esters. Chemistry & Physics of Lipids, 58, 219-224

Gunstone, F.D., 2007. ^{13}C-NMR Spectroscopy of fatty acids and derivatives: Alkanoic acids. [Online avaialable: http://lipidlibrary.aocs.org/nmr/nmrsat/index.htm] [Last accessed: 02/09/14]

Harper, D.B., O'Hagan, D., 1994. The Fluorinated Natural products. Natural Products Report 11, 123-133.

Heyman, H.M. 2014. Identification of anti-HIV compounds in *Helichrysum* (Asteraceae) species by means of NMR-based metabolomic guided fractionation. PhD Thesis, University of Pretoria. Pretoria

Knothe, G., 2006. ^{1}H-NMR Spectroscopy of fatty acids and their derivatives: Saturated fatty acids and methyl esters. [Online avaialable: http://lipidlibrary.aocs.org/nmr/1NMRsat/index.htm] [Last accessed: 02/09/14]

Knothe, G., 2014. ^{1}H-NMR Spectroscopy of fatty acids and their derivatives: Glycerol esters. [Online avaialable: http://lipidlibrary.aocs.org/nmr/1NMRglyc/index.htm] [Last accessed: 02/09/14]

O. Neill, M.J., 2006. The Merck Index: An encyclopedia of chemicals, drugs and biologicals. ^{14}th Ed. Merck & Co., Inc. New Jersey. USA.

Pinheiro, E.T., Gomes, B.P.F.A., Drucker, D.B., Zaia, A.A., Ferraz, C.C.R., Souza-Filho, F.J., 2004. Antimicrobial susceptibility of *Enterococcus faecalis* isolated from canals of root filled teeth with periapical lesions. International Endodontic Journal 37. 756-763.

Sahm, D.F., Boonlayangoor, S., Iwen, P.C., Baade, J.L., Woods, G.L., 1991. Factors Influencing determination of high-level aminoglycoside resistance in *Enterococcus faecalis*. Journal of Clinical Microiology 29(9), 1934-1939.

Sakdarat, S., Shuyprom, A., Pientong, C., Ekalaksananan, T., Thongchai, S., 2009. Bioactive constituents from the leaves of *Clinacanthus nutans* Lindau. Bioorganic and Medicinal Chemistry 17, 1857-1860

Schwikkard, S.L., Mulholland, D.A., Hutchings, A., 1998. Phaeophytins from *Tapura fischeri*. Phytochemistry 49(8), 2391-2394

Sigma-Aldrich., 2014. Derivatization of Fatty Acids to FAMEs. [Online available: http://www.sigmaaldrich.com/analytical-chromatography/analytical-products.html?TablePage=105120181] [Last accessed: 17/10/14]

Tan, D.H.S., Kaul, R., Walsmley, S., 2009. Left out but not forgotten: Should closer attention be paid to coinfection with herpes simplex virus type 1 and HIV? Canadian Journal of infectious diseases and medical microbiology 20(1), e1 – e7.

Vickery, B., Vickery, M.L., Ashu, J.T., 1972. Analysis of plants for fluoroacetic acids. Phytochemistry 12, 145-147.

Chapter 4:

Leaf morphology and bacterial endophytes of *T. fischeri*

4.1 Introduction

The term endophyte refers to organisms such as bacteria, fungi or any other organism living inside a plant (Gliménez *et al*., 2007) and showing no external signs of infection or negative effect on the host (Ryan *et al*., 2007). Although the endophyte profit from its living environment by gaining enhanced nutrient availability, the plant also benefits from the organism, yielding a mutualistic relationship (Hardoim *et al*., 2008).

The advantages that plants gain include controlling plant pathogens (Ryan *et al*., 2007). An important disease of citrus is citrus variegated chlorosis (CVC) caused by *Xylella fastidiosa*. In many affected orchards, a few unaffected trees were observed. The endophyte *Curtobacterium flaccumfaciens* was found to be associated mainly with asymptomatic trees, and this bacterium could be a possible biocontrol agent against CVC (Araújo *et al*., 2002).

Other endophytes can produce toxins, which protect the plant against herbivores. The toxic alkaloid from locoweed species (*Astragalus* and *Oxytropis* spp), known as swainsonine (Figure 4.1) result in livestock losses each year. It has recently been determined that a fungal endophyte, *Embellisia* spp., is solely responsible for swainsonine production, and thereby transfers toxicity to the plant (Ralphs *et al*., 2008).

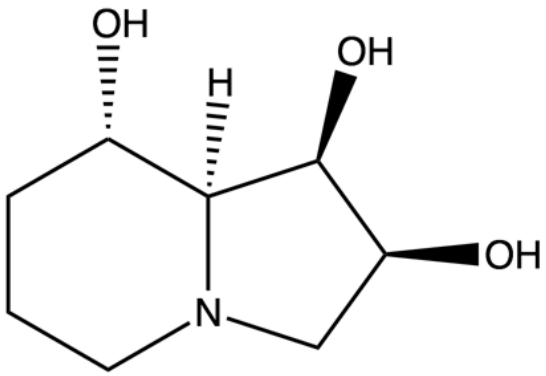

Figure 4.1: Chemical structure of swainsonine (Sibi & Christensen, 1999)

The question remains whether the fluorinated compound present in *T. fischeri* is produced by a bacterial endophyte, or by the plant itself. In previous studies conducted by Hendriks (2012) no endophytes from *T. fischeri* producing fluorinated compounds was isolated, although a few endophytes from *D. cymosum* produced a fluorinated compound with a chemical shift between -131 to -133 ppm.

4.2 Methodology

4.2.1 Endophyte isolation from fresh plant material

Plant material was collected from the Onderstepoort campus of the University of Pretoria during autumn and both leaves and stems were sterilized on the outside. For sterilization, plant material was washed in distilled water, followed by 3.5 % (v/v) hypochlorite solution and then 100 % ethanol. Stems were left in each solution for one minute, while leaves were left for 30 seconds in each. After the ethanol treatment the material was rinsed in autoclaved distilled water, to rinse off the remaining ethanol.

After sterilization the stems were cut into 0.5 cm pieces and placed on soy flour mannitol (SFM) medium, to allow internal bacterial growth. A piece of leaf material was also cut out across the central vain and grinded in 500 µl SFM broth. The grounded material was placed on SFM plates. As positive control unsterilized leaf material was pressed onto a SFM plate, to observe microbial growth present on the outer leaf surface. The plates were incubated at a temperature of 25 °C in the dark.

The SFM growth medium consisted of 20 g nutrient agar powder, 20 g soy flower agar powder and 20 g mannitol dissolved in 1 L of distilled water. Sodium fluoride (0.42 g, 10 mM NaF) was added as a fluorine source. The solution was autoclaved and poured into petri dishes and allowed to solidify.

From the isolation plates, the different endophytes were placed onto new SFM plates to obtain pure single colonies. After single colonies were obtained, the bacteria were marked and grown in SFM broth, consisting of 20 g nutrient broth, 20 g soy flour broth and 20 g of mannitol dissolved in 1 L of distilled water. 0.42 g of NaF was once again added as fluorine source, and endophytes were grown at 25 °C. After 48 hrs the different bacterial solutions were prepared for ^{19}F NMR by drying them on a rotavapor and then dissolving them in D_2O for fluorine NMR.

Prior to drying, a sample of each endophyte was stored at -70 °C. A drop of endophyte in SFM broth was placed in an Eppendorf tube. Glycerol was added and the tube was placed in liquid nitrogen for quick freezing and then placed in the -70 °C freezer for storage.

4.2.2 Light microscopy

Leaf material was collected during spring from the Onderstepoort campus of the University of Pretoria, and the external leaf morphology studied. Fresh material was used, and particular emphasis was placed on visualizing the outer surface of the glandular structures present on the leaves hypothesised to contain bacterial endophytes.

Plant material was collected a second time from the Onderstepoort campus during summer. Leaf material was embedded as will be described in the transmission electron microscopy section 4.2.3. The embedded material was cut with a glass knife into 2-3 µm sections; the cross sections were places on temporary microscope slides and stained with toluidine blue for 30 seconds and then rinsed with water and allowed to dry. The slides were covered with a cover slip and visualized using light microscopy.

4.2.3 Transmission electron microscopy

Plant material was collected during autumn from the Onderstepoort campus, University of Pretoria. The material collected included mostly older leaf material. Cuttings were made of the glands, leaf veins and the growth point.

Leaf material was collected a second time during summer of the following year and cuttings were made of the veins and glandular structures for internal microscopy work.

The material was fixed in 2.5 % glutaraldehyde in 0.075 M phosphate buffer with a pH of 7.4 for 1- 2 hours at room temperature. To prepare the 2.5 % glutaraldehyde, 1.0 ml 25 % glutaraldehyde was added to 5.0 ml 0.15 M phosphate buffer and 4.0 ml distilled water. After two hours the material was rinsed three times with 0.075 M-phosphate buffer. Each rinse cycle was done for 10 minutes. The material was fixated in 0.5 % aqueous osmium tetroxide for 1-2 hours, followed by three wash cycles with distilled water. Using various concentrations of ethanol, the material was dehydrated. The concentrations of ethanol were 30 %, 50 %, 70 %, 90 %, followed by three times using 100 % ethanol. The material was left in each ethanol concentration for 10 minutes.

Ten gram quetol 651 epoxy resin was prepared for infiltration. To prepare 10 g, 3.89 g of quetol, was added to 4.46 g MNA (methyl nadic anhydride), 1.66 g of DDSA (dodecenyl succinic anhydride), 0.20 g RD2 (1,4-butanediol diglycidyl ether) and 0.10 g S1 (2-dimethylaminoethanol). The plant material was infiltrated using 30 % quetol in ethanol for 1 hour, followed by 60 % quetol in ethanol for another hour. Pure quetol was added to the plant material to allow infiltration; this was done for 4 hours. Embedding was done by drying the samples at 60 °C for 48 hours.

The prepared samples were cut for TEM using a diamond knife into 1.2 – 1.5 µm sections and placed onto 200 mesh grids for visualization under the microscope. The grid samples were stained for 2 minutes with 4 % aqueous uranyl acetate, rinsed thoroughly in water and followed by 2 minutes with Reynolds lead acetate, and again thoroughly rinsed in water. Each grid was thoroughly searched for the presence of endophytes and any other unusual structures present in the plant samples.

4.3 Results and Discussion

4.3.1 Endophyte isolation and NMR results

Bacteria were isolated from *T. fischeri* plant material on two occasions. Both stems and leaves (young and old) were used for isolation. The first isolation process yielded a single bacterial colony from a stem cutting and none from the leaves (Figure 4.2 A). This bacterial endophyte was named TA1. During the second bacterial isolation, two additional bacterial endophytes were isolated from young leaf material (Figure 4.2 B) they were named TB 1 and TB 2.

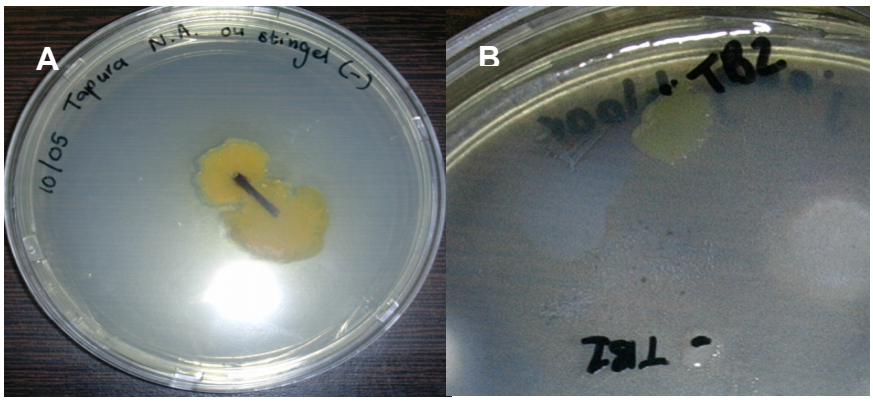

Figure 4.2: Bacterial endophytes from *T. fischeri*. Plate A contains a single bacterial endophyte (TA1) from old stems. Plate B with 2 bacterial endophytes (TB1 and TB2) isolated from young leaves.

The three bacterial endophytes were purified to obtain single colonies, and then grown up in SFM broth. Each endophyte was dried and used for NMR spectroscopy to determine whether any fluorinated compound is being produced by these bacteria. Sodium fluoride (NaF) was added to the broth as precursor molecule for fluoroactete synthesis.

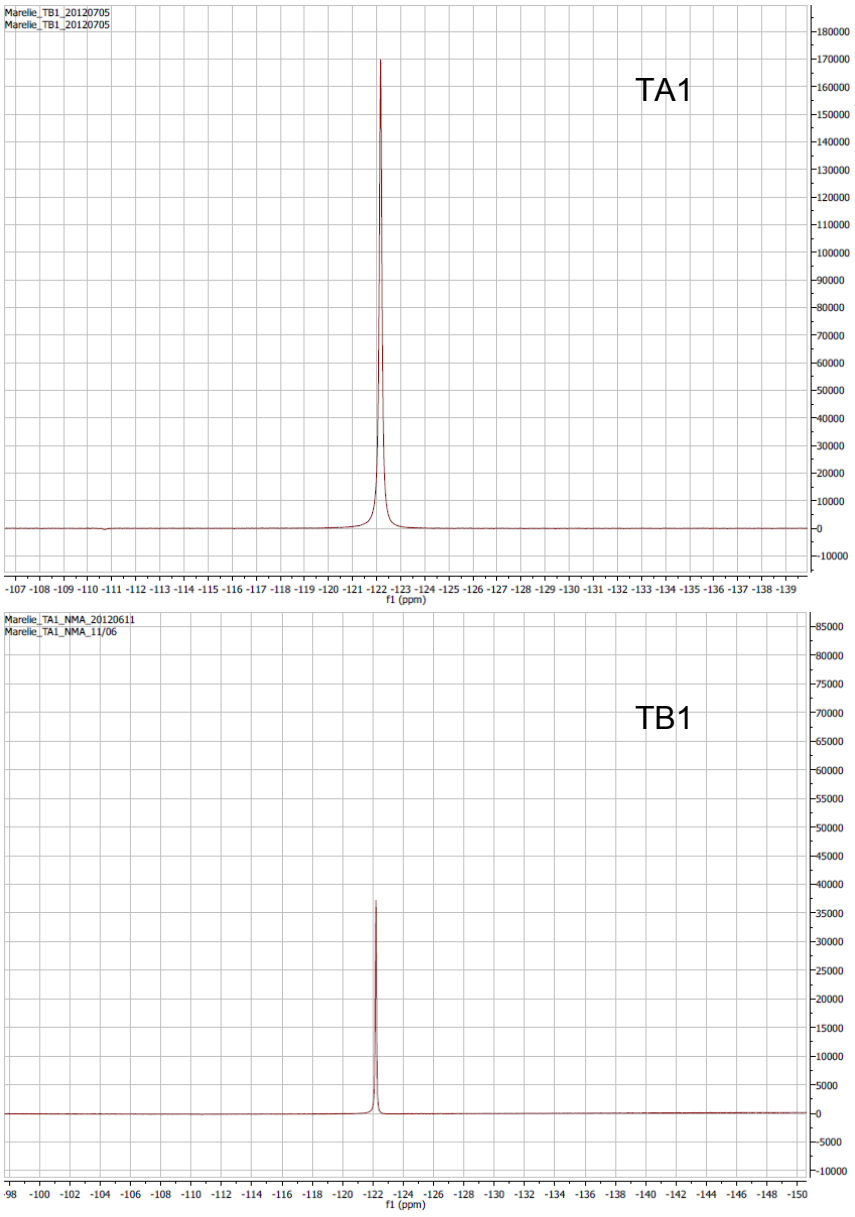

Figure 4.3: NMR spectra from the two bacterial endophytes TA 1 and TB 1. Both yielded no additional fluorinated peaks other than the precursor NaF at -122 ppm.

From Figure 4.3 it is clear that both TA1 and TB1 did not produce a fluorinated compound from NaF. Only a single peak is visible from both NMR spectra at – 122 ppm, which is the peak for free fluorine. Due to their lack of producing fluorinated compounds these endophytes were not used for further studies.

The third endophyte TB 2 however did produce a fluorinated compound with a peak at -136.1 ppm. From Figure 4.4 B it is clear that the sample contained both free fluorine (-122 ppm) and an additional molecule at -136.1 ppm. This however is not the same fluorinated molecule present in the plant, which showed a peak at -75.87 ppm. The molecule produced by the bacterium is probably a precursor molecule, which can be used to produce the compound present in the plant, either by the same bacterium, a different endophyte or the plant itself. The SFM broth was also analyzed and contained no fluorinated peak (Figure 4.4 A).

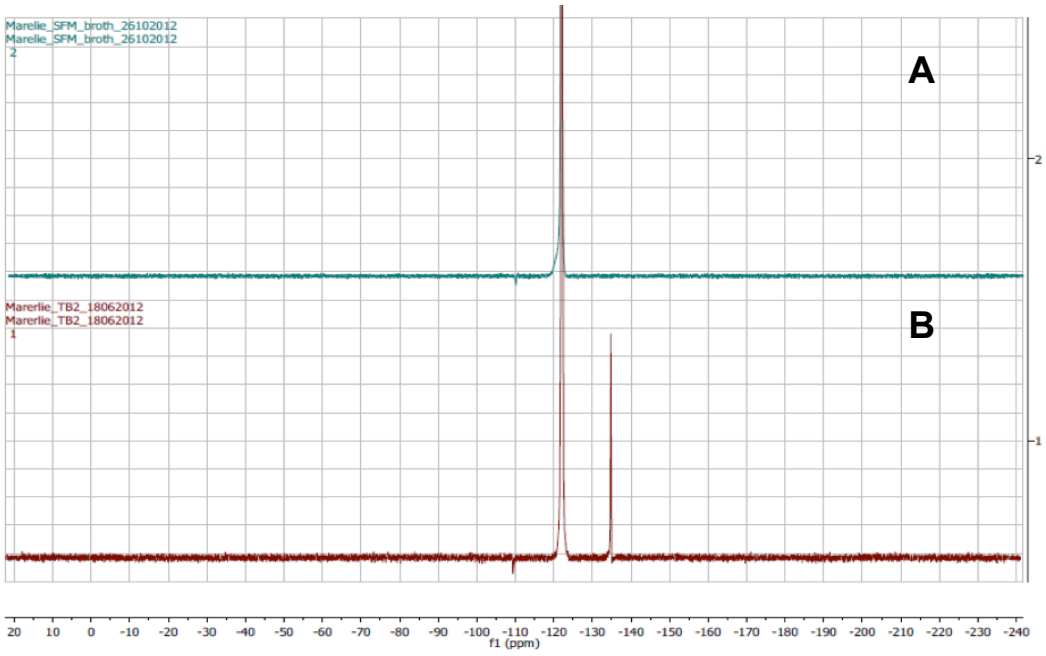

Figure 4.4: (A) SFM broth containing no endophytes. (B) NMR results for the endophyte TB2, showing an additional peak at -136.1 ppm, as well as the free fluorine peak at -122 ppm.

This compound is very similar to the compounds isolated from *D. cymosum* endophytes (-133 ppm) (Hendriks, 2012). It could be speculated that similar species of endophytes are responsible for the production of a precursor molecule in the two plants. Meyer *et al*. (1990) isolated an endophyte (*Pseudomonas cepacia*) from *D. cymosum* capable of metabolizing fluoroacetate, by breaking the C-F bond. A possibility is that similar endophytes in the two plants produce the precursor molecule at -136 ppm. Different organisms such as *P. cepacia* in *D. cymosum* might be responsible for the breakdown of these molecules to the respective fluorinated compounds obtained in the two plants.

When the freeze-dried TB2 was used to grow up more of this bacterium to obtain enough of the compound for analysis, the shaking incubator was out of order which resulted in anaerobic growth of the bacterium during the first five days. The next five days the incubator was working and the bacteria received sufficient oxygen for growth. This second set of TB2 endophyte, showed completely different results. Figure 4.5 shows the NMR results for this endophyte. Unlike the first NMR a compound at -136 ppm was not synthesized, instead two small peaks at -71.75 ppm and -76.35 ppm were observed. The compound at -76.35 ppm is possibly the same compound obtained in the plant. These results however indicate that the same endophyte is capable of synthesizing both compounds. The reason as to why these different results were obtained might be due to the anaerobic conditions that the endophytes underwent during the second experiment. Another possibility is that the compound at -136 ppm is a precursor for the compound at -76.3 ppm, and that due to the long incubation period all the precursor molecules have been converted into the final product.

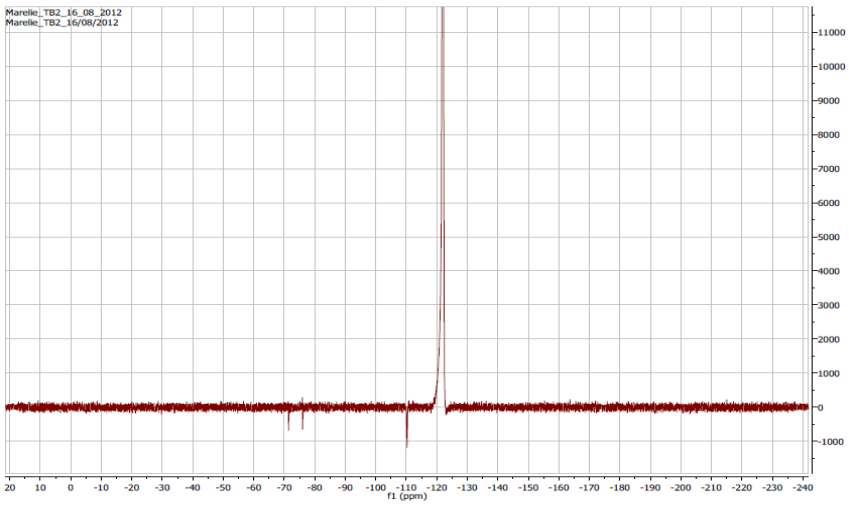

Figure 4.5: Different fluorinated compounds produced by TB2 than during the first isolation. One of the compounds have a similar chemical shift (-76.3 ppm) to the compound extracted from the plant. ca. -75.8 ppm. The other peak is at -71.7 ppm.

The bacterium was grown again in SFM broth, although no growth was obtained. It was initially thought that the bacterial cultures might have died, however it was later discovered that the specific bacterium is inhibited at a growth temperature of 36 °C. When the temperature was adjusted to 25 °C, bacterial colonies were once again obtained and showed to produce a fluorinated compound at -136 ppm (Figure 4.6).

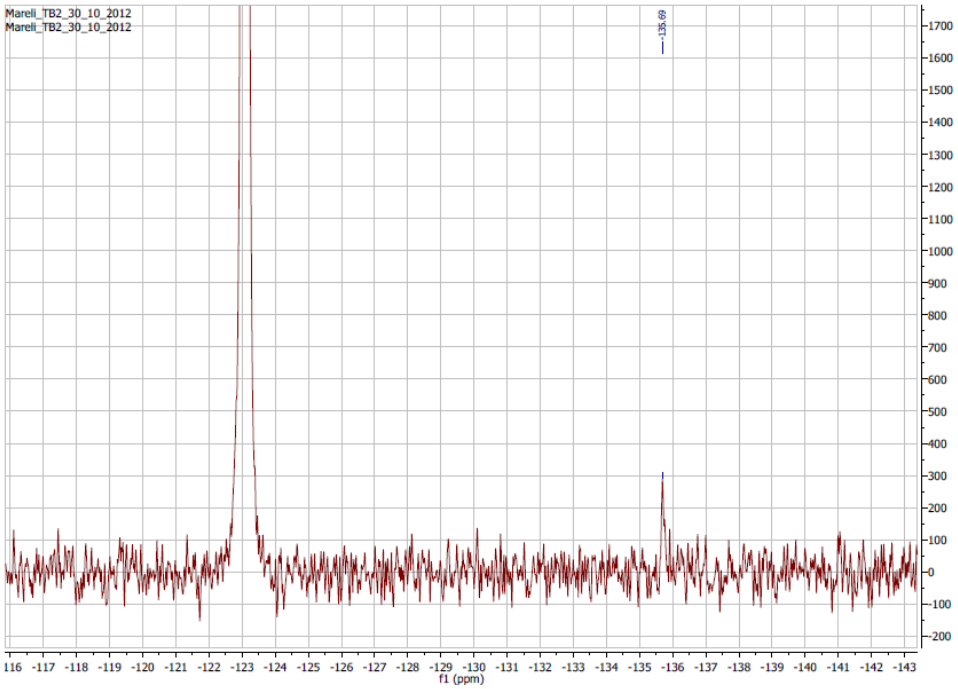

Figure 4.6: Fluorinated compound produced by TB2 confirmed to be at -136 ppm

4.3.2 Microscopy

4.3.2.1 Morphology of the glandular structures on *T. fischeri* leaves.

Upon studying the surface of the leaf material, various structures were observed. Close inspection of the leaf, especially the younger leaves; revealed buldging structures. These structures look similar to bacterial nodules; Figure 4.7 shows what might be a bacterial nodule. A plant family well known to have these leaf nodules is the Rubiaceae, especially the genus *Pavetta*, and a few species of *Psychotria*. The size of the structures in *T. fischeri* is much smaller than the bacterial nodules, which are known to be between 1-2 mm in diameter (van Wyk & van Wyk, 2007). No reference to any Dichapetalaceae species containing bacterial nodules could be obtained and the identity of these structures remains unknown.

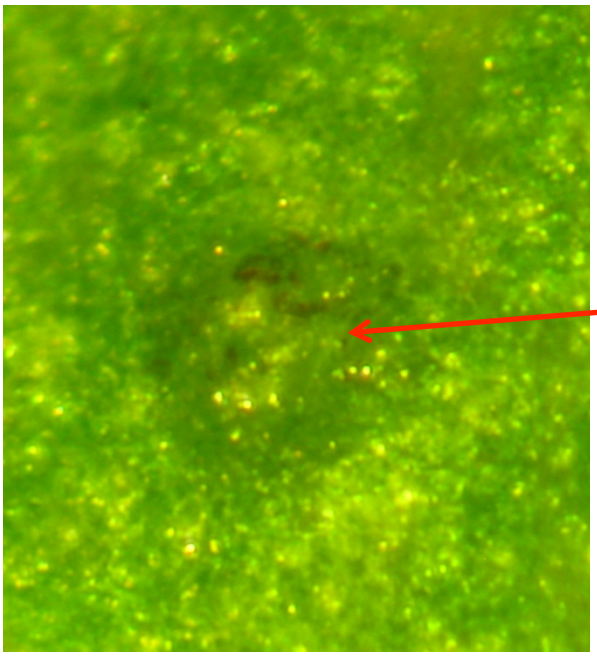

Figure 4.7: Unknown glandular type structure (red arrow) present in *T. fischeri*.

The second type of structure looks like some sort of glandular structure. Under the microscope, it seems as though a watery excretion is secreted from these structures. Figure 4.8 compare the glandular structure present in *T. fischeri* (B) to the extrafloral nectaries present in the duikerberry tree (*Sclerocroton integerrimus*) (A). Extrafloral nectaries that might be the structures in *T. fischeri*, normally occur on the lower surface of the leaf, and the number of structures present per leaf is relatively few. One feature of these structures not consistent in *T. fischeri* is the presence of ants around these structures (van Wyk & van Wyk, 2007). No ant accumulation was present on these structures, however most of the flowers were not open yet, and it is possible that the structures are not fully functional yet.

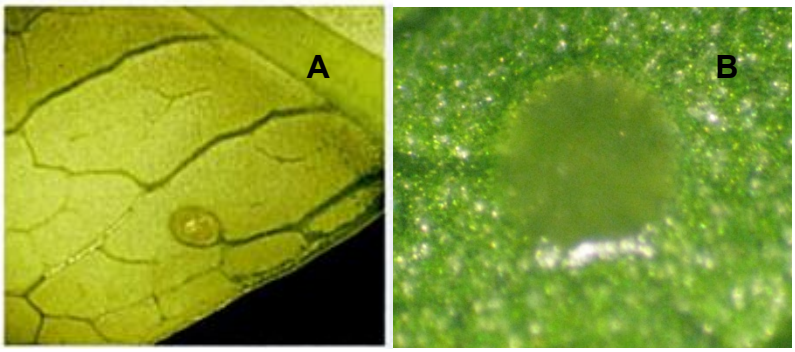

Figure 4.8: (A) Extrafloral nectaries present on leaves of duikerberry tree (*Sclerocroton integerrimus*) (van Wyk & van Wyk, 2007). (B) Glandular structures present on the leaves of *T. fischeri*.

In previous studies conducted by Hendriks (2012) he found that a nymph of tobacco whitefly (*Bemisia tabaci*) or a greenhouse whitefly (*Trialeurodes vaporariorum*) is often associated with the leaves, showing resemblance to the glandular structures in size and shape. He further observed damaged material within the structure, possibly made by the piercing mouthparts of the nymph. The origin of the glands is still however unsure and further investigation should be done. It is also possible that the structures are formed by the plant and that the nymph feeding on it, causes the damage observed.

The third type of interesting structures seen in *T. fischeri* is domatia occurring in the axils between the midrib and the main side veins (Figure 4.9). These structures can be clearly seen with the naked eye, and are particularly visible on the older leaves. The formation of the structures can be seen on the maturing leaves. Domatia are formed by the plant itself, and serve as a housing structure for fungus eating mites, or mites feeding on plant mites (van Wyk & van Wyk, 2007).

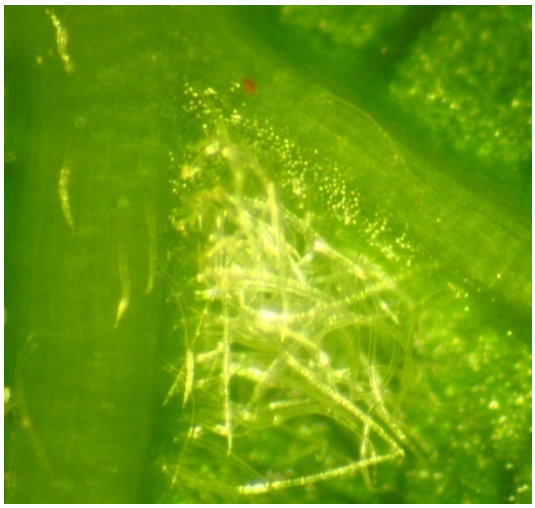

Figure 4.9: Domatium in the axil of the midrib and primary side vein of *T. fischeri* leaf.

3.3.2.2 Transmission electron microscopy in search of endophytes

Microscope sections of the growth point, leaf midrib and glands were prepared for observation under a transmission electron microscope. The main aim was to determine whether bacteria are present in the intracellular spaces as are the case with many Rubiaceae members, such as the genus *Pavetta* and certain *Psychotria* species (Glimenez *et al*., 2007; van Wyk & van Wyk, 2007).

No bacteria were seen within the intercellular spaces, of either the leaf midrib, glandular or growth point material. However in previous studies Hendriks (2012) observed unusual structures among the thylakoids of the chloroplast associated with parenchyma cells underneath the damaged glandular structures. Similar structures between 5 – 8 nm has also been observed in the current study (Figure 4.10), however in a much lower concentration as were seen in the previous studies. These structures are suggested to be virus-like particles (VLP's) deposited by viruses associated with the nymphs of the whitefly.

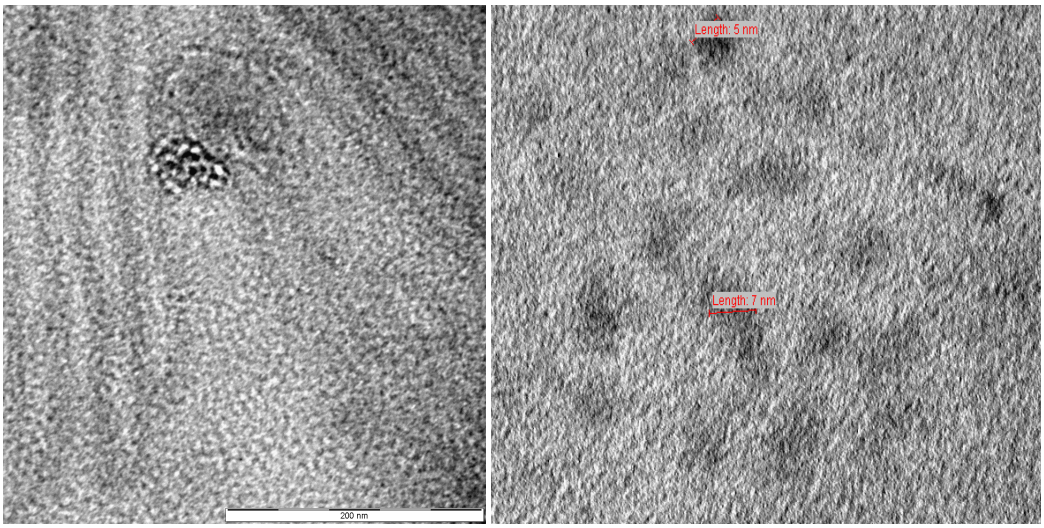

Figure 4.10: Virus-like particles associated with thylakoids in the chloroplasts of the parenchyma cells associated with the glandular structures observed on the leaves.

It has also been suggested that these structures might be phytoferritin molecules, compounds responsible for binding iron. These compounds were initially known to be associated with differentiating immature plastids, however in later studies these structures were obtained in mature plastids also, as well as in virus-infected plastids in sugar beet. It is however unclear whether these particles are the virus itself, or structures formed by the plant as a response to the infection (Robards & Humpherson, 1967).

4.3.2.3. Anatomical study of the glandular structures of *T. fischeri*

Cross section were made of embedded glandular structures cut from leaf material, and visualized with light microscopy. From Figure 4.11 it can be observed that in the normal tissue palisade parenchyma cells are longitudinal and tightly packed under the upper epidermis. The spongy mesophyll cells are rounder in shape with large intracellular spaces as would be expected in dicot leaves. When this is compared to the glandular structure (bulging part) it is clear that although palisade parenchyma cells look similar, major

differences occur in the spongy mesophyll cells. These cells are mostly irregular shaped with very small to no intracellular spaces.

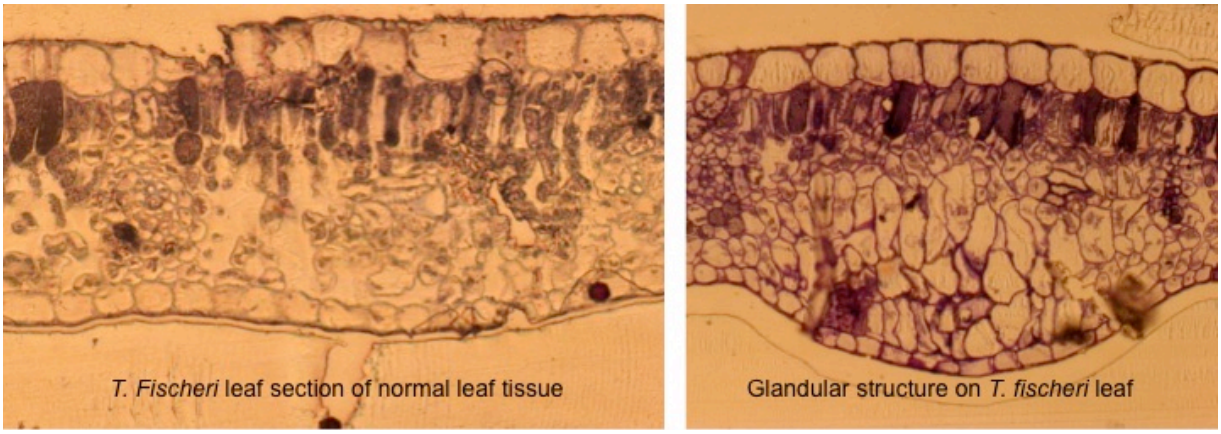

Figure 4.11: Comparison of *T. fischeri* normal leaf tissue and that with glandular structures under light microscopy (20 x magnification).

The sections were then visualized with TEM microscopy in an attempt to better understand the reason for such an occurrence in these structures.

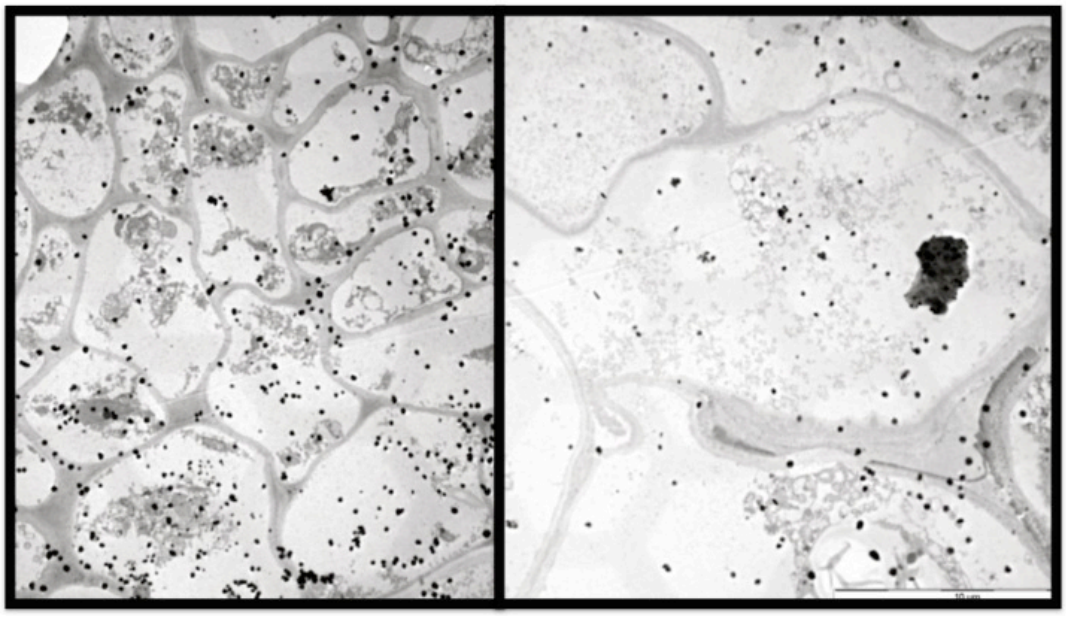

Figure 4.12: TEM Microscopy of glandular structures on *T. fischeri* leaves, showing irregularity of spongy mesophyll cells

TEM microscopy once again showed the irregular spongy mesophyll cells with no to very small intracellular spaces. From Figure 4.12 it seems as though the cells are undergoing plasmolysis. Upon inspection of these images no large vacuoles, or healthy chloroplasts could be observed. Cells seem to be dying, with all the organelles occurring together in a small area of the cell due to the cytoplasm shrinking. The difference between the cells of normal plant tissue compared to the dying cells of the glandular structures can clearly be seen in Figure 4.13.

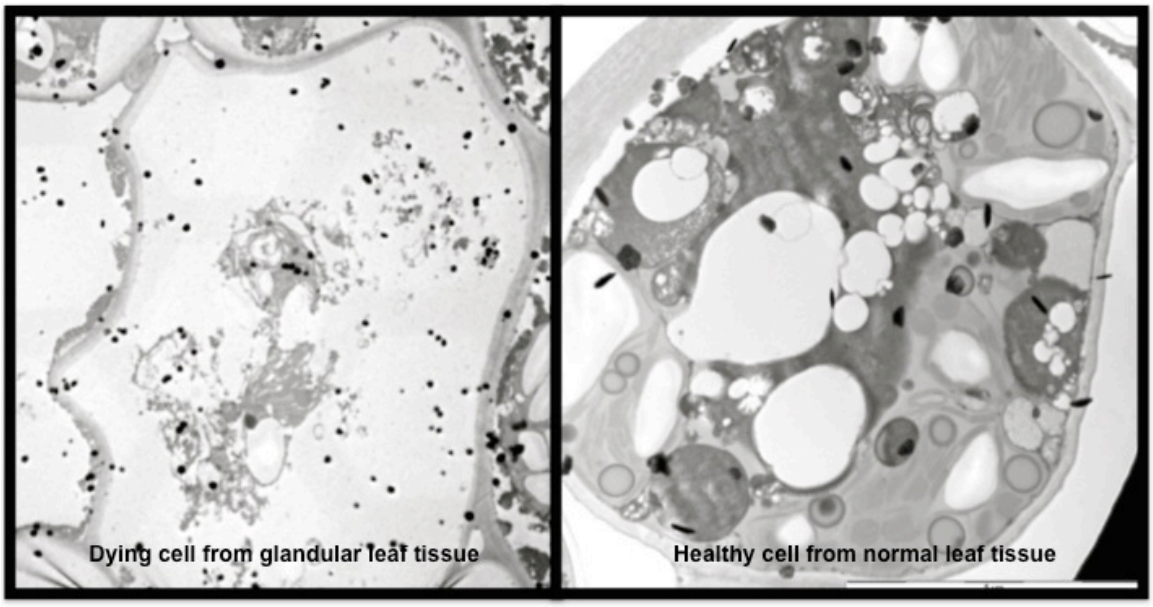

Figure 4.13: Healthy cell of normal leaf tissue compared to dying cell of glandular structure.

From the TEM images no explanation can be given as to the reason of these cells dying, as no bacteria, viruses or VLP's were observed. As was mentioned before, glandular structures of *Dichapetalum cymosum* is possibly due to whitefly insects, however those structures were associated with a abnormality in the palisade parenchyma cells and possibly VLP structures. This however is not the case in *T. fischeri*, and further work should be done to determine why these cells are dying.

It is a possibility that these are normal structures associated with these plants, possibly playing a role in defense, and that the cells die off in order to be filled with a defense related compounds/substances such as tannins (Chafe and Durzan, 1973).

4.4 Conclusion

Bacterial endophytes were isolated from *T. fischeri* stems (one endophyte) and leaves (two endophytes). These were tested for fluorinated compound production. One of the endophytes isolated from the leaves produced a compound at -136 ppm, very similar to endophytes isolated form *D. cymosum* (Hendriks, 2012). More bacterial cultures of the endophyte were grown in SFM broth and NMR analysis repeated. The endophytes this time produced a compound at -76 ppm, which was concluded to be the same compound produced in the plant. During the incubation process the shaker was out of order for a time, which created an anaerobic environment, which might be responsible for the difference in compounds produced. Another possibility is that the initial compound at -136 ppm might have been converted into the second compound at -76 ppm, due to prolonged incubation.

Three morphological structures are associated with *T. fischeri* leaves. Glandular structures excreting a watery substance is believed to be either extrafloral nectaries, or formed by a whitefly nymph. The mature leaves are associated with housing structures known as domatia. These structures serve as a hide for leaf protecting mites. The third type of structure might possibly be bacterial nodules, however there are no data supporting this. Using a transmission electron microscope, particles believed to be virus-like particles, phytoferritin, or phytoferritin produced in response to a viral infection were observed in the parenchyma cells.

The glandular structures seen on the leaves was fixated and prepared for TEM microscopy, the structures revealed a abnormality in the spongy mesophyll of these structures, where

the cells become irregular with very little intracellular spaces. Reasons for this phenomenon is not yet explained, and require further investigation.

4.5 References

Araújo, W.L., Marcon, J., Maccheroni, J.W., van Elsal, J.D., van Vuurde, J.W.L., Azevedo, J.L., 2002. Diversity of Endophytic Bacterial Populations and their interactions with *Xylella fastidiosa* in Citrus Plants. Applied Environmental Microbiology 68, 4906-4914.

Chafe, S.C., Durzan, D.J. 1973. Tannin inclusions in cell suspension cultures of white spruce. Planta 113 (3), 251-262.

Gliménez, C., Cabrera, R., Reina, M., González-Coloma, A., 2007. Fungal Endophytes and their role in Plant Production. Current Organic Chemistry 11, 707-720.

Hardoim, P.R., van Overbeek, L.S., van Elsas, J.D., 2008. Properties of bacterial endophytes and their proposed role in plant growth. Trends in Microbiology 16, 463-471.

Hendriks, C.B.S. 2012. The role of endophytes in the metabolism of fluorinated compounds in the South African Dichapetalaceae. MSc dissertation, University of Pretoria. Pretoria.

Meyer, J.J.M., Grobbelaar, N., Steyn, P.L., 1990. Fluoroacetate-Metabolizing Pseudomonas isolated from *Dichapetalum cymosum*.. Applied Environmental Microbiology 56, 2152-2155.

Ralphs, M.H., Creamer, R., Baucom, D., Gardner, D.R., Welsh, S.L., Graham, J.D., Hart, C., Cook, D., Stegelmeier, B.L., 2008. Relationship between the endophyte *Embellisia* spp. and the toxic alkaloid Swainsonine in major locoweed species (*Astragalus* and *Oxytropis*). Journal of Chemical Ecology 34, 32-38.

Robards, A.W., Humpherson, P.G., 1967. Phytoferritin in Plastids of the Cambial Zone of Willow. Planta 76, 169-178.

Ryan, R.P., Germaine, K., Franks, A., Ryan, D.J., Dowling, D.N., 2007. Bacterial endophytes: recent developments and applications. FEMS Microbiology Letters 278, 1-9.

Sibi, M.P., Christensen, J.W., 1999. Enantiospecific synthesis of (-) Slafranine and related hydroxylated indolizines. Utilization of a nucleophilic alaninol synthon derived from Serine. Journal of Organic Chemistry 64, 6343 – 6442.

van Wyk, B., van Wyk, P., 2007. How to identify trees in southern Africa. Struik Publishers, Cape Town.

Chapter 5:

General conclusions and future prospects

5.1 General Conclusions

Tapura fischeri is a plant belonging to the Dichapetalaceae, a family known to contain many toxic species, such as the only other member of this family naturally occurring in South Africa, *D. cymosum* which is toxic due to the presence of the fluorine containing compound, monofluoroacetate. Toxic plants are often in nature associated with endophytes, producing either the toxic compound itself or a precursor thereof. The primary aim of this study was to determine whether *T. fischeri* also produces monofluoroacetate, or another fluorinated compound, and whether there might be a relationship with endophytes in the production of the fluorinated compound.

During the study it was determined that *T. fischeri* do produce a fluorinated compound, this compound was preliminary identified to be tri-fluorinated due to the single ^{19}F NMR peak observed at -76 ppm. It was established that that the fluorinated compound is volatile, due to the absence of the fluorinated compound in older plant extracts. For this reason it was hypothesized that the fluorinated compound could be trifluoroacetate (TFA), a volatile compound with a single peak and chemical shift close to -76 ppm on NMR. Trifluoroactetate standard was analysed on ^{19}F NMR, forming a single peak at the same place as the fluorinated compound in the *T. fischeri* extract.

The presence of trifluoroacetate was confirmed with GCMS. The trifluoroacetate was derivatized to its methyl ester form (MTFA), further increasing the volatility of the compound. The standard eluted from the GC after 4.6 minutes, with three prominent ions *m/z* 59, 69 and 99 on the MS. The extract was derivatized in the same manner and again the MTFA eluted after 4.6 minutes, which was then quantified to be 238.40 µg/g and 153.63 µg/g MTFA per gram fresh leaf material for the OP (Onderstepoort) and LBG (Lowveld botanical garden) plants respectively. TFA is often formed as a pollutant derived from the break down

of hydrofluorocarbons (HFC's) and hydrochlorofluorocarbons (HCFC's) in the trophosphere. However previous studies conducted on the accumulation of TFA in plants have never reported such elevated levels of TFA as seen in the current study. It is for this reason that it is believed that TFA is produced in *T. fischeri* as a possible defence chemical, similar as monofluoroacete in *D. cymosum.*

Bacterial endophytes were isolated from the plant material, of these one was capable of producing a fluorinated compound. The compound produced by the endophyte was different than the compound present in the plant. The role the endophyte play in the production of the fluorinated compound found in the plant is still uncertain.

Thin layer chromatography indicated that the plant extract is toxic to the Gram-positive bacterium, *Enterococcus faecalis*. The compounds responsible for the antibacterial activity were isolated during column chromatography. This was confirmed by spraying TLC plates with *E. faecalis*, and after 24 hours spraying the same plate with the colouring agent INT. The pure compounds were identified as fatty acids with the use of ^{1}H and ^{13}C 400 MHz NMR. The NMR spectrum of the first compound was consistent with a long chain saturated fatty acid, and the second compound with a long chain saturated fatty acid attached to position 1 of a glycerol. With the use of GCMS it was attempted to identify these two compounds. The derivatisation methods of the fatty acids to their methyl ester forms (FAMEs) were however unsuccessful, and the identity of the compounds are therefore still unknown.

Since these compounds are fatty acids the possibility existed that the antibacterial results were false positives due to their hydrophobic nature, thereby repelling the water based nutrient broth containing the bacterial colonies or the water based INT. The antibacterial activity was therefore also tested using 96 well microtitre plates, in order to test the activity

in a liquid form. The results indicated that both the compounds and the plant extract do not exhibit antibacterial activity against the Gram-positive *E. faecalis*, and that the previous results were in fact false positives.

Transmission electron microscopy was used to determine whether endophytes are present in the leaf material; however no bacterial colonies were observed in the intercellular spaces of the plant material. On the younger leaves glandular structures were observed using light microscopy; cross sections of these structures were made and observed both with light microscopy and transmission electron microscopy. These structures showed abnormalities but the cause of this is unexplained.

Although the nature of the fluorinated compound has been explained, the origin of it is still unsure. Is it absorbed as a pollution or is it formed in the plant with the help of endophytes?

5.2 Future Prospects

The primary question in further studies would be to determine how trifluoroacetate is synthesized, and whether it is present in other *Tapura* members such as *T. amazonica*. The question should also be asked whether this compound is responsible for the toxicity associated with some *Tapura* members. The toxicity of *T. fischeri* against various vertebrates should be confirmed, since it still only speculated to be a toxic plant.

Future work should also focus on the relationship of the bacterial endophytes capable of forming a fluorinated compound. Are these endophytes responsible for the presence of the TFA, or are they capable of breaking down TFA, obtained from the plant or from pollution, to a less toxic form? The identity of the endophyte producing the fluorininated compound should also be established.

If TFA is not present in other *Tapura spp.*, focus should be placed on the compounds responsible for the toxicity, and lethality of species such as *T. amazonica.*